Information from the Universe:

Cosmological Branes and Perturbation

of Strong Gravity

Elcio Abdalla

Abstract

We aim at gathering information from gravitational interaction in the Universe, especially in limiting situations, where gravity can be tested at its most extreme forms.

First we briefly consider perturbations of strong gravity solutions to Einstein Equations, and the type of signs derived thereof.

Subsequently, using the solutions to Einstein equations and boundary conditions we study the kind of constraints to the number of e-foldings in inflation.

Later we analyse a dynamical membrane world in a space-time with scalar bulk matter described by domain walls, as well as a dynamical membrane world in empty Anti de Sitter space-time.

We finally investigate the possibility of having shortcuts for gravitons leaving the membrane and returning subsequently. In comparison with photons following a geodesic inside the brane, we verify that shortcuts exist. For some Universes they are small, but sometimes are quite effective.

In the case of matter branes, we argue that at times just before nucleosynthesis the effect is sufficiently large to provide corrections to the inflationary scenario, especially as concerning the horizon problem and the Cosmological Radiation Background.

Introduction

Although standard model of particle physics has been established as the uncontested theory of all interactions down to distances of 10^{-17}m, there are good reasons to believe that there is a new physics arising soon at the experimental level.

Introduction

String theory provides an excelent background to solve long standing problems of theoretical high energy physics.

M-theory can be a reasonable description of our Universe.

In the field theory limit: described by a solution of the 11-dimensional Einstein equations with a cosmological constant by means of a four dimensional membrane. In this picture only gravity survives in the extra dimensions; remaining matter and gauge interactions are typically four dimensional.

This avenue presents us a possibility of tackling with two different problems at the same time, namely provide a means of testing the up to now far from experimental and observational data string theory, and providing a theoretical framework to cosmology, whose theoretical background needs a full understanding of quantum gravity in order to correctly deal with the puzzling question of the initial singularity.

General Relativity always evaded quantization.

Einstein gravity is a nonrenormalizable theory at a low loop level.

Atempts to include supersymmetry in order to cancel divergencies only postponed the problem to a higher loop.

String Theory showed a way, from its very basis of how to succesfully quantize gravity. At the same time, and especially after the discovery of the anomaly cancellation mechanism (first superstring revolution).

Strings are quasi unique. Moreover, the further discovery of the duality symmetry, such a uniqueness has been further enhanced (duality), leading to the concept of a universal theory: M-theory (largely unknown)

describing an eleven dimensional misterious, master theory, mother of all string descriptions on their side related by duality, and containing in their field theory limit a version of 11-dimensional supergravity.

What can turn a higher dimensional theory into something realistic, describing our four dimensional world. Some hints are know since almost a century, and which have been used before in the context of supergravity.

Kaluza Klein approach: extra dimensions are compactified, curled up into a size that cannot be observed.

Although appealing several problems, being still an active field of inquire. Still there are proposals where some of these dimensions are large enough to be probed by microphysics.

Universe as a Membrane.

Horava and Witten: our universe can be seen as a solution of a higher dimensional theory.

Strings can be open or closed.

The closed string sector contains gravity and further components. The open string sector contains matter fields, isolated into their extremities.

The open string extremities containing the matter fields are restrained to live in the physical universe.

Randall and Sundrum

The universe as a solution of the higher dimensional field equations with boundary conditions describing the membrane: full fledged extra dimensions, but with a warp, such that the effective penetration of gravitons in the extra dimensions is small, and the effective gravitational interaction is, observationally, four dimensional.

Possibility that gravitational fields, while propagating out of the brane speed up, reaching farther distances in smaller time as compared to light propagating inside the brane, a scenario that for a resident of the brane (as ourselves) implies shortcuts.

FRW Brane Universe.

The brane evolves in a non-trivial way in a static AdS background, we can construct explicitly the causal structure of null geodesics leaving and subsequently returning to the brane.

Shortcuts are common, although harmless at the present days (the delay is vanishingly small), but could be large in the era before nucleosynthesis if high redshits were available.

Strings and Observations

Moreover, one of the main goals of string theory nowadays is to prove itself able of coping with experimental evidences.

Branes: useful tools to understand the physics of strings and M-theory.

Brane Universes: relics of extra dimensions in the cosmic microwave background.

If inflation took part on the brane, the causal structure can be changed by gravitational shortcuts.

We may have distinct predictions in the cosmic microwave background structure for inflationary models.

Further Motivations and Brane Cosmology

Planck mass: natural scale where string effects becomes important.

Not possible in accelerators.

Cosmology: alternative laboratory for string theory.

General relativity in higher dimensions together with scalar and tensor fields.

Extensive used of specific properties of strings, such as the T-duality may provide simple explanations of several properties of the universe, though of course an observational check is always missing. Nonetheless, a pre big-bang scenario turns out to be described, providing a very sophisticated physical picture of the universe. Several solutions indicating inflationary results have been obtained, in what is now usually called brane cosmology.

CMB data

Cosmic Microwave Background: pioneering COBE satelite, WMAP.

Avenue for precision cosmology: results with error bars less and a percent are now available.

A chance of favouring, or discarding, string inspired models of cosmology, or brane cosmology.

Towards Inflation

Scalar potential directly from string theory has been an important issue.

Scalar interaction from a brane-brane interaction.

Different and new forms for the inflaton potential have been derived, showing that at least one can hope to derive inflationary models directly from the properties which caracterize string theory and its consequences.

Perturbations of Einstein Equations in a General Setup

Exact solutions of Einstein Equations are many, but reality can be much more difficult, and much more is needed.

Perturbations of Black Hole Solutions

Wave dynamics outside black holes.

Schematic picture regarding the dynamics of waves outside a spherical collapsing object.

Static observer outside BH: three successive stages of the wave evolution.

Initial pulse.

Quasi–normal ringing (information about the structure of the background spacetime; and is believed to be a unique fingerprint to the black hole existence).

Gravitational wave observation.

At late times, quasinormal oscillations are swamped by the relaxation process.

Relaxation: Price, power law tail.

Further results on non asymptotically flat spaces.

Inclusion of charges.

Hod and Piran: usual inverse power–law accompanied by an oscillatory behavior, with self interactions.

Non–asymptotically flat exteriors of Schwarzschild–de Sitter and RN de Sitter black holes: exponential decay.

Inverse power–law tails as seen in asymptotically flat black hole spacetimes are not a general feature of wave propagation in curved spacetime.

Besides some relation to the perturbative field, the relaxation process reflects a characteristic of the background geometry.

AdS

Anti–de Sitter/Conformal Field Theory (AdS/CFT) correspondence makes the investigation in AdS black hole background more appealing.

The quasinormal frequencies of AdS black hole have direct interpretation in terms of the dual *Conformal Field Theory* (CFT).

In terms of the AdS/CFT correspondence, the black hole corresponds to an approximately thermal state in the field theory, and the decay of the test–field corresponds to the decay of the perturbation of the state.

Real and imaginary parts of the quasinormal frequencies scale linearly with the black hole temperature. The time scale for approaching the thermal equilibrium is detected by the imaginary part of the lowest quasinormal frequency and is proportional to the inverse of the black hole temperature.

AdS

Considering that the RN AdS solution provides a better framework than the Schwarzschild AdS geometry and may contribute significantly to our understanding of space and time.

Charge in RN AdS black hole showed a richer physics concerning quasinormal modes and further information on AdS/CFT correspondence.

The bigger the black hole charge is, the quicker for their approach to thermal equilibrium in CFT.

New window of information from the cosmos by means of the hopefully nearly coming discovery of gravitational waves.

Especially strong when emitted by black holes.

Small but non vanishing (and positive) cosmological constant.

Quasi Normal Modes

First described by G. Gamow in the content of nuclear physics, the wave describes properties more connected with the background space rather than the font itself.

Also WKB method: accurate and systematic means to find quasinormal modes.

The results cannot in general be obtained in analytic form, but describe reasonably the behaviour of waves scattered by the black hole solutions providing information about the caracteristics of the background.

Our intention here is to provide methods for dealing with perturbations of strong gravity solutions.

Scalar, Electromagnetic and Gravitational Perturbation

Schwarzschild-de Sitter metric:

$$ds^2 = -h(r)dt^2 + h(r)^{-1}dr^2 + r^2\left(d\theta^2 + \sin^2\theta d\phi^2\right) \ , \tag{1}$$

$$h(r) = 1 - \frac{2m}{r} - \frac{\Lambda r^2}{3} \ . \tag{2}$$

m is the black hole mass. $\Lambda = \frac{3}{a^2}$.

$$r_+ = \frac{2}{\Lambda^{1/2}} \sin\left[\frac{1}{3}\sin^{-1}\left(3m\Lambda^{1/2}\right)\right] \ , \tag{3}$$

$$r_c = \frac{2}{\Lambda^{1/2}} \sin\left[\frac{1}{3}\sin^{-1}\left(3m\Lambda^{1/2}\right) + \frac{2\pi}{3}\right] \ , \tag{4}$$

$$r_n = -(r_+ + r_c) \ . \tag{5}$$

$$a^2 = r_+^2 + r_c^2 + r_+ r_c \ , \tag{6}$$

$$2ma^2 = r_+ r_c (r_+ + r_c) \ , \tag{7}$$

‘Tortoise” radial coordinate

$$x(r) = \frac{1}{2\kappa_c}\ln(r_c - r) - \frac{1}{2\kappa_+}\ln(r - r_+) + \frac{1}{2\kappa_n}\ln(r - r_n)\ , \tag{8}$$

$$\kappa_i = \frac{1}{2}\left|\frac{dh(r)}{dr}\right|_{r=r_i}\ . \tag{9}$$

κ_+ and κ_c: surface gravity associated with the event and cosmological horizons.

Scalar field Φ

$$\nabla^2 \Phi = 0 \ , \tag{10}$$

$$\Phi = \sum_{\ell\, m} \frac{1}{r} \psi^{es}_{\ell}(t,r) Y_{\ell}(\theta,\phi) \ , \tag{11}$$

$$-\frac{\partial^2\psi_\ell^{es}}{\partial t^2}+\frac{\partial^2\psi_\ell^{es}}{\partial x^2}=V^{es}(x)\psi_\ell\ , \tag{12}$$

with the effective potential V^{es} given by

$$V^{es}(r)=h(r)\left[\frac{\ell(\ell+1)}{r^2}+\frac{2m}{r^3}-\frac{2}{a^2}\right]\ . \tag{13}$$

In the non charged black hole geometry, it is possible to have pure electromagnetic and gravitational perturbations. In this case, the potential of the corresponding Schrödinger type equation is given by the expression

$$V^{el}(r) = h(r)\frac{\ell(\ell+1)}{r^2} \ . \tag{14}$$

$$V^{ax}(r) = h(r)\left[\frac{\ell(\ell+1)}{r^2} - \frac{6m}{r^3}\right] \ , \tag{15}$$

$$V^{po}(r) = \frac{2h(r)}{r^3}\frac{9m^3 + 3c^2mr^2 + c^2(1+c)r^3 + 3m^2(3cr - \Lambda r^3)}{(3m+cr)^2} \ , \tag{16}$$

with $c = (\ell-1)(\ell+2)/2 = [\ell(\ell+1) - 2]/2$.

For perturbations with $\ell > 0$, we can show explicitly that the effective potentials $V(x) \equiv V(r(x))$ are positive definite. For scalar perturbations with $\ell = 0$, its effective potential has one zero point x_n, and it is negative for $x > x_n$.

Numerical and Semi-analytic Methods

Characteristc integration

$u = t - x$ and $v = t + x$:

$$-4\frac{\partial^2}{\partial u \partial v}\psi(u,v) = V(r(u,v))\psi(u,v)\ . \tag{17}$$

$$\psi(u = u_0, v) = \exp\left[-\frac{(v - v_c)^2}{2\sigma^2}\right] \ , \tag{18}$$

$$\psi(u, v = v_0) = 0 \ . \tag{19}$$

$$\psi(N) = \psi(W) + \psi(E) - \psi(S) \\ - \Delta^2 V(S) \frac{\psi(W) + \psi(E)}{8} + \mathcal{O}(\Delta^4) \ , \tag{20}$$

$N = (u + \Delta, v + \Delta)$, $W = (u + \Delta, v)$, $E = (u, v + \Delta)$, $S = (u, v)$ and $S = (u + \Delta/2, v + \Delta/2)$.

After the integration is completed, the values $\psi_l(u_{max}, v)$ and $\psi_l(u, v_{max})$ are extracted, where u_{max} (v_{max}) is the maximum value of u (v) on the numerical grid. Taking sufficiently large u_{max} and v_{max}, we have good approximations for the wave function at the event and cosmological horizons.

Non-characteristc integration

$$\psi''(t,x) = \frac{\psi(t,x+2dx) - 16\psi(t,x+dx) + 30\psi(t,x) - 16\psi(t,x-dx) + \psi(t,x-2dx}{12dx^2} \tag{21}$$

$$\ddot{\psi}(t,x) = \frac{\psi(t+dt,x) - 2\psi(t,x) + \psi(t-dt,x)}{dt^2}. \tag{22}$$

$$E = \frac{1}{2}\int \left(\left(\psi'(t,x)\right)^2 + \left(\dot{\psi}(t,x)\right)^2 + V\psi(t,x)^2 \right) dx. \tag{23}$$

Exhaustive analysis of the asymptotic behavior

$$\begin{aligned} \psi(0,x) &= C_0 \exp\left[-\frac{(x-x_0)^2}{2\sigma_0^2}\right], \\ \dot{\psi}(0,x) &= C_1 \exp\left[-\frac{(x-x_1)^2}{2\sigma_1^2}\right]. \end{aligned} \tag{24}$$

Results do not depend on the details of initial conditions, are compatible with the ones obtained by the usual characteristic integration.

$\dot{\psi}(0,x)$ determines the asymptotic value for the $\ell = 0$ modes of scalar fields.

WKB analysis

$$\frac{d^2\psi(x)}{dx^2} - \left[s^2 + V(x)\right]\psi(x) = 0 \ . \tag{25}$$

$$\lim_{x\to-\infty} \hat{\psi}_\ell \, e^{sx} = 1 \ , \tag{26}$$

$$\lim_{x\to+\infty} \hat{\psi}_\ell \, e^{-sx} = 1 \ . \tag{27}$$

$s = i\omega$: usual quasinormal mode boundary conditions. ω (or s) are called quasinormal frequencies.

High order WKB approximation scheme: by

$$\omega_n = (V_0 + P) - i\left(n + \frac{1}{2}\right)\left(-2V_0^{(2)}\right)^{1/2}(1 + Q) \tag{28}$$

$$P = \frac{1}{8}\left[\frac{V_0^{(4)}}{V_0^{(2)}}\right]\left(\frac{1}{4} + \alpha^2\right) - \frac{1}{288}\left[\frac{V_0^{(3)}}{V_0^{(2)}}\right]^2\left(7 + 60\alpha^2\right) \ , \tag{29}$$

$$\begin{aligned} Q \ = \ & \frac{1}{-2V_0^{(2)}}\left\{\frac{5}{6912}\left[\frac{V_0^{(3)}}{V_0^{(2)}}\right]^4\left(77 + 188\alpha^2\right) - \frac{1}{384}\left[\frac{V_0^{(3)2}V_0^{(4)}}{V_0^{(2)}}\right]\left(51 + 100\alpha^2\right)\right. \\ & \left. + \frac{1}{2304}\left[\frac{V_0^{(4)}}{V_0^{(2)}}\right]^2\left(67 + 68\alpha^2\right) + \frac{1}{288}\left[\frac{V_0^{(3)}V_0^{(5)}}{V_0^{(2)2}}\right]\left(19 + 28\alpha^2\right)\right. \end{aligned}$$

$$- \frac{1}{288}\left[\frac{V_0^{(6)}}{V_0^{(2)}}\right]\left(5+4\alpha^2\right)\Bigg\} \tag{30}$$

$\alpha = n + 1/2$

Intermediary Region in Parameter Space

Scalar Fields with $\ell = 0$

Zero angular momentum sector.

Constant tail.

Fields with $\ell > 0$

We can have scalar and vector fields with angular momentum $\ell = 1$, and with $\ell > 1$.

Three phases confirmed.

Separation of the horizons increases: quasinormal frequencies deviate from those predicted before.

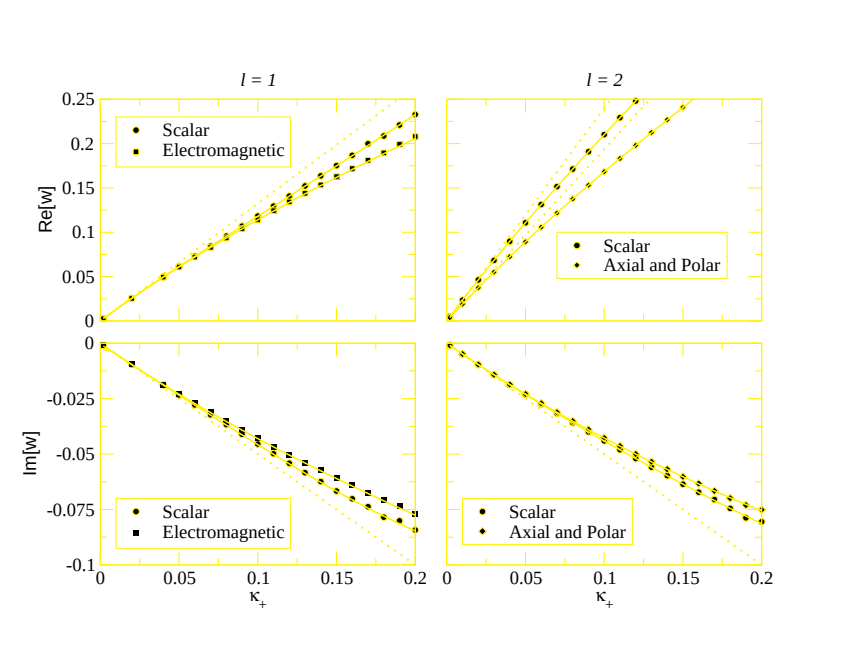

Figure 1: *Graph of the real and imaginary part of the fundamental frequencies* $(n = 0)$ *with* κ_+. *The dotted lines are the near extreme results, the symbols are the numerical results and the continuous curves are the semi-analytic results.*

Agreement is good, for the hole range of Λ.

In the table 1, we illustrate these observations with a few values of Λ.

		Numerical		Semi-analytical	
ℓ	Λ	Re(ω)	-Im(ω)	Re(ω)	-Im(ω)
1	1.000E-5	2.930E-01	9.753E-01	2.911E-01	9.780E-02
	1.000E-4	2.928E-01	9.764E-02	2.910E-01	9.797E-02
	1.000E-3	2.914E-01	9.726E-02	2.896E-01	9.771E-02
	1.000E-2	2.770E-01	9.455E-02	2.753E-01	9.490E-02
	1.000E-1	8.159E-02	3.123E-02	8.144E-02	3.137E-02
2	1.000E-5	4.840E-01	9.653E-02	4.832E-01	9.680E-02
	1.000E-4	4.833E-01	8.948E-02	4.830E-01	9.677E-02
	1.000E-3	4.816E-01	8.998E-02	4.809E-01	9.643E-02
	1.000E-2	4.598E-01	8.880E-02	4.592E-01	9.290E-02
	1.000E-1	1.466E-01	3.068E-02	1.466E-01	3.070E-02

Table 1: *Fundamental frequency ($n = 0$) of the scalar field, obtained using the numerical and semi-analytical methods.*

		Numerical		Semi-analytical	
ℓ	Λ	Re(ω)	-Im(ω)	Re(ω)	-Im(ω)
1	1.000E-5	2.481E-01	9.226E-02	2.459E-01	9.310E-02
	1.000E-4	2.481E-01	9.223E-02	2.457E-01	9.307E-02
	1.000E-3	2.475E-01	9.176E-02	2.448E-01	9.270E-02
	1.000E-2	2.374E-01	8.839E-02	2.352E-01	8.896E-02
	1.000E-1	8.035E-02	3.027E-02	8.023E-02	3.033E-02
2	1.000E-5	4.577E-01	8.985E-02	4.571E-01	9.506E-02
	1.000E-4	4.575E-01	8.991E-02	4.569E-01	9.502E-02
	1.000E-3	4.559E-01	9.439E-02	4.551E-01	9.464E-02
	1.000E-2	4.371E-01	8.941E-02	4.364E-01	9.074E-02
	1.000E-1	1.458E-01	3.037E-02	1.458E-01	3.038E-02

Table 2: *Fundamental frequency ($n = 0$) of the electromagnetic field, obtained using the numerical and semi-analytical methods.*

		Numerical		Semi-analytical	
ℓ	Λ	Re(ω)	-Im(ω)	Re(ω)	-Im(ω)
2	1.000E-5	3.738E-01	8.883E-02	3.731E-01	8.921E-02
	1.000E-4	3.737E-01	8.880E-02	3.730E-01	8.918E-02
	1.000E-3	3.721E-01	8.850E-02	3.715E-01	8.888E-02
	1.000E-2	3.566E-01	8.538E-02	3.560E-01	8.572E-02
	1.000E-1	1.179E-01	3.020E-02	1.179E-01	3.023E-02

Table 3: *Fundamental frequency ($n = 0$) of the axial and polar gravitational fields, obtained using the numerical and semi-analytical methods.*

Higher modes cannot be obtained from the numerical solution, but can be calculated by the semi-analytical method. As the cosmological constant decreases, the real and imaginary parts of the frequencies increase, up to the limit where the geometry is asymptotically flat.

Behavior of the modes illustrated in figure 2. The behavior of the electromagnetic field is similar.

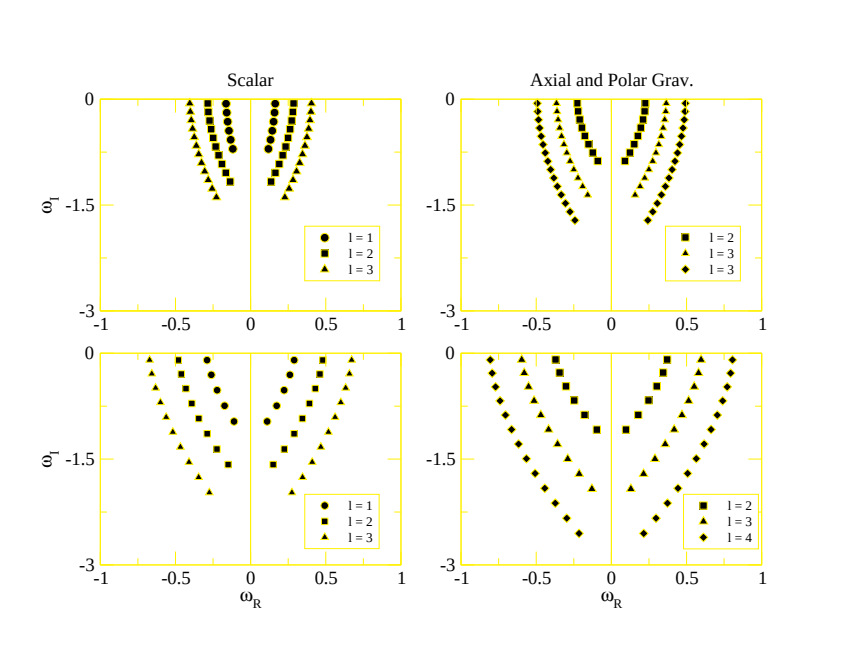

Figure 2: *Quasinormal modes of the scalar, axial and polar gravitational fields, for higher modes.*

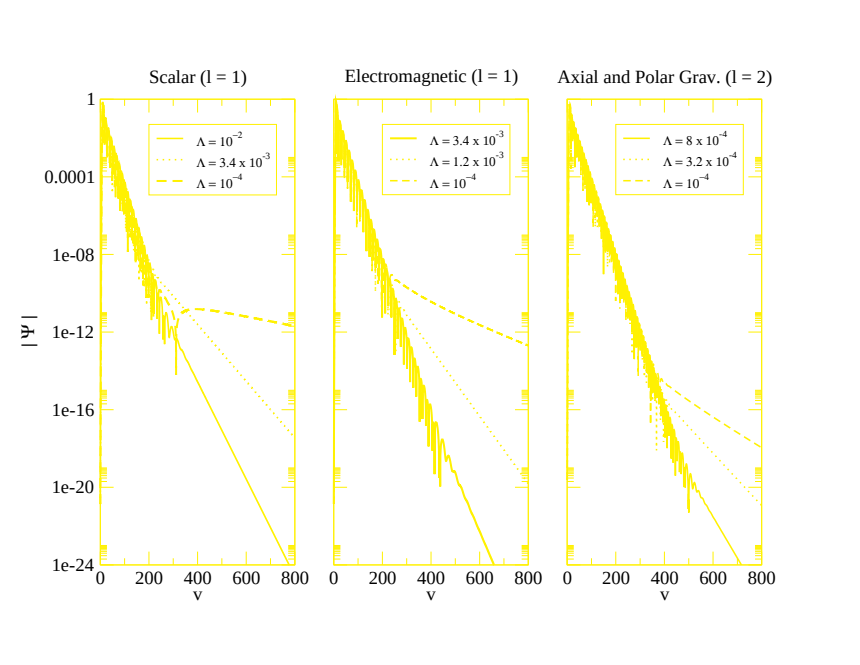

Figure 3: *Exponential tail for the scalar and electromagnetic fields with $\ell = 1$, and for the axial and polar gravitational field with $\ell = 2$.*

Figure 3 shows that the massless scalar, electromagnetic and gravitational perturbations in SdS geometry behave as

$$\psi_\ell^{es} \sim e^{-k_{exp}^{es} t} \quad \text{com} \quad t \to \infty \tag{31}$$

$$\psi_\ell^{el} \sim e^{-k_{exp}^{el} t} \quad \text{com} \quad t \to \infty \tag{32}$$

$$\psi_\ell^{ax} \sim e^{-k_{exp}^{ax} t} \quad \text{com} \quad t \to \infty \tag{33}$$

$$\psi_\ell^{po} \sim e^{-k_{exp}^{po} t} \quad \text{com} \quad t \to \infty \tag{34}$$

for t sufficiently large. At the event and the cosmological horizons t is substituted, respectively by v and u.

The numerical simulations: interesting transition between oscillatory modes and exponentially decaying modes.

As the cosmological constant decreases, the absolute value of $-\mathrm{Im}(\omega)$ decreases as well.

Up to a certain critical value of Λ we do not observe the exponential tail, since the coefficient k_{exp} is larger than $-\mathrm{Im}(\omega)$ thus the decaying quasinormal mode dominates.

For Λ smaller than this critical value, $-\mathrm{Im}(\omega)$ turns out to be larger than k_{exp} and the exponential tail dominates.

For a small enough cosmological constant the exponential tail dominates in the various cases considered here.

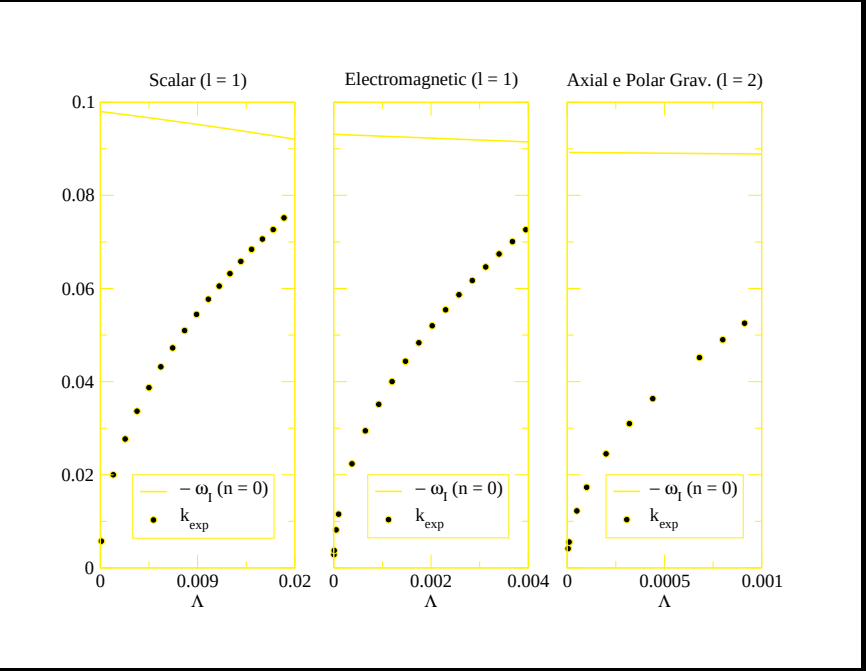

Figure 4: *Approaching of the constants $-Im(\omega)$ (fundamental mode) and k_{exp}, for the scalar, electromagnetic and gravitational fields.*

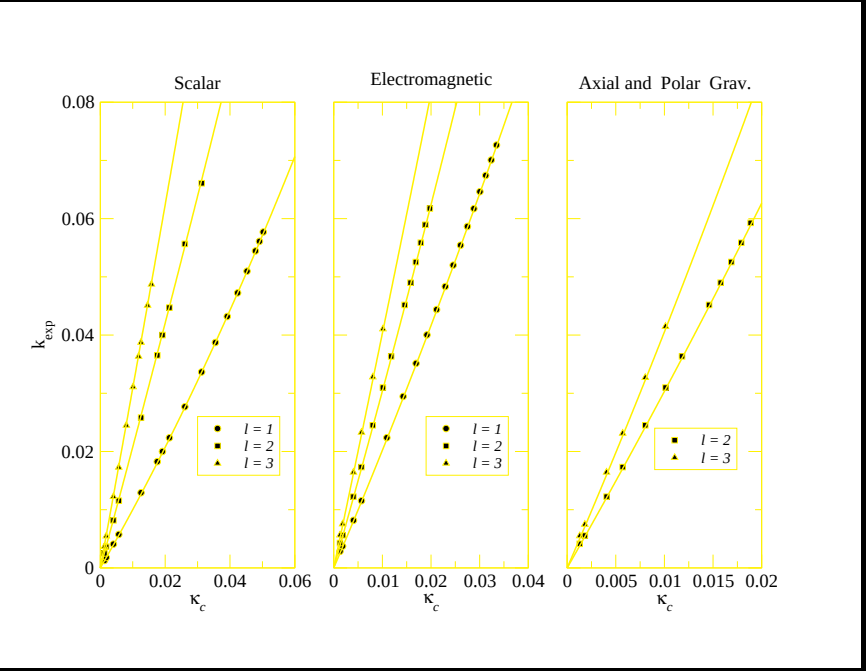

Figure 5: *Dependence of the coefficient k_{exp} with κ_c and ℓ. The symbols indicate the estimated numerical values. The solid lines are the appropriate quadratic fittings.*

Perturbations of Early Universe and Relics of Inflation

Not very much is known from the early universe prior to nucleosynthesis.

Cosmic Microwave Background is homogeneous to one part in a hundred thousand.

Absence of magnetic monopoles and flatness: before nucleosynthesis the universe underwent an epoch of high inflation.

The universe was filled with nothing but a scalar field.

A very strong expansion, increasing the overall sizes by at least sixty orders of magnitude.

Strings and Cosmology: New Methods

Likeliness of the inflationary scenario deepened by the COBE/WMAP experiments.

However, very little is known about a possible derivation of inflation from first principles.

Search of experimental support of string theory.

Both can find a meeting point, what would be a new era in the physics of fundamental objects.

The main calculations in inflationary models concern the density perturbations, or else its Fourier components $\delta_{\vec{k}}$. Its modulus squared, $|\delta_{\vec{k}}|^2$ defines the power spectrum, $\mathcal{P}(\vec{k})$, which is the main experimental data available from the CMB results.

Main Results from Standard Inflationary Models

Inflationary models: cornerstone for the understanding of the origin and evolution of large scale structure, of the large scale isotropy of the Microwave Background Radiation and of the flatness of the universe.

Describe the universe in terms of an unperturbed Friedmann equation, derived from a perfect fluid of the form

$$T^{\mu\nu} = pg^{\mu\nu} + (\rho + p)u^{\mu}u^{\nu} \tag{35}$$

ρ energy density, p pressure, u^{μ} fluid four-velocity. $u^{\mu} = \delta^{\mu}_{0}$

$$ds^2 = dt^2 - a^2(t)\delta_{ij}dx^i dx^j \quad . \tag{36}$$

Independent modes of perturbations: density, pressure and velocity fields, as well as pure perturbations of the metric, generating gravitational waves.

Friedmann equation:

$$H^2 = \frac{8\pi G}{3}\rho - \frac{K}{a^2} \tag{37}$$

$H = \frac{\dot{a}}{a}$ Hubble constant, K constant describing the curvature.

Perturbation: $\delta\rho$, δK describing the observed inhomogeneities. The spectrum pf perturbations is obtained, from the observational side, from the COBE/WMAP satelites describing the Cosmic Microwave Background.

Theoretical side: the large scale quasi-homogeneity of the universe is predicted by inflation.

Driven by a scalar field coupled to gravity, the inflaton field:

$$\begin{aligned} \rho &= \frac{1}{2}\dot{\varphi}^2 + V(\varphi) \\ p &= \frac{1}{2}\dot{\varphi}^2 - V(\varphi) \quad , \end{aligned}$$

$V(\varphi)$ is a potential for the inflaton.

$$\ddot{\varphi} + 3H\dot{\varphi} + V'(\varphi) = 0 \quad . \tag{38}$$

Inflation: the scale factor increses very fast, as $e.\ g.$ exponentially.

Potential is almost constant,kinetic energy is very small, giving rise to an effective cosmological constant, and a de Sitter like expantion. In such a slow roll approximation we define the very usefull parameters

$$\begin{aligned} \epsilon &\sim [V'/V]^2 \\ \eta &\sim [V''/V] \\ \zeta &\sim \frac{V'''V''}{V'^2} \end{aligned}$$

Slow roll approximation: parameters are very small, that is, we neglect the second derivative of φ obtaining

$$\dot{\varphi} \approx -\frac{1}{3H}V' \quad . \tag{39}$$

An observationally important parameter describes the deviation from scale invariance of the density perturbation, that is,

$$\delta^2 \approx k^{n-1} \quad \Rightarrow n-1 = \frac{d\ln\delta^2}{d\ln k} \quad . \tag{40}$$

In terms of the slow roll parameters

$$n = 1 + 2\eta - 6\epsilon \quad . \tag{41}$$

Observations give n near unit, somewhat larger than one at large scales, and smaller at small scales.

The junction conditions

The formulation of proper junction conditions at surfaces of discontinuity is a fundamental problem in gravitational theory. Well-known examples are the Schwarzschild and Oppenheimer-Snyder problems, which require the junction of the interior field of a static or collapsing star to the exterior vacuum field.

In newtonian theory the problem is directly solved by imposing the standard continuity and jump conditions connecting the potential and its first derivatives across the surface. In general relativity, however, the gravitational potential is not only determined by the smoothness of physical conditions but also by the smoothness of the coordinates we are using to describe spacetime.

A pioneering work on these subjects was made in 1922 by C. Lanczos; W. Israel based his landmark formalism forty years later.

G. Darmois derived junction conditions for the special case of a boundary surface, i.e. a surface through which both the metric and the extrinsic curvature tensor are continuous.

Darmois-Israel junction/thin-shell formalism, which has found wide application in general relativity and cosmology, including further studies of gravitational collapse, the evolution of bubbles and domain walls in a cosmological setting, wormholes and more recently in brane cosmology.

Junction formalism as it was first derived by Israel. We also derive the Darmois-Israel conditions from the gravitational action in the context of D-dimensional theories and give an alternative approach using distribution theory.

The Formalism

Spacetime M (riemannian manifold with signature $(-+++)$) with metric $g_{\alpha\beta}(x^\gamma)$ in the coordinate system (x^γ).

The absolute derivative of a smooth vector function $\mathbf{A}$ defined on a curve on this spacetime parametrized by t is given by

$$\nabla_t A^\alpha \equiv \frac{\partial A^\alpha}{\partial t} + A^\lambda \Gamma^\alpha_{\lambda\mu} \frac{dx^\mu}{dt} \,. \tag{42}$$

Let Σ be a smooth hypersurface in M with metric $g_{ij}(\xi^c)$ in the coordinates ξ^c, which separates M into two four-dimensional manifolds M^- and M^+, each containing Σ as part of its boundary.

The unit 4-normal $\mathbf{n}$ to this hypersurface in M labels Σ as timelike (spacelike) for $\epsilon(\mathbf{n}) \equiv \mathbf{n} \, . \, \mathbf{n} = -1 \, (1)$.

We define a natural frame of three linearly independent tangent vectors $e^{\alpha}_{(i)}$ associated with the intrinsic coordinates ξ^i as

$$e^{\alpha}_{(i)} = \frac{\partial x^{\alpha}}{\partial \xi^i}\,, \tag{43}$$

which gives the induced metric on Σ as

$$g_{ij} \equiv \mathbf{e}_{(i)} \,.\, \mathbf{e}_{(j)} = \frac{\partial x^{\alpha}}{\partial \xi^i}\frac{\partial x^{\beta}}{\partial \xi^j} g_{\alpha\beta}\,. \tag{44}$$

The intrinsic covariant derivative of $\mathbf{A}$ with respect to ξ^i is the projection of the vector $\partial\mathbf{A}/\partial\xi^j$ onto Σ,

$$A_{i;j} = \mathbf{e}_{(i)} \cdot \frac{\partial \mathbf{A}}{\partial \xi^j} = \frac{\partial A}{\partial \xi^j} - A_h \Gamma^h_{ij} \, . \tag{45}$$

Intrinsic covariant differentiation does not depend on the nature of the embedding.

Non-intrinsic character: the way in which Σ "bends" in M.

Measured by the variations $\partial\mathbf{n}/\partial\xi^i$ of the unit normal,

$$\partial\mathbf{n}/\partial\xi^i = K_i^j \mathbf{e}_{(j)}\,, \tag{46}$$

what defines the *extrinsic curvature 3-tensor* K_{ij} of Σ,

$$K_{ij} = e_{(j)} \cdot \frac{\partial \mathbf{n}}{\partial \xi^i} \equiv \frac{\partial x^\alpha}{\partial \xi^i}\frac{\partial x^\beta}{\partial \xi^j}\nabla_\alpha n_\beta = -n_\gamma \left(\frac{\partial^2 x^\gamma}{\partial \xi^i \partial \xi^j} + \Gamma^\gamma_{\alpha\beta}\frac{\partial x^\alpha}{\partial \xi^i}\frac{\partial x^\beta}{\partial \xi^j} \right)\,. \tag{47}$$

Let K^-_{ij}, K^+_{ij} be the extrinsic curvatures of Σ associated with its embeddings in M^-, M^+. If $K^-_{ij} \neq K^+_{ij}$, Σ is called a singular hypersurface of order one, $surface\ layer$ or $thin\ shell$. If $K^-_{ij} = K^+_{ij}$, Σ is called a hypersurface of higher order or $boundary\ surface$.

The Darmois conditions for the joining of M^- and M^+ through Σ are [66]

$$[g_{ij}] = 0\,, \tag{48}$$

$$[K_{ij}] = 0\,, \tag{49}$$

where $[X] = X^+ - X^-$ is the jump of X through the hypersurface Σ.

A boundary surface satisfies both equations, while a thin shell only satisfies (48). Condition (49) as it stands is ambiguous since the orientation of the 4-vector field $\mathbf{n}$ has not been specified. The Israel formalism will require the normals in M to point from M^- to M^+.

The majority of the existing literature deals with spherical symmetry where the direction of the normal is clear, but in more complicated cases great care must be taken.

The Israel formulation of thin shells follows from the Lanczos equation

$$[K_{ij}] - g_{ij}[K^a_a] = -8\pi G S_{ij}\,, \tag{50}$$

or equivalently

$$[K_{ij}] = -8\pi G(S_{ij} - \frac{1}{2}g_{ij}S)\,, \tag{51}$$

where S_{ij} is the surface stress-energy tensor of Σ.

By regarding a thin shell as the limit of a layer of uniform finite thickness ϵ as $\epsilon \to 0$, we can give a heuristic justification for the name $surface\ stress\text{-}energy\ tensor$.

Let Σ^-, Σ^+ be the two boundary surfaces separating the finite layer from the regions M^-, M^+. In gaussian coordinates the equations of Σ^- and Σ^+ are $x^1 = 0$, $x^1 = \epsilon$.

In terms of the extrinsic curvature tensor and in the gaussian system of coordinates the Ricci tensor can be written as

$$ {}^4R_{ij} = \frac{\partial K_{ij}}{\partial x^1} + Z_{ij} \,, \tag{52} $$

where

$$ Z_{ij} = {}^3R_{ij} - K K_{ij} + 2K_i^p K_{pj} \,. \tag{53} $$

Integration of the Einstein field equations

$$R_{\alpha\beta} = -8\pi G(T_{\alpha\beta} - \frac{1}{2}g_{\alpha\beta}T)\,, \tag{54}$$

through the layer gives

$$-8\pi G\int_0^\epsilon (T_{ij} - \frac{1}{2}g_{ij}T)dx^1 = [K_{ij}] + \int_0^\epsilon Z_{ij}dx^1\,. \tag{55}$$

In the limit $\epsilon \to 0$ for fixed K^-_{ij}, K^+_{ij}, K_{ij} remains bounded inside the layer. Hence, the integral of Z_{ij} tends to zero. Comparing this result with (51) we see that

$$S_{ij} = \lim_{\epsilon\to 0}\int_0^\epsilon T_{ij}dx^1\,. \tag{56}$$

Thus, S_{ij} is the integral of Einstein's energy tensor through the thickness of the layer.

Matching Conditions from the Action

The problem of junction conditions in the context of D-dimensional theories.

Introduce the concept of $domain\ wall$. In a D-dimensional spacetime a domain wall can be defined as an extended object with $D-2$ spatial dimensions, which divides the spacetime in different domains. Here we will use this term to make reference to any $D-2$ brane moving in D dimensions.

Let M be a D-dimensional manifold containing a domain wall Σ, which splits M into two parts M^- and M^+. The metric must be continuous everywhere, while its derivatives must be continuous everywhere except on Σ. We will denote $\Sigma^\pm$ as being the two sides of Σ.

Varying the Einstein-Hilbert action in $M^{\pm}$,

$$\delta S_{EH} = -\frac{1}{2}\int_{\Sigma^{\pm}} d^{D-1}x\sqrt{-h}\, g^{MN} n^{P}(\nabla_{M}\delta g_{NP} - \nabla_{P}\delta g_{MN})\,, \qquad (57)$$

n_M is the unit normal pointing into $M^{\pm}$ and the induced metric on $\Sigma^{\pm}$ is given by the tangential components of the projection tensor $h_{MN} = g_{MN} - n_M n_N$.

If we contract the quantity in parenthesis with $n^M n^N n^P$, it vanishes, so we can replace g^{MN} by h^{MN}.

The expression (57) contains a normal derivative of the metric variation, which is discontinuous across Σ according to our initial hypothesis, so the contributions from $M^{\pm}$ will not necessarily cancel out.

It is necessary to add a Gibbons-Hawking boundary term on each side of the domain wall,

$$S_{GH} = -\int_{\Sigma^{\pm}} d^{D-1}x\sqrt{-h}\,K\,, \tag{58}$$

with K being the trace of the extrinsic curvature of Σ, *i.e.* $K = h^{MN}K_{MN}$ where $K_{MN} = h^{P}_{M}h^{Q}_{N}\nabla_{P}n_{Q}$.

The variation of this new term is

$$\delta S_{GH} = -\int_{\Sigma^{\pm}} d^{D-1}x\sqrt{-h}\,(\delta K + \frac{1}{2}Kh^{MN}\delta g_{MN})\,, \tag{59}$$

$$\delta K = -K^{MN}\delta g_{MN} - h^{MN}n^{P}(\nabla_{M}\delta g_{NP} - \frac{1}{2}\nabla_{P}\delta g_{MN}) + \frac{1}{2}Kn^{P}n^{Q}\delta g_{PQ}\,. \tag{60}$$

Thus, the total variation is

$$\delta S_{EH}+\delta S_{GH} = \int_{\Sigma^{\pm}} d^{D-1}x\sqrt{-h}\left[\frac{1}{2}h^{MN}n^{P}\nabla_{M}\delta g_{NP}+K^{MN}\delta g_{MN}- -\frac{1}{2}Kn^{M}n^{N}\delta g_{MN}-\frac{1}{2}Kh^{MN}\delta g_{MN}\right]. \quad (61)$$

The first term in the rhs of (61) can be written as

$$h^{MN}n^{P}\nabla_{M}\delta g_{NP}=\bar{\nabla}_{M}(h^{MN}n^{P}\delta g_{NP})+Kn^{M}n^{N}\delta g_{MN}-K^{MN}\delta g_{MN}\,, \quad (62)$$

$\bar{\nabla}$ is the covariant derivative associated to h.

We substitute this last result into (61):

$$\delta S_{EH} + \delta_{GH} = \frac{1}{2}\int_{\Sigma^{\pm}} d^{D-1}x\sqrt{-h}\,(K^{MN} - Kh^{MN})\delta g_{MN}\,. \qquad (63)$$

If the domain wall has an action given by

$$S_{dw} = \int_{\Sigma} d^{D-1}x\sqrt{-h}\, L_{dw}\,, \tag{64}$$

whose variation is

$$\delta S_{dw} = \int_{\Sigma} d^{D-1}x\sqrt{-h}\, t^{MN}\delta g_{MN}\,, \tag{65}$$

$t^{MN} \equiv \frac{2}{\sqrt{-h}}\frac{\delta S_{dw}}{\delta h_{MN}}$ is tangential to the domain wall; we can replace δh_{MN} by δg_{MN}.

Variation of the total action $S = S_{EH} + S_{GH} + S_{dw}$ gives the Darmois-Israel conditions

$$[K_{MN} - Kh_{MN}] = -t_{MN}\,, \tag{66}$$

where the brackets stand for the jump of K through the domain wall Σ.

Junction Conditions from Distribution Theory

The Darmois-Israel conditions describe the motion of the domain wall through the bulk. However, sometimes it will be required to have a static brane, in this case the Darmois-Israel conditions reduce to some relations between the energy density and pressure on the brane and the coefficients of the bulk metric. An alternative derivation of these relations can be done using distribution theory as follows.

Example: 5-dimensional bulk metric of the form

$$ds^2_{(5)} = -n^2(t,y)dt^2 + a^2(t,y)\gamma_{ij}dx^k dx^j + b^2(\tau,y)dy^2\,, \qquad (67)$$

γ_{ij} represents a maximally symmetric metric on the 3-brane located in $y = 0$ with $k = -1, 0, 1$ parametrizing the spatial curvature.

Stress-energy tensor in $G_{AB} = \kappa^2_{(5)} \mathcal{T}_{AB}$ can be written as

$$\mathcal{T}_{AB} = \hat{T}_{AB} + T_{AB} \, , \tag{68}$$

$\hat{T}_{AB}$ stress-energy tensor of the matter on the bulk.

T_{AB}: matter content on the brane,

$$T^A_B = \frac{\delta(y)}{b} diag(-\rho, p, p, p, 0) \quad . \tag{69}$$

ρ and p independent of the position on the brane in order to recover homogeneous cosmology.

$$\tilde{G}_{00} = 3\left\{\frac{\dot{a}}{a}\left(\frac{\dot{a}}{a}+\frac{\dot{b}}{b}\right)-\frac{n^2}{b^2}\left(\frac{a''}{a}+\frac{a'}{a}\left(\frac{a'}{a}-\frac{b'}{b}\right)\right)+k\frac{n^2}{a^2}\right\}, \quad (70)$$

$$\tilde{G}_{ij} = \frac{a^2}{b^2}\gamma_{ij}\left\{\frac{a'}{a}\left(\frac{a'}{a}+2\frac{n'}{n}\right)-\frac{b'}{b}\left(\frac{n'}{n}+2\frac{a'}{a}\right)+2\frac{a''}{a}+\frac{n''}{n}\right\}+$$

$$+\frac{a^2}{n^2}\gamma_{ij}\left\{\frac{\dot{a}}{a}\left(-\frac{\dot{a}}{a}+2\frac{\dot{n}}{n}\right)-2\frac{\ddot{a}}{a}+\frac{\dot{b}}{b}\left(-2\frac{\dot{a}}{a}+\frac{\dot{n}}{n}\right)-\frac{\ddot{b}}{b}\right\}-k\gamma_{ij}, \quad (71)$$

$$\tilde{G}_{05} = 3\left(\frac{n'}{n}\frac{\dot{a}}{a}+\frac{a'}{a}\frac{\dot{b}}{b}-\frac{\dot{a}'}{a}\right), \quad (72)$$

$$\tilde{G}_{55} = 3\left\{\frac{a'}{a}\left(\frac{a'}{a}+\frac{n'}{n}\right)-\frac{b^2}{n^2}\left(\frac{\dot{a}}{a}\left(\frac{\dot{a}}{a}-\frac{\dot{n}}{n}\right)+\frac{\ddot{a}}{a}\right)-k\frac{b^2}{a^2}\right\}, \quad (73)$$

In order to have a well defined geometry the metric must be continuous across the brane.

Derivatives with respect to y can be discontinuous in $y = 0$. Thus, there is a Dirac delta function in the second derivatives of the metric with respect to y.

$$a'' = \hat{a}'' + [a']\delta(y)\,, \tag{74}$$

$\hat{a}''$ stands for the non-distributional part of the second derivative of a, $[a']$ is the jump of the first derivative across $y = 0$,

$$[a'] = a'(0^+) - a'(0^-)\,. \tag{75}$$

Terms with a delta function appearing in the Einstein tensor must be matched to the distributional part of the stress-energy tensor in order to satisfy the Einstein's equations.

Matching the Dirac delta functions in the components (70) and (71):

$$\begin{aligned} \frac{[a']}{a_0 b_0} &= -\frac{\kappa_{(5)}^2}{3}\rho\,, \\ \frac{[n']}{n_0 b_0} &= \frac{\kappa_{(5)}^2}{3}(3p+2\rho)\,, \end{aligned} \tag{76}$$

0 means that the metric coefficients take their values on the brane.

This result is known as the *junction conditions* for a static brane embedded in a generic bulk.

Application of quantum cosmology:

an upper bound for the number of e-foldings

Motivated by the well-known example of black hole entropy, an influential holographic principle has put forward, suggesting that microscopic degrees of freedom that build up the gravitational dynamics actually reside on the boundary of space-time.

This principle developed to the Maldacena's conjecture on AdS/CFT correspondence and further very important consequences, such as Witten's identification of the entropy, energy and temperature of CFT at high temperatures with the entropy, mass and Hawking temperature of the AdS black hole.

We seek at a description of the powerful holographic principle in cosmological settings, where its testing is subtle.

The question of holography therein: for flat and open FLRW universes the area of the particle horizon should bound the entropy on the backward-looking light cone.

FLRW universe filled with CFT with a dual AdS description: Verlinde revealed that when a universe-sized black hole can be formed, an interesting and surprising correspondence appears between entropy of CFT and Friedmann equation governing the radiation dominated closed FLRW universes.

Generalization broader class of universes including a cosmological constant: Friedmann equation to Cardy formula holds for de Sitter closed and AdS flat universes.

However for the remaining de Sitter and AdS universes, the argument fails due to breaking down of the general philosophy of the holographic principle. In high dimensions, various other aspects of Verlinde's proposal have also been investigated in a number of works.

Further light on the correspondence Friedmann equation/Cardy formula for Randall-Sundrum.

CFT dominated universe as a co-dimension one brane with fine-tuned tension in a background of an AdS black hole, Savonije and Verlinde found the correspondence between Friedmann equation and Cardy formula for the entropy of CFT when the brane crosses the black hole horizon.

Confirmed for a brane-universe filled with radiation and stiff-matter, quantum-induced brane worlds and radially infalling brane.

The discovered relation between Friedmann equation and Cardy formula for the entropy shed significant light on the meaning of the holographic principle in a cosmological setting.

A general proof for this corresp. is still difficult at the moment.

Our motivation here is the use of the correspondence between the CFT gas and the Friedmann equation establishing an upper bound for the number of e-foldings during inflation.

Banks and Fischler: the problem of the number of e-foldings in a universe displaying an asymptotic de Sitter phase, as our own. As a result the number of e-foldings is not larger than 65/85 depending on the type of matter considered.

Here we reconsider the problem from the point of view of the entropy content of the Universe, and considering the correspondence between the Friedmann equation and Cardy formula in Brane Universes.

Upper Bound for e-foldings

The existence of an upper bound for the number of e-foldings has been discussed.

In general it is model dependent. Has been obtained in some very simple cosmological settings, while it is still difficult to be obtained in nonstandard models.

Using the holographic principle, the consideration of physical details connected to the universe evolution can be avoided. We have obtained the upper bound for the number of e-foldings for a standard FRW universe as well as non-standard cosmology based on the brane inspired idea of Randall and Sundrum models.

Metric

Starting point: the scalar factor.

Brane cosmology: Darmois-Israel.

$$ds_5^2 = -f dt^2 + f^{-1} dr^2 + r^2 d\Sigma_K^2, \tag{77}$$

$f = k + \frac{r^2}{L^2} - \frac{m}{r^2}$, L is the curvature radius of AdS spacetime. $k = 0, -1, +1$; $d\Sigma_k^2$ is the corresponding metric on the unit three dimensional section.

Black Hole Horizon

The black hole horizon is located at

$$r_H^2 = \frac{L^2}{2}(-k + \sqrt{k^2 + 4m/L^2}). \tag{78}$$

Relation between m and the Arnowitt-Deser-Misner (ADM) mass of the five dimensional black hole M is

$$M = \frac{3\omega_3}{16\pi G_5} m \tag{79}$$

ω_3 is the volume of the unit 3 sphere.

Metric on the Brane.

Here, the location and the metric on the boundary are time dependent. We can choose the brane time such that $\dot{r}^2 = f^2\dot{t}^2 - f$.

The metric on the brane is thus

$$ds_4^2 = -d\tau^2 + r^2(\tau)d\Sigma_3^2 \quad . \tag{80}$$

CFT on the Brane

The Conformal Field Theory lives on the brane, the boundary of the AdS hole.

Energy for a CFT on a sphere with volume $V = r^3\omega_3$: $E = \frac{L}{r}M$.

Density of the CFT energy

$$\rho_{CFT} = E/V = \frac{3mL}{16\pi G_5 a^4} = \frac{3m}{8\pi G_4 a^4} \quad . \tag{81}$$

Entropy.

Entropy of the CFT on the brane is equal to the Bekenstein-Hawking entropy of the AdS black hole:

$$S_{CFT}(4D) = S_{BH}(5D) = \frac{V_H}{4G_5}, \quad V_H = a_H^3 \omega_3 \quad . \tag{82}$$

The entropy density of the CFT on the brane is

$$\sigma = \frac{S}{V} = \frac{a_H^3 \omega_3}{4G_5} \frac{1}{a^3 \omega_3} \overset{G_5 = \frac{G_4 L}{2}}{=} \frac{a_H^3}{2G_4 L a^3} \quad . \tag{83}$$

From the matching conditions $\Rightarrow$ cosmological equations in the brane,

$$H^2 = -\frac{k}{r^2} + \frac{m}{r^4} - \frac{1-(\sigma/\sigma_c)^2}{L^2} \quad , \tag{84}$$

$\sigma_c = \frac{3}{8\pi G_5 L}$ is the critical brane tension.

Taking $\sigma = \sigma_c$, (84) reduces to Friedmann equation of CFT radiation dominated brane universe without cosmological constant.

If $\sigma > \sigma_c$ or $\sigma < \sigma_c$, the brane-world is a de Sitter universe or AdS universe, respectively. Using

$$\rho_{CFT} = E/V = \frac{3mL}{16\pi G_5 a^4} = \frac{3m}{8\pi G_4 a^4} \quad . \tag{85}$$

Friedmann equation can be written in the form

$$H^2 = -\frac{k}{a^2} + \frac{8\pi G_4}{3}\rho_{CFT} + \frac{\lambda}{3} \quad , \tag{86}$$

λ is the effective positive cosmological constant in four dimensions.

Using $\rho = \frac{9mL}{16\pi^2 a_H^3 a^4} S$ Friedmann equation becomes

$$(\dot{a})^2 + k - \frac{3G_4 mLS}{2\pi a_H^3 a^2} - \frac{\lambda}{3} a^2 = 0 \quad , \tag{87}$$

$i.\ e.$ movement of a mechanical nonrelativistic particle in a given potential.

For a closed universe there is a critical value for which there is no big crunch:

$$S < \frac{2\pi a_H^3 \lambda a^4}{9 G_4 m L} \overset{a \approx \lambda^{-1/2}}{\rightarrow} \frac{2\pi a_H^3 \lambda^{-1}}{9 G_4 m L} \quad . \tag{88}$$

The entropy in such a universe can be rewriten as

$$S = \sigma V = \frac{4}{3}\pi a^3 \frac{4\pi a_H^3 a}{3mL}\rho \tag{89}$$

at the end of inflation.

Take ρ: energy density during inflation, $\rho \sim \Lambda_I$.

Scale factor at the exit of inflation: $a \approx \Lambda_I^{-1/2} e^{Ne}$,

$\Lambda_I^{-1/2}$: apparent horizon during inflation,

$$N_e = \ln a + \frac{1}{2} \ln \Lambda_I \quad . \tag{90}$$

Using now (89) in (88) we get

$$a < (8\pi G_4 \Lambda_I \lambda)^{-1/4} \quad , \tag{91}$$

$$N_e < \frac{1}{4}\ln\frac{\Lambda_I}{\lambda} - \frac{1}{4}\ln(8\pi G_4) \approx 64 \quad , \tag{92}$$

where we used the usual values $\Lambda_I^{1/4} \approx 10^{16}$GeV and $\lambda^{1/4} \approx 10^{-3}$eV.

Brane corrections to Friedmann equation

$$H^2 = -\frac{k}{a^2} + \frac{8\pi}{3M_4^2}\rho + \frac{4\pi}{3M_4^2}\frac{\rho^2}{l} + \frac{\lambda_4}{3} \approx -\frac{k}{a^2} + \frac{4\pi}{3M_4^2}\frac{\rho^2}{l} + \frac{\lambda_4}{3} \quad , \qquad (93)$$

l is the brane tension; in the very high energy limit the ρ^2 term dominates.

Within the high-energy regime, the expansion laws corresponding to matter and radiation domination are slower than in the standard cosmology.

Slower expansion rates lead to a larger value of the number of e-foldings. However, the full calculation has not been obtained due to the lack of knowledge of this high-energy regime.

Energy density of the CFT and the entropy density relation:

$$\rho_{CFT} = \frac{3m}{8\pi G_4 a^4} \quad , \quad \sigma = \frac{a_H^3}{2G_4 L a^3} \quad ,$$
$$\rho = \frac{9mLS}{16\pi^2 a_H^3 a^4} \quad , \tag{94}$$

Substitute in the Friedmann equation, and

$$S^2 = \frac{256\pi^4 a_H^6 a^8 \rho^2}{81 m^2 L^2} < \frac{64\pi^3 l a_H^6}{243 G_4 m^2 L^2 \lambda^3}$$
$$a^8 < \frac{3l}{4\pi G_4 \rho^2 \lambda_4^3} \quad , \tag{95}$$

Era when the quadratic energy density is important:

$l < (1\mathrm{MeV})^4$.

$\Lambda_I \approx 10^{64}\mathrm{GeV}^4$ and $\lambda \approx 10^{-12}\mathrm{eV}^4$:

$$N_e < 75 \quad . \tag{96}$$

The number of e-foldings obtained is bigger than the value in standard FRW cosmology, which is consistent with the arguments in the literature (Liddle).

In summary: upper limit for the number of e-foldings based upon the arguments relating Friedmann equation and Cardy formula.

Standard FRW universe: agreement with literature.

Brane inspired cosmology in four dimensions: larger bound. The expansion laws are slower than in the standard cosmology, and result can again be considered to be consistent with the known arguments.

Holographic point of view avoids a complicated physics during the universe evolution and give a reasonable value for the upper bound of the number of e-foldings.

Shortcuts: Scenarios

Two kinds of scenarios:

1. Brane wall model based on the exact solution of Einstein Equations and boundary conditions, where the brane is a socalled domain wall embedded in a space-time containing a singularity (a type of black hole) and a cosmological constant.

2. Friedmann-Robertson-Walker type of membrane.

First Scenario

Gravitational action in a D-dimensional bulk with a scalar field, a bulk dilaton, a domain wall potential and a Gibbons-Hawking term,

$$S = \int_{bulk} d^D x \sqrt{-g} \left(\frac{1}{2} R - \frac{1}{2} (\partial \phi)^2 - V(\phi) \right) - \int_{dw} d^{D-1} x \sqrt{-h} ([K] + \hat{V}(\phi)) \,, \tag{97}$$

ϕ the bulk dilaton, K the extrinsic curvature, $V(\phi)$ and $\hat{V}(\phi)$ are bulk and domain wall potentials, g and h bulk and domain wall metrics.

The potentials are here considered to be of the Liouville type:

$$V(\phi) = V_0 e^{\beta \phi} \,, \tag{98}$$

$$\hat{V}(\phi) = \hat{V}_0 e^{\alpha \phi} \,. \tag{99}$$

We consider the bulk metric as being static and invariant under rotation, being given by

$$ds^2 = -U(r)dt^2 + U(r)^{-1}dr^2 + R(r)^2 d\Omega_k^2\,, \tag{100}$$

$d\Omega_k^2$ is the line element on a $D-2$ dimensional space of constant curvature depending on a parameter k.

Considerations

We might also consider the brane to have a static metric, in which case the solution of the bulk would be more complicated.

Metric has mirror symmetry Z_2.

Useful for Darmois-Israel conditions.

$$K_{MN} = -\frac{1}{2(D-2)}\hat{V}(\phi)h_{MN} \quad . \tag{101}$$

$$K_{MN} = h^P_M h^Q_N \bigtriangledown_P n_Q \quad , \tag{102}$$

$$n_M = \frac{1}{\sqrt{U - \frac{\dot{r}^2}{U}}}(\dot{r}\,, -1\,, 0 \ldots, 0)\,. \tag{103}$$

The ij component of boundary condition:

$$\frac{R'}{R} = \frac{\hat{V}(\phi)}{2(D-2)U}\sqrt{U - \frac{\dot{r}^2}{U}}\,, \tag{104}$$

00 component is

$$\left(\frac{R'}{R}\right)^{-1}\left(\frac{R'}{R}\right)' = \frac{\hat{V}'(\phi)}{\hat{V}(\phi)} - \frac{R'}{R}\,. \tag{105}$$

The equation of motion for the dilaton can be solved

$$\phi(r) = \phi_\star - \frac{\alpha(D-2)}{\alpha^2(D-2)+1}\log r\,, \tag{106}$$

$$R(r) = (\alpha^2(D-2)+1)C\hat{V}_0 e^{\alpha\phi_\star} r^{\frac{1}{\alpha^2(D-2)+1}}\,, \tag{107}$$

$\phi_\star$ and C are arbitrary integration constants.

The motion of the domain wall is governed by the ij component of the Darmois-Israel conditions (104). That equation can be written in terms of the brane proper time τ as

$$\frac{1}{2}\left(\frac{dR}{d\tau}\right)^2 + F(R) = 0\,. \tag{108}$$

The induced metric on the domain wall is Friedmann-Robertson-Walker describes the evolution of the scale factor $R(\tau)$.

This equation is the same as that one for a particle of unit mass and zero energy rolling in a potential $F(R)$ given by

$$F(R) = \frac{1}{2} U R'^2 - \frac{1}{8(D-2)^2} \hat{V}^2 R^2 \, . \tag{109}$$

Solution only exists when $F(R) \leq 0$.

Induced domain wall metric: relation between the time parameter on the brane (τ) and in the bulk (t),

$$dt = \frac{\sqrt{U + \left(\frac{dr}{d\tau}\right)^2}}{U} d\tau \ ,$$

$$\dot{r} \equiv \frac{dr}{dt} = \frac{dr}{d\tau}\frac{d\tau}{dt} = \frac{dr}{d\tau}\frac{U}{\sqrt{U + \left(\frac{dr}{d\tau}\right)^2}} \ , \tag{110}$$

$\frac{dr}{d\tau} = \frac{dR}{d\tau}\left(\frac{dR}{dr}\right)^{-1}$ can be obtained from (108).

(110) describes the motion of a domain wall in the static background as seen by an observer in the bulk.

Consider two points on the brane. In general, there are more than one null geodesic connecting them in the D-dimensional spacetime. The trajectories of photons must be on the brane and those of gravitons may be outside. We consider the shortest path for both photons and gravitons.

For the gravitons the geodesic equation is obtained from the bulk metric (static):

$$\ddot{r}_g + \left(\frac{1}{r_g} - \frac{3}{2}\frac{U'}{U}\right)\dot{r}_g^2 + \frac{1}{2}U\,U' - \frac{U^2}{r_g} = 0\,. \tag{111}$$

The solutions of (110) and (111) in terms of the bulk proper time t were obtained by means of a **MAPLE** program. Now we discuss the possibility of shortcuts in the cases of the various solutions describing different Universes defined by the domain wall solution.

Second Scenario

The bulk is a purely Anti-de-Sitter space-time of the form,

$$ds^2 = h(a)dt^2 - \frac{da^2}{h(a)} - a^2 d\Sigma^2,$$

$h(a) = k + \frac{a^2}{l^2}$, $l \sim 0.1mm$ is the Randall-Sundrum lenght scale and $d\Sigma^2$ represents the metric of the three dimensional spatial sections with $k = 0\ ,\ \pm 1$,

$$d\Sigma^2 = \frac{dr^2}{1 - kr^2} + r^2[d\theta^2 + \sin^2(\theta)d\phi^2].$$

The brane is localized at $a_b(\tau)$, where τ is the proper time on the brane. The unit vector normal to the brane is defined as (overdot and prime superscript denote differentiation with respect to τ and a respectively)

$$n = \dot{a}_b(\tau)dt - \dot{t}(\tau)da \quad . \tag{112}$$

The normalization of n implies the relation between the bulk time t and the brane time τ,

$$h(a_b)\dot{t}^2 - \dot{a_b}^2 h^{-1}(a_b) = 1 \tag{113}$$

and also the usual FRW expression for the distance in the brane ,

$$ds^2 = d\tau^2 - a_b^2 d\Sigma^2 \quad .$$

Junction Conditions:

$$K_{ij} = e_i^\alpha e_j^\nu \nabla_\alpha n_\nu \quad ,$$

$$\begin{aligned} K_{rr} &= -\frac{a_b h}{(1-kr^2)}\dot{t} \quad , \\ K_{\theta\theta} &= -a_b r^2 h\dot{t} \quad , \\ K_{\phi\phi} &= -a_b r^2 \sin^2(\theta) h\dot{t} \end{aligned}$$

$$K_{\tau\tau} = \frac{1}{h\dot{t}}\left(\ddot{a}_b + \frac{h'}{2}\right) \quad .$$

With a Z_2 symmetric configuration,

$$K_{ij} = \frac{1}{2}\kappa^2_{(5)}\left(S_{ij} - \frac{1}{3}h_{ij}S\right) \quad , \tag{114}$$

we relate the discontinuity in the second fundamental form through the brane and the energy momentum tensor in the brane, S_{ij}.

For an isotropic distribution of matter, as given by

$$S_{ij} = \epsilon_T u_i u_j - p_T(h_{ij} - u_i u_j) \quad , \tag{115}$$

$$\frac{d\epsilon_T}{d\tau} = -3\frac{\dot{a}_b}{a_b}(\epsilon_T + p_T)$$

$$\frac{\dot{a}_b^2}{a_b^2} + \frac{h}{a_b^2} = \frac{\kappa_{(5)}^4 \epsilon_T^2}{36} \quad .$$

Introduce an intrinsic non-dynamical energy density ϵ_0 defined by means of $\epsilon_T = \epsilon_0 + \epsilon$, $p_T = -\epsilon_0 + p$.

ϵ and p corresponds to the brane matter. Junction condition:

$$\frac{d\epsilon}{d\tau} = -3\frac{\dot{a}_b}{a_b}(\epsilon + p) \tag{116}$$

Modified Friedmann equation:

$$H^2 = \left(\frac{\dot{a}_b}{a_b}\right)^2 = \frac{\Lambda_4}{3} + \frac{1}{M_{Pl}^2}\left(\frac{\epsilon}{3} + \frac{\epsilon^2}{6\epsilon_0}\right) - \frac{k}{a_b^2} \quad ,$$

hierarchy

$$M_{PL}^{-2} = \frac{\kappa_5^4 \epsilon_0}{6} \tag{117}$$

cosmological constant in the brane

$$\frac{\Lambda_4}{3} = \left(\frac{\kappa_5^4 \epsilon_0^2}{36} - \frac{1}{l^2}\right). \tag{118}$$

Present density of the Universe is

$$\epsilon(0) = \Omega_0 \epsilon_c = \Omega_0 3 M_{PL}^2 H_0^2 \quad ,$$

Ω_0 is the ratio of the density and the critical density of the Universe.

Friedmann equation can be written as

$$H^2 = \frac{\Lambda_4}{3} + \Omega_0 H_0^2 \frac{a_{b0}^q}{a_b^q}\left(1 + \frac{\Omega_0}{4(1+\Lambda_4 l^2/3)}\frac{L_c^q}{a_b^q}\right) - \frac{k}{a_b^2} \quad , \tag{119}$$

where $L_c^q = a_{b0}^q l^2 H_0^2$.

Phases of evolution of the Universe

We thus verify that there exist three phases in the evolution of the Universe.

When $a_b >> L_c$ the linear term in the energy density prevails in the Friedmann equation, leading to the standard cosmology.

Because $H_0 l \sim 10^{-29}$ this happens in a redshift of $a_{b0}/a_b \sim 10^{15}$, much earlier than the nucleosynthesis.

For $a_b << L_c$ the Universe expands at a slower pace as compared to the standard model, $a_b \propto \tau^{1/q}$, and the quadratic term is the prevailing one. In an intermediate era where $a_b \sim L_c$, both phases coexist.

We see that all the cosmological information is already known: the position of the brane in the extra dimension, $a_b(\tau)$, is just the scale factor of the FRW metric and the junction conditions imply that the cosmological evolution of the brane is obtained by the usual energy conservation and the modified Friedmann equations.

We are particularly interested in the evolution of the brane with respect to the bulk. This relation can be obtained using

$$h(a_b)\dot{t}^2 - \dot{a_b}^2 h^{-1}(a_b) = 1 \tag{120}$$

and transforming from the time of the brane to the time of the bulk. The position of the brane can also be treated as a function of the bulk proper time satisfying

$$\frac{da_b}{dt} = \frac{da_b}{d\tau}\frac{d\tau}{dt} = \dot{a}_b(\tau)\frac{h(a_b)}{\sqrt{h(a_b) + \dot{a}_b(\tau)^2}} \quad .$$

Solutions of the Geodesic Equation for a Domain Wall

Type I Solutions We define the type I brane solutions as those for which $\alpha = \beta = 0$. Consequently, the potentials become cosmological constants. The solution also has a constant dilaton $\phi = \phi_0$. A simple rescaling in the metric leads us to

$$ds^2 = -U(R)dt^2 + U(R)^{-1}dR^2 + R^2 d\Omega_k^2 \, , \tag{121}$$

with

$$U(R) = k - 2MR^{-(D-3)} - \frac{2V_0}{(D-1)(D-2)}R^2 \, , \tag{122}$$

which corresponds to a topological black hole solution in D dimensions with a cosmological constant.

If the domain wall has positive energy density ($\hat{V}_0 > 0$), the relevant part of the bulk spacetime is $R < R(\tau)$, which is the region containing the singularity. If it has negative energy density ($\hat{V}_0 < 0$), the relevant part is $R > R(\tau)$, which is non-singular unless the wall reaches $R = 0$.

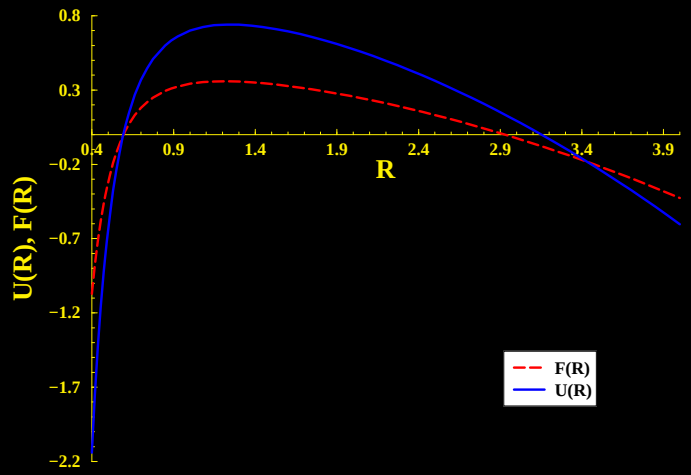

(a)

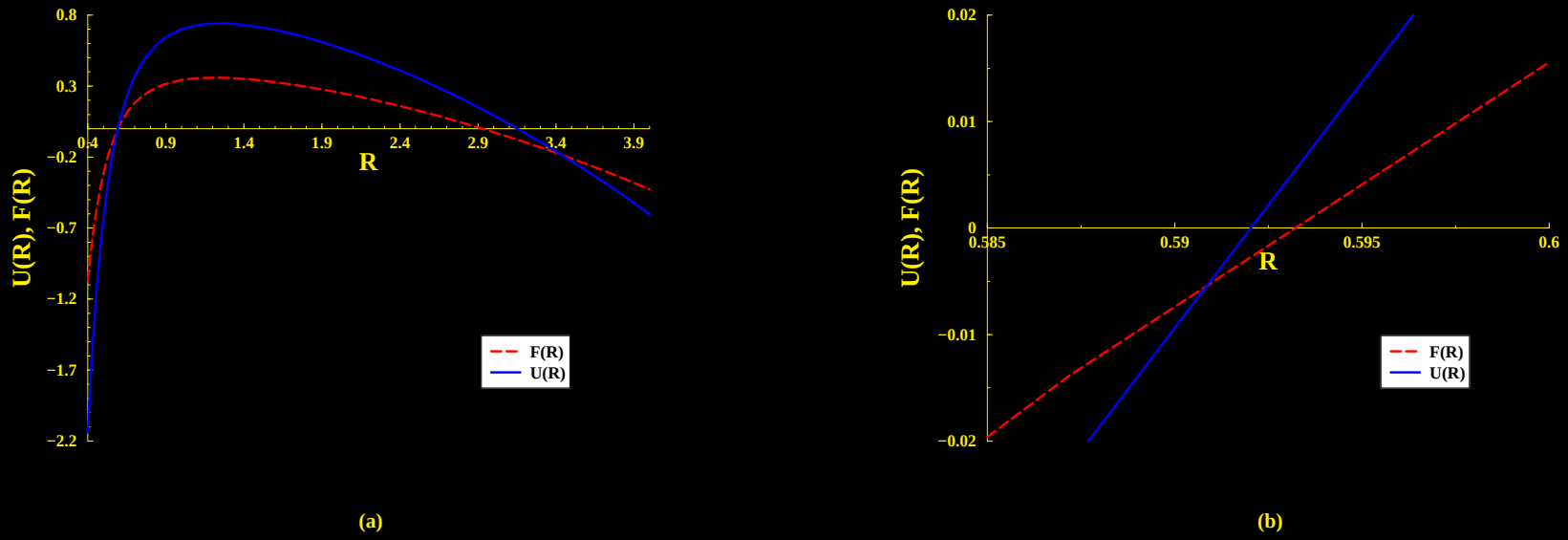

(a) $U(R)$ and $F(R)$ for type I solutions with $M = 1/10$, $V_0 = 1$ and $\hat{V}_0 = \pm 1$, (b) Zoom of the event horizon region.

[htb!]

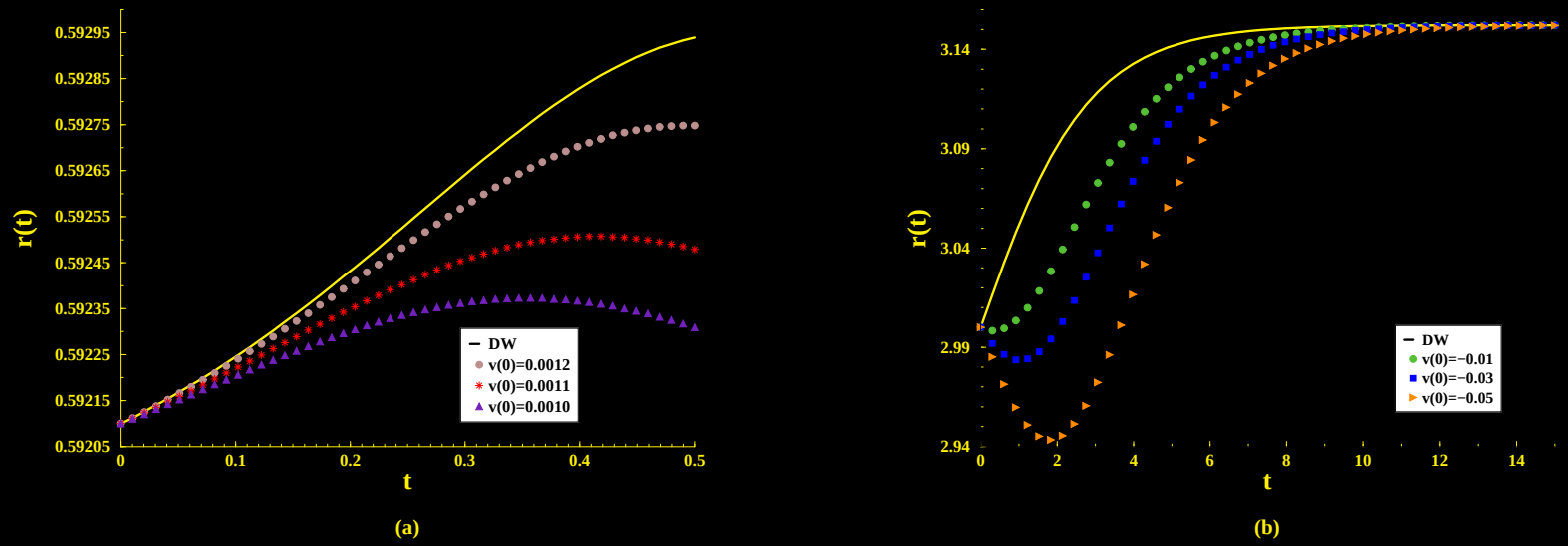

Domain wall motion and geodesics for type I solutions with $M = 1/10$, $V_0 = 1$ and $\hat{V}_0 = 1$ in (a) region I and, (b) region II.

[htb!]

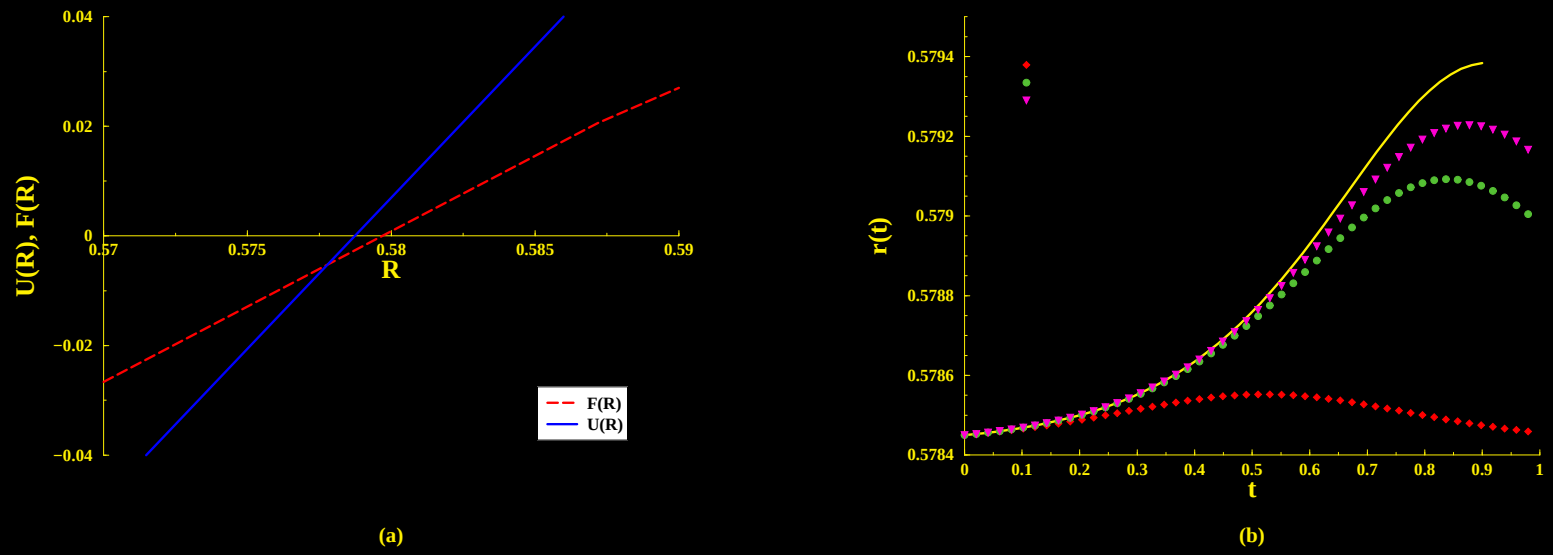

(a) Zoom of the region where (125) holds from the graph of $U(R)$ and $F(R)$ with $\hat{\Lambda} < 0$ and $M > 0$ for type I solutions, (b) Domain wall motion and geodesics for type I solutions with $M = 1/10$, $V_0 = -1$ and $\hat{V}_0 = 1$.

[htb!]

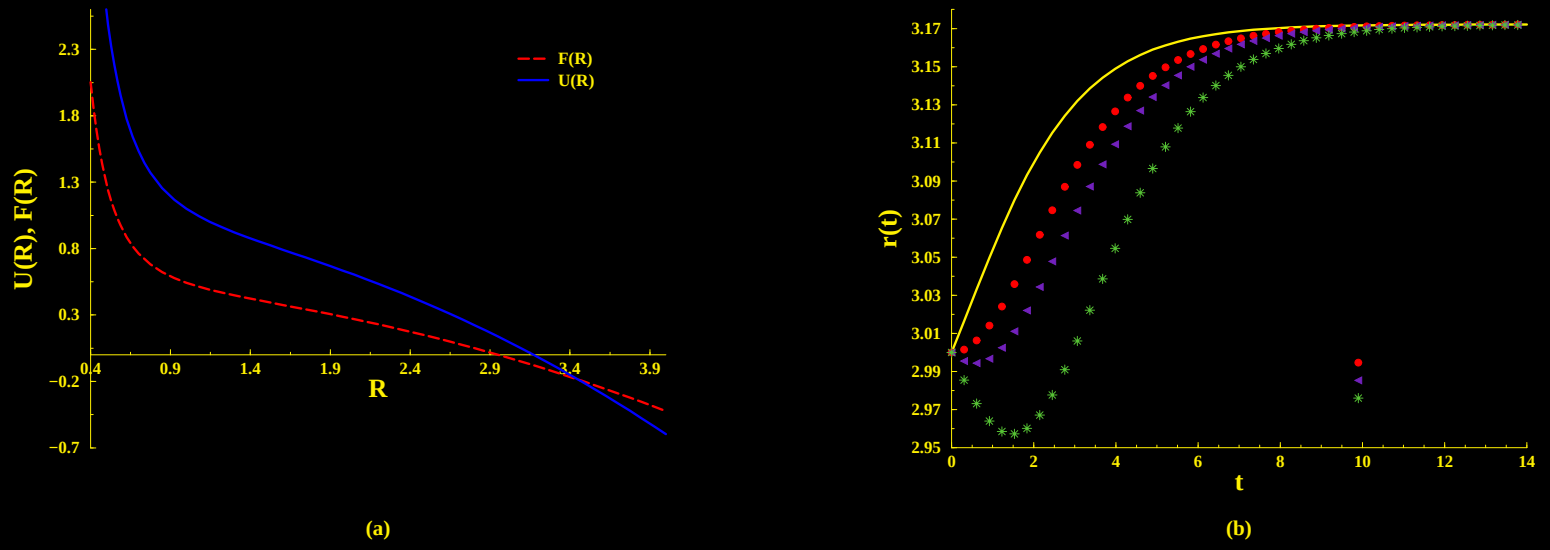

(a) (b)

(a) $U(R)$ and $F(R)$ with $\hat{\Lambda} > 0$ and $M < 0$ for type I solutions, (b) Domain wall motion and geodesics for $M = -1/10$, $V_0 = 1$ and $\hat{V}_0 = 1$.

[htb!]

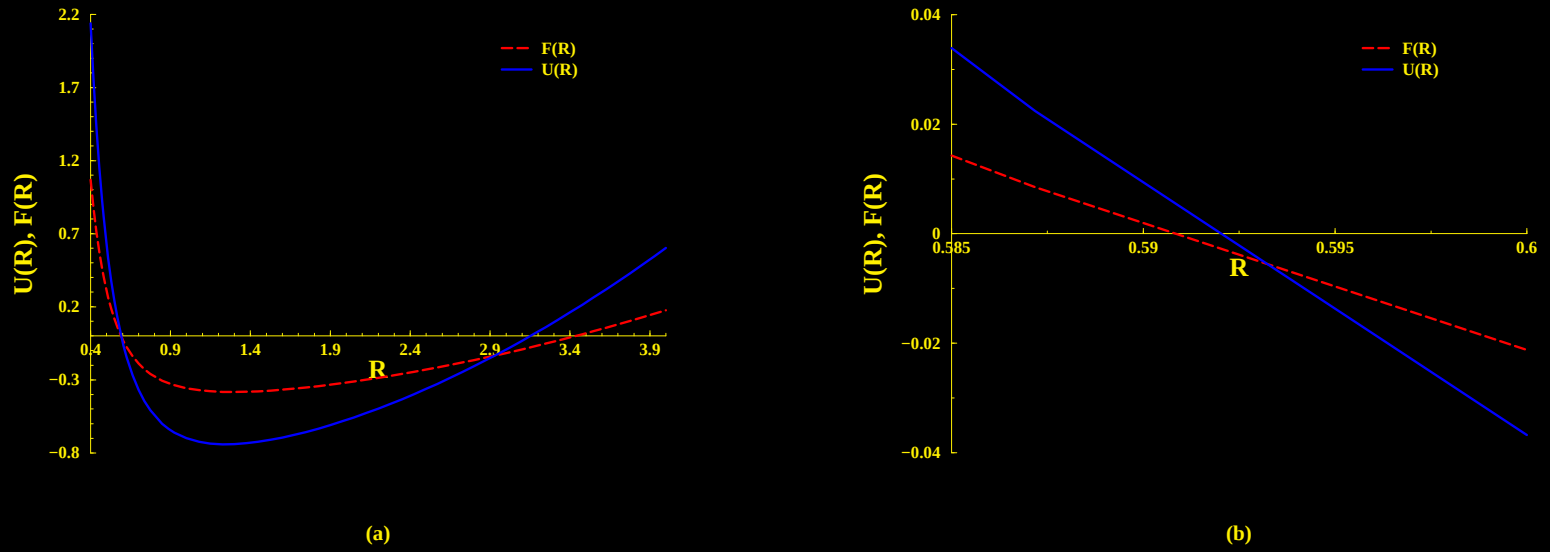

(a) $U(R)$ and $F(R)$ with $\hat{\Lambda} < 0$ and $M = -1/10$ for type I solutions, (b) Zoom of the event horizon region.

The potential $F(R)$ ruling the evolution of the scale factor is

$$F(R) = \frac{k}{2} - MR^{-(D-3)} - \hat{\Lambda}R^2\,, \tag{123}$$

where the effective cosmological constant on the domain wall is given by

$$\hat{\Lambda} = \frac{1}{D-2}\left[\frac{V_0}{D-1} + \frac{\hat{V}_0^2}{8(D-2)}\right]\,. \tag{124}$$

We shall analyze each of the four cases.

As we have previously stated, the equation of motion has a solution only when $F(R) \leq 0$. This is automatic only if $U(R) < 0$, $i.e.$ if r is a time coordinate; therefore, we look for solutions with $U(R) > 0$. In fact, both conditions,

$$F(R) \leq 0 \qquad \text{and} \qquad U(R) > 0\,, \tag{125}$$

can coexist in some cases as we will see in what follows. In order to ilustrate the following examples we have chosen $D = 6$ dimensions.

$\hat{\Lambda} > 0$, $M > 0$ From the graph of $U(R)$ (see Fig.6) we can choose the initial condition for the domain wall assuming that

$$U(R) = k - 2MR^{-(D-3)} - \frac{2V_0}{(D-1)(D-2)}R^2 \,,$$

describes a dS-Schwarzschild bulk with event and cosmological horizons when $M > 0$ and $V_0 > 0$.

We thus choose the initial condition for the domain wall inside this region and where r is a space coordinate. From Fig.6 let us notice that there are two small regions, $r_H \leq r < 0.593$ and $2.93 \leq r < r_C$, where (125) holds. The results are shown in Fig.7. We see that for region I the geodesics follow the domain wall for a while and then decouple falling into the event horizon. For region II all the geodesics and the domain wall converge to the cosmological horizon r_C independently of the value of $\hat{V}_0$.

$\hat{\Lambda} < 0,\ M > 0$ This case describes an AdS-Schwarzschild bulk. The condition (125) is fullfilled inside a very small range as we can see in Fig.8(a). However, all the geodesics fall into the event horizon after following some path on the brane (see Fig.8(b)).

$\hat{\Lambda} > 0,\ M < 0$ From Fig.9(a) we choose the initial condition for the domain wall equation of motion inside the region where (125) holds. As we can see from Fig.9(b), the domain wall and the geodesic converge to the cosmological horizon r_C. However, after some threshold initial velocity the geodesics diverge to the timelike naked singularity.

$\hat{\Lambda} < 0,\ M < 0$ In this case (108) can only have solution when $k = -1$. This is a topological black hole in an asymtotically AdS space. From Fig.10 we see that there is no solution fulfilling (125) between event and cosmological horizons.

Type II Solutions

[htb!]

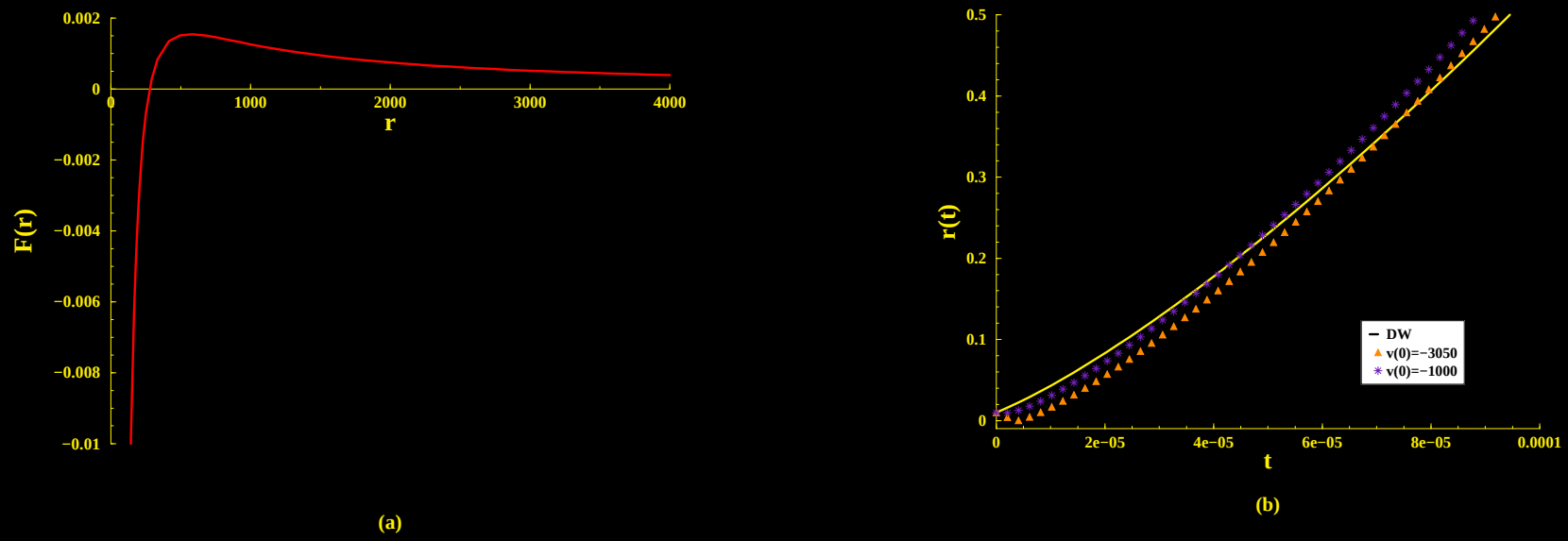

(a) $F(r)$ with $\hat{\Lambda} > 0$ and $M < 0$ for type II solutions, (b) Domain wall motion and geodesics for $V_0 = 1$, $\hat{V}_0 = 6$, $M = -10$ and $\beta = \sqrt{10}$.

[htb!]

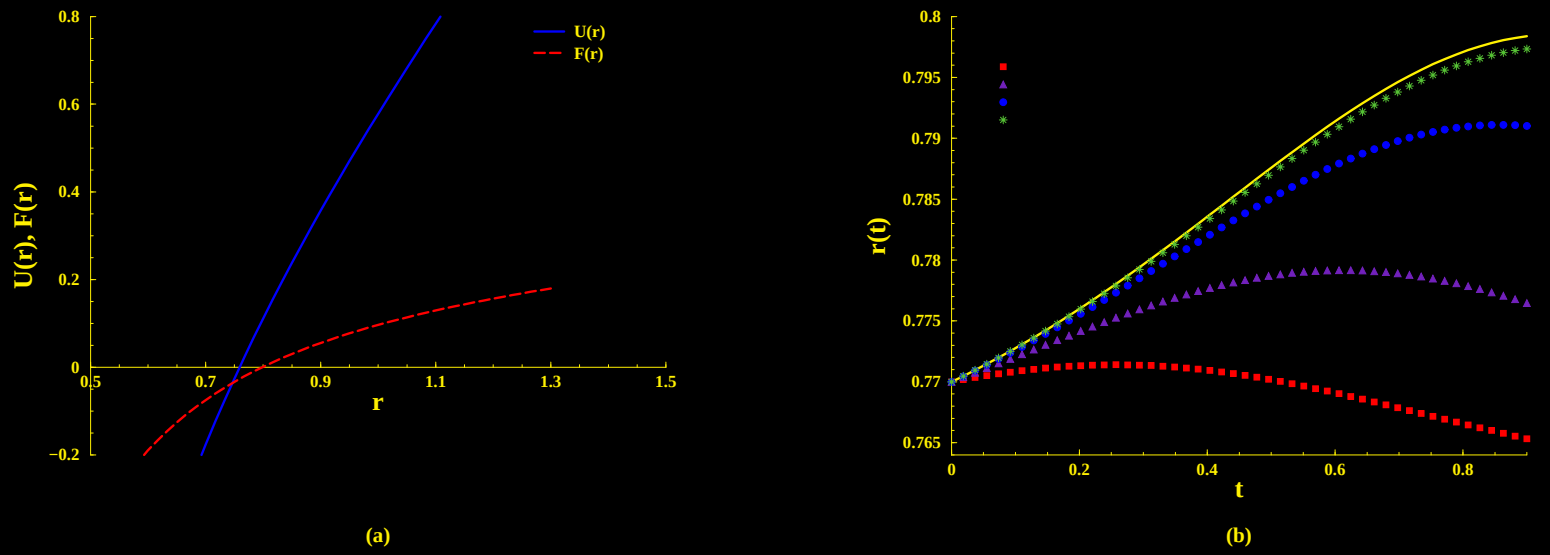

(a) $U(r)$ and $F(r)$ with $\hat{\Lambda} < 0$ and $M > 0$ for type II solutions, (b) Domain wall motion and geodesics for $V_0 = -1$, $\hat{V}_0 = 1$, $M = 1/10$ and $\beta = 1/\sqrt{2}$.

[htb!]

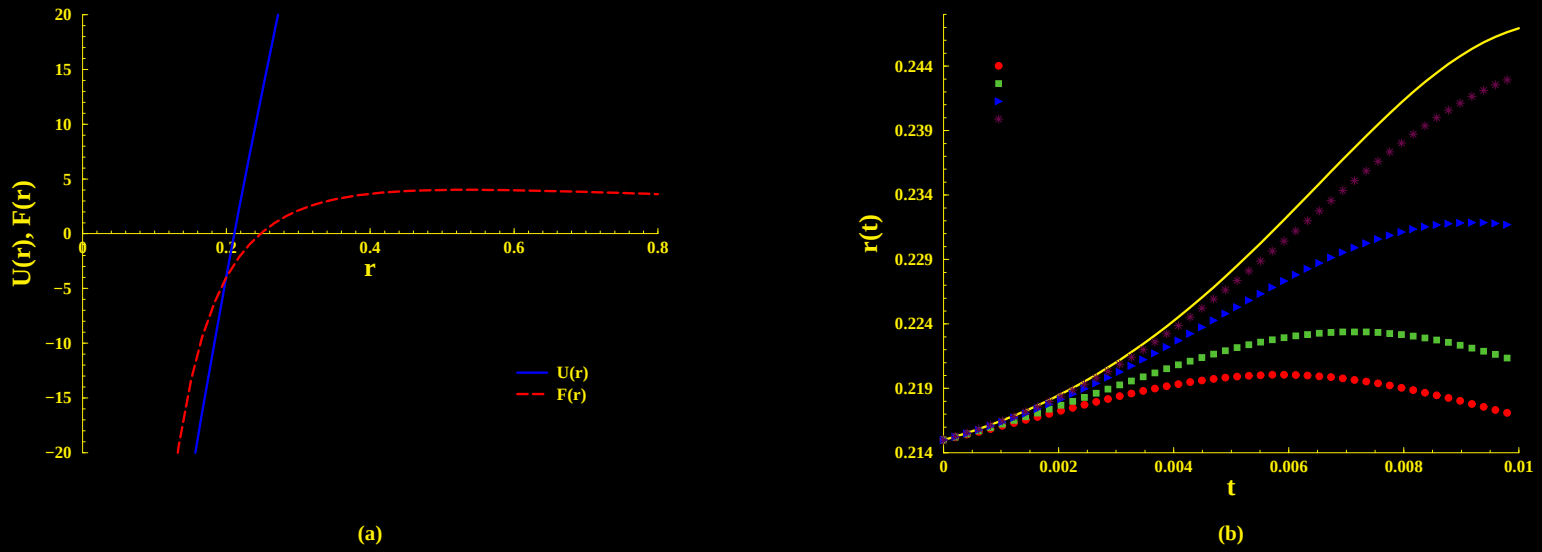

(a) $U(r)$ and $F(r)$ with $\hat{\Lambda} < 0$ and $M > 0$ for type II solutions, (b) Domain wall motion and geodesics for $V_0 = -1$, $\hat{V}_0 = 1$, $M = 10$ and $\beta = 2$.

The type II solutions have $\alpha = \beta/2$ and $k = 0$. The metric is given by

$$U(r) = (1+b^2)^2 r^{\frac{2}{1+b^2}} \left(-2Mr^{-\frac{D-1-b^2}{1+b^2}} - \frac{2\Lambda}{(D-1-b^2)} \right) , \tag{126}$$

and the scale factor is

$$R(r) = r^{\frac{1}{1+b^2}} , \tag{127}$$

where

$$\Lambda = \frac{V_0 e^{2b\phi_0}}{D-2} , \tag{128}$$

$$b = \frac{1}{2}\beta\sqrt{D-2} . \tag{129}$$

The potential is given by the expression

$$F(R) = -R^{2(1-b^2)}\left(MR^{-(D-1-b^2)} + \hat{\Lambda}\right) \ , \tag{130}$$

where

$$\hat{\Lambda} = \frac{e^{2b\phi_0}}{D-2}\left(\frac{V_0}{D-1-b^2} + \frac{\hat{V}_0^2}{8(D-2)}\right) \ . \tag{131}$$

There are twelve cases from which we choose those ones where r is a spatial coordinate. When $b^2 < D-1$, r is a spatial coordinate if $V_0 < 0$. When $b^2 > D-1$, r is spatial if $M < 0$.

We should also rewrite (125) as

$$F(r) \leq 0 \quad \text{and} \quad U(r) > 0\,. \tag{132}$$

$\hat{\Lambda} > 0,\ M < 0,\ b^2 > D-1$

In this case $U(r)$ is always positive, whereas $F(r)$ is negative for small r. From Fig.11 we see that some microscopic shortcuts appear in the very beginning of the solution and after crossing the domain wall they escape to infinity.

$\hat{\Lambda} < 0,\ M > 0,\ b^2 < 1$

This case describes a black $(D-2)$ brane solution in AdS space. Here there is a very small region where (132) holds after the event horizon as we can see from Fig.12. We show the entire domain wall solution and we see that geodesics follow it and then decouple to fall into the event horizon at later times.

$\hat{\Lambda} < 0,\ M > 0,\ 1 < b^2 < D-1$

This case is also a black brane in AdS space. The region where (132) is respected is shown in Fig.13. As in the previous case all the geodesics follow the domain wall and at later times fall into the event horizon.

$\hat{\Lambda} < 0,\ M < 0$

As $F(r)$ is always positive for all b^2, no solutions to (110) exist.

Type III Solutions

[htb!]

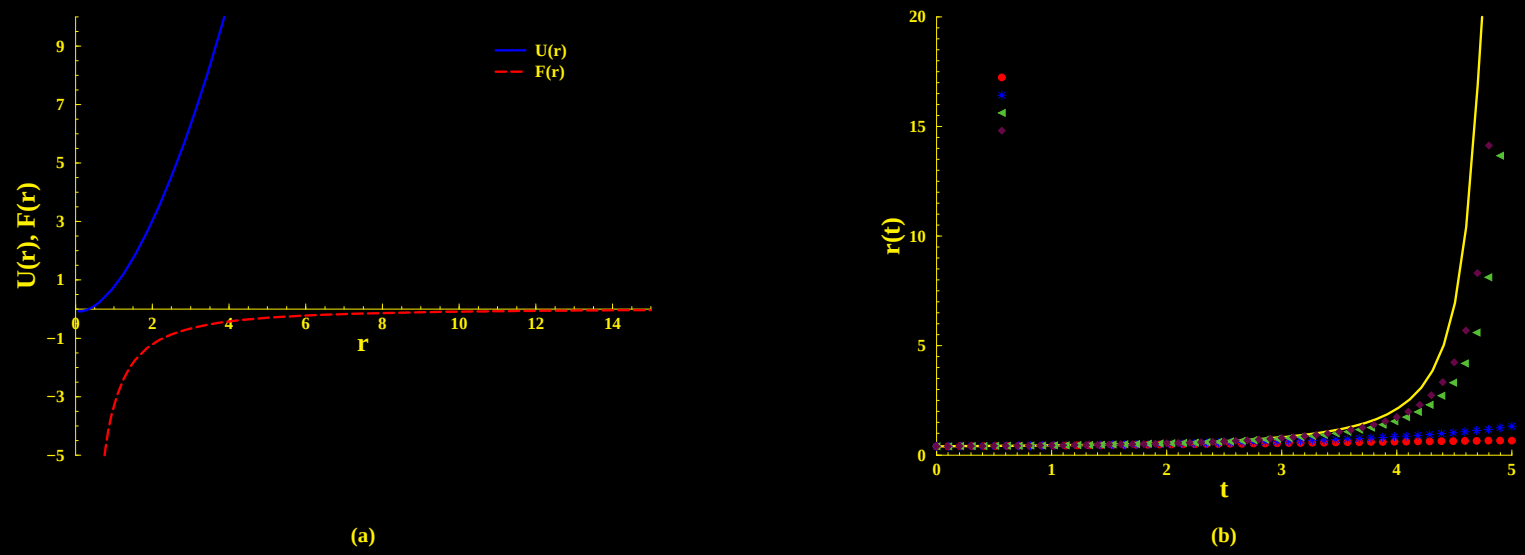

(a) $U(r)$ and $F(r)$ for Type III solutions with $k=-1$, $M=1/10$ and $\beta^2 < \frac{1}{(D-2)}$,
(b) Domain Wall motion and geodesics for $V_0=-1$, $\hat{V}_0=1$, $\phi_0=1$ and $\beta=1/\sqrt{6}$.

[htb!]

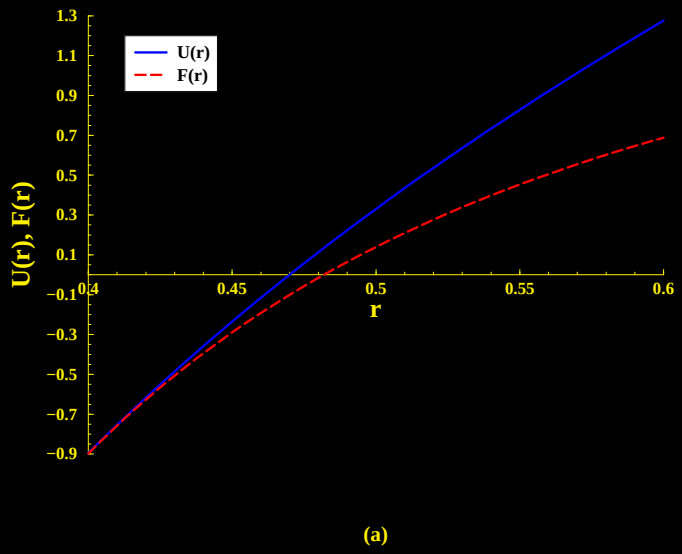

(a)

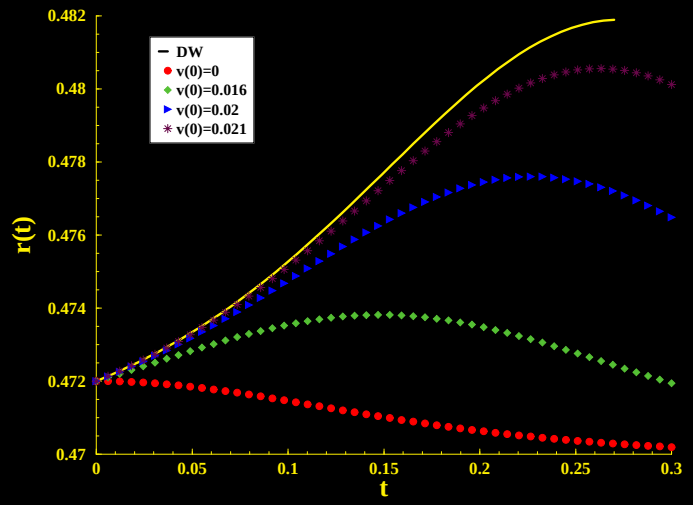

(b)

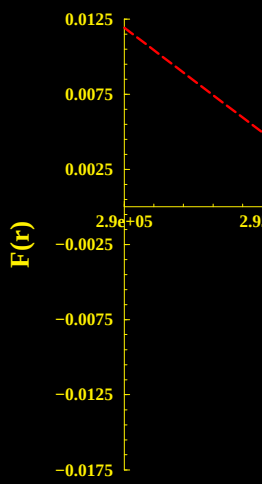

(a) $U(r)$ and $F(r)$ for $M = 1/10$ and $V_0 < 0$ in Type III solutions, (b) Domain wall motion and geodesics with $V_0 = -1$, $\hat{V}_0 = 1$, $\phi_0 = 1$ and $\beta = \sqrt{5}/2$, (c) $F(r)$ in the region of interest, (d) Domain wall motion and geodesics under the same conditions as (b).

[htb!]

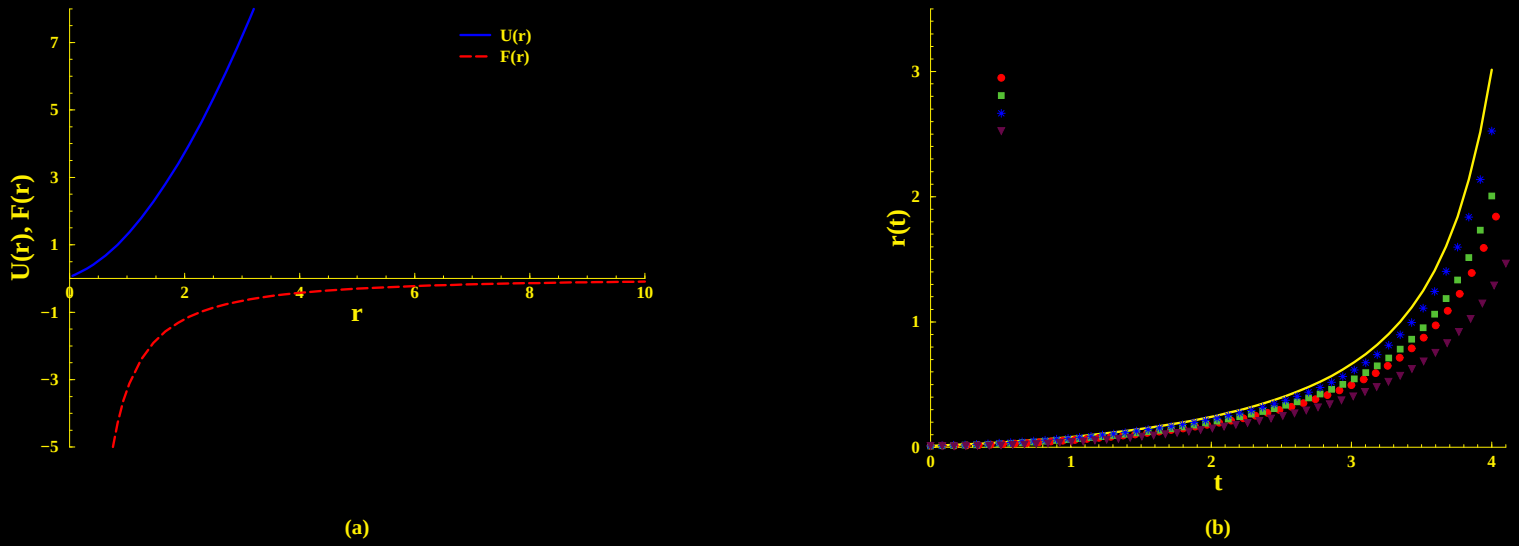

(a) $U(r)$ and $F(r)$ for type III solutions when $k=-1$, $M=-1/10$ and $b^2<\frac{1}{(D-2)}$,
(b) Domain wall motion and geodesics for $V_0=-1$, $\hat{V}_0=1$, $\phi_0=1$ and $\beta=1/\sqrt{6}$.

[htb!]

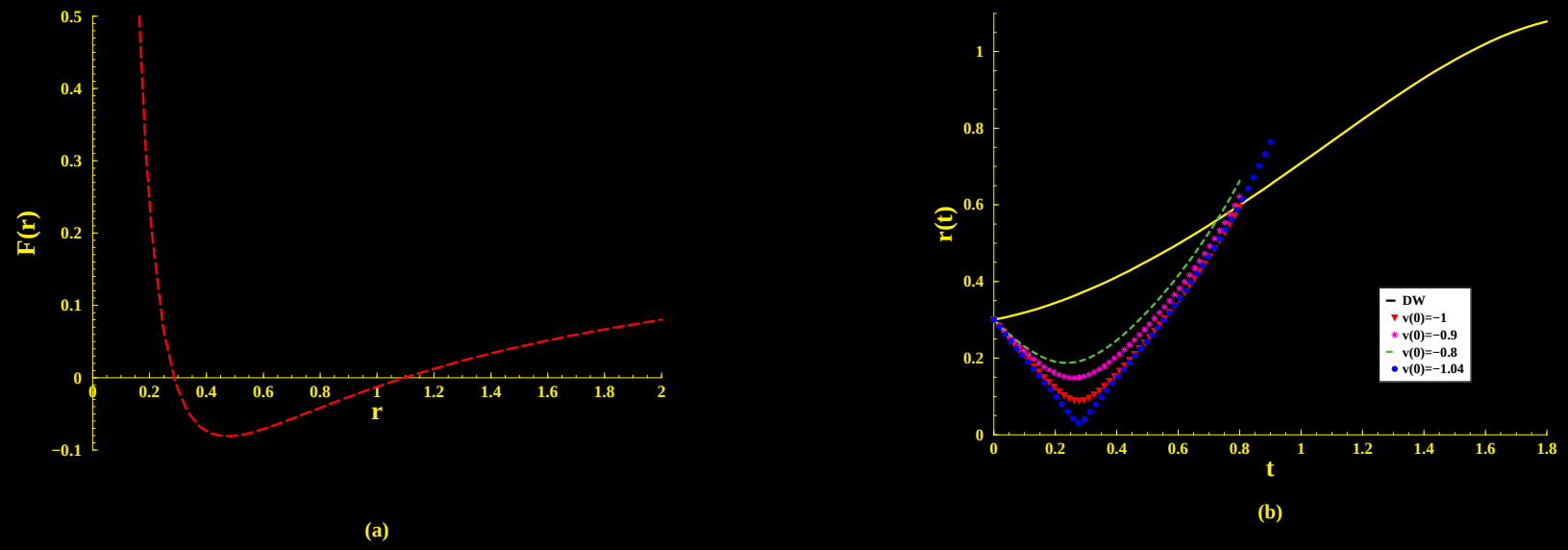

(a) $F(r)$ for type III solutions when $k=-1$, $M=-1/10$ and $\frac{1}{(D-2)}<b^2<1$, (b) Domain wall motion and geodesics for $V_0=-1$, $\hat{V}_0=1$, $\phi_0=1$ and $\beta=1/\sqrt{2}$.

[htb!]

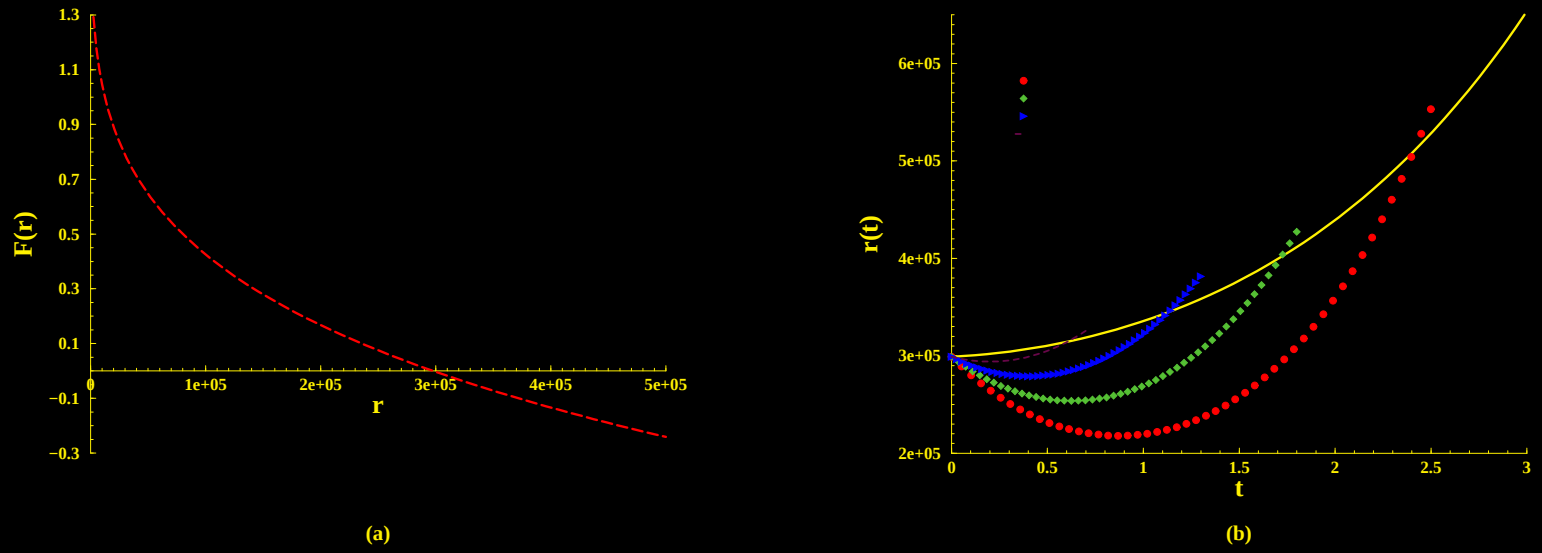

(a) $F(r)$ for type III solutions when $M = -1/10$ and $b^2 > 1$, (b) Domain wall motion and geodesics for $V_0 = -1$, $\hat{V}_0 = 1$, $\phi_0 = 1$ and $\beta = \sqrt{5}/2$.

The type III solutions have $\alpha = \frac{2}{\beta(D-2)}$. In this case, the metric is given by

$$U(r) = (1+b^2)^2 r^{\frac{2}{1+b^2}} \left(-2Mr^{\frac{-1+b^2(D-3)}{1+b^2}} - \frac{2\Lambda}{(1+b^2(D-3))} \right) , \tag{133}$$

scale factor

$$R(r) = \gamma r^{\frac{b^2}{1+b^2}} , \tag{134}$$

where

$$\gamma = \left(\frac{(D-3)}{2k\Lambda(1-b^2)} \right)^{\frac{1}{2}} . \tag{135}$$

The values of Λ and b are the same as those given in (128) and (129).

The potential $F(R)$ is

$$F(R) = -\frac{(D-3)b^4}{2k(1-b^2)(1+b^2(D-3))} - M\gamma^2 b^4 \left(\frac{R}{\gamma}\right)^{-\left(D-3+\frac{1}{b^2}\right)} - -\frac{\hat{V}_0^2 e^{\frac{2\phi_0}{b}}\gamma^2}{8(D-2)^2}\left(\frac{R}{\gamma}\right)^{-2\left(\frac{1}{b^2}-1\right)}. \quad (136)$$

If $V_0 > 0$, r turns out to be a time coordinate, while for $V_0 < 0$, it is a spatial coordinate.

From the twelve cases we choose those where it is a spatial coordinate. For all these solutions the condition (132) applies.

$V_0 < 0$, $M > 0$, $b^2 < \frac{1}{(D-1)}$ This case describes a topological black hole in AdS space. From Fig.14 we can see the region where (132) holds. There are no shortcuts in this interval, and all the geodesics follow the brane and then either diverge to infinity or fall into the event horizon.

$V_0 < 0$, $M > 0$, $\frac{1}{(D-1)} < b^2 < 1$ We again have a topological black hole in AdS space. There is a small interval where (110) has solution as we can see from Fig.15(a). Our results are shown in Fig.15(b). Notice that the domain wall equation of motion has a solution only inside the interval shown there. This means that only a group of geodesics with initial velocity $\dot{r}(0) > v_c$ can meet the domain wall after a roundabout in the bulk. It is also shown that negative initial velocities force geodesics to fall into the event horizon.

$V_0 < 0$, $M > 0$, $b^2 > 1$ The black hole in AdS space appearing here has round spatial section. In this case $U(r)$ is always positive (then r is always a spatial coordinate); however, as we must fulfill (132), we should notice that $F(r) \leq 0$ for $r \geq 3 * 10^5$. We found that shortcuts are possible for several initial velocities if $M = 0$.

The case $M > 0$ is shown in Fig.16. We have two regions of interest after the event horizon depending only on the sign of $F(r)$ since $U(r)$ is positive in this range. In the first region all the geodesics initially follow the brane and fall into the event horizon at later times. In the second region we have shortcuts again for several initial velocities.

$V_0 < 0$, $M < 0$, $b^2 < \frac{1}{(D-1)}$ Here $U(r)$ is always positive while $F(r)$ is negative in the range shown in Fig.17. The domain wall and the geodesics diverge after some time near the end of the range where (110) has a solution.

$V_0 < 0$, $M < 0$, $\frac{1}{(D-1)} < b^2 < 1$ In this case $U(r)$ is always positive while $F(r)$ is negative for a small range as seen in Fig.18. There are several shortcuts in the region where the domain wall equation of motion has solution; nevertheless, there is a threshold velocity after which the geodesics can not return. As we can notice from Fig.18(b), the last curve displayed here ($v(0) = -1.04$) can not be consider a real shortcut since it is not a continuous solution of the geodesic equation, but represents a transition between shortcuts and geodesics falling into the naked singularity.

$V_0 < 0$, $M < 0$, $b^2 > 1$ Now $U(r)$ is always positive and $F(r)$ will determine the initial condition for the domain wall equation of motion. As we can see from Fig.19, several shortcuts appear.

Domain Wall Time and Time Delays

The time delay between the photon traveling on the domain wall and the gravitons traveling in the bulk can be calculated as follows. Since the signals cover the same distance,

$$\int \frac{d\tau_\gamma}{r(\tau_\gamma)} = \int \frac{dt_g}{r_g(t_g)} \sqrt{U(r_g) - \frac{\dot{r}_g(t)^2}{U(r_g)}}, \tag{137}$$

The difference between photon and graviton time of flight can approximately be written as

$$\frac{\Delta\tau}{r} \simeq \int_0^{\tau_f+\Delta\tau} \frac{d\tau_\gamma}{r(\tau_\gamma)} - \int_0^{\tau_f} \frac{d\tau_g}{r(\tau_g)}\,, \tag{138}$$

In terms of the bulk time

$$\Delta\tau \simeq r(t_f)\int_0^{t_f} dt\left(\frac{1}{r_g(t)}\sqrt{U(r_g)-\frac{\dot{r}_g(t)^2}{U(r_g)}}-\frac{1}{r(t)}\frac{d\tau}{dt}\right)\,. \qquad (139)$$

The elapsed bulk time t, the corresponding domain wall time τ and the delays (139) are shown in Table 4 for all the shortcut examples considered in the present paper. Notice that $\Delta\tau < 0$ for the last geodesic solution in Fig.18 what, in fact, shows that this curve can not be considered a shortcut (it is probably falling into the naked singularity).

Type II Shortcuts			
Conditions	t	τ	$\Delta\tau$
Fig.11, $v(0) = -3050$	7.5×10^{-5}	0.0025	0.0466
Fig.11, $v(0) = -1000$	4.4×10^{-5}	0.0014	0.0027
Type III Shortcuts			
Fig.15, $v(0) = 0.145$	1.49	0.970	0.210
Fig.15, $v(0) = 0.140$	1.75	1.394	0.523
Fig.16, $v(0) = -5 \times 10^4$	0.58	353	3.51
Fig.16, $v(0) = -10^5$	1.11	683	26.6
Fig.16, $v(0) = -1.2 \times 10^5$	1.33	823	48.1
Fig.16, $v(0) = -1.5 \times 10^5$	1.69	1058	104
Fig.18, $v(0) = -0.8$	0.73	0.753	0.123
Fig.18, $v(0) = -0.9$	0.78	0.808	0.148
Fig.18, $v(0) = -1$	0.81	0.842	0.111
Fig.18, $v(0) = -1.04$	0.80	0.831	-0.129
Fig.19, $v(0) = -5 \times 10^4$	0.61	372	4.11
Fig.19, $v(0) = -10^5$	1.14	703	29.2
Fig.19, $v(0) = -1.5 \times 10^5$	1.72	1081	112
Fig.19, $v(0) = -2 \times 10^5$	2.42	1568	354

A Six-Dimensional Model

We consider a six-dimensional model, such as the one constructed by Kanti et. al. [72]. We also search for a solution of six-dimensional Einstein equation in AdS space of the form

$$ds^2 = -n^2(t,y,z)dt^2 + a^2(t,y,z)d\Sigma_k^2 + b^2(t,y,z)\left\{dy^2 + c^2(t,y,z)dz^2\right\} \quad (140)$$

where $d\Sigma_k^2$ represents the metric of the three dimensional spatial sections with $k = -1,\, 0,\, 1$ corresponding to a hyperbolic, a flat and an elliptic space, respectively.

The total energy-momentum tensor can be decomposed in two parts corresponding to the bulk and the brane as

$$\tilde{T}_N^M = \breve{T}_N^{M(B)} + T_N^{M(b)}\,, \quad (141)$$

where the brane contribution can be written as

$$T_N^{M(b)} = \frac{\delta(z-z_0)}{bc}\, diag\left(-\rho, p, p, p, \hat{p}, 0\right). \tag{142}$$

In order to have a well-defined geometry, the metric must be continuous across the brane; however, its derivatives with respect to z can be discontinuous at the position of the brane, generating a Dirac δ-function in the second derivatives of the metric with respect to z [81]. These δ function terms must be matched with the components of the brane energy-momentum tensor (142) in order to satisfy Einstein equations. Thus, we obtain the following Darmois-Israel conditions,

$$\begin{aligned}
\frac{[\partial_z a]}{a_0 b_0 c_0} &= -\frac{\kappa_{(6)}^2}{4}(p - \hat{p} + \rho)\,, \\
\frac{[\partial_z b]}{b_0^2 c_0} &= -\frac{\kappa_{(6)}^2}{4}\left\{\rho - 3(p - \hat{p})\right\}\,, \\
\frac{[\partial_z n]}{b_0 c_0 n_0} &= \frac{\kappa_{(6)}^2}{4}\left\{\hat{p} + 3(p + \rho)\right\}\,.
\end{aligned} \tag{143}$$

A metric of the form (140) satisfying six dimensional Einstein equations is given by

$$ds^2 = -h(z)dt^2 + \frac{z^2}{l^2}d\Sigma_k^2 + h^{-1}(z)dz^2\,, \tag{144}$$

where

$$d\Sigma_k^2 = \frac{dr^2}{1-kr^2} + r^2 d\Omega_{(2)}^2 + (1-kr^2)dy^2\,, \tag{145}$$

and

$$h(z) = k + \frac{z^2}{l^2} - \frac{M}{z^3} \quad , \quad \text{for AdS-Schwarzschild bulk}\,, \tag{146}$$

$$h(z) = k + \frac{z^2}{l^2} - \frac{M}{z^3} + \frac{Q^2}{z^6} \quad , \quad \text{for AdS-Reissner-Nordström bulk}\,, \tag{147}$$

with $l^{-2} \propto -\Lambda$ (Λ being the cosmological constant), which describes a black hole in the bulk, located at $z = 0$.

Following [12], we find a further solution by means of a Z_2 symmetry inverting the space with respect to the brane position. That is, considering a metric of the form

$$ds^2 = -A^2(z)dt^2 + B^2(z)d\Sigma^2_{(4)} + C^2(z)dz^2 \tag{148}$$

and the brane to be defined at $z = z_0$, there is a solution given by

$$\begin{aligned} A(z),\ B(z),\ C(z) \qquad\quad &, \quad \text{for} \quad z \leq z_0\,, \\ A(z_0^2/z),\, B(z_0^2/z),\, C(z_0^2/z)\tfrac{z_0^2}{z^2} \quad &, \quad \text{for} \quad z \geq z_0\,. \end{aligned} \tag{149}$$

The Z_2-symmetry corresponds to $z \to z_0^2/z$.

The static brane still has to obey the Darmois-Israel conditions (143), which for the metric (144) are written as

$$\begin{aligned} \frac{[\partial_z a]}{a_0^2 c_0} &= -\frac{\kappa_{(6)}^2}{4}\rho\,, \\ \frac{[\partial_z n]}{a_0 c_0 n_0} &= \frac{\kappa_{(6)}^2}{4}(4p+3\rho)\,, \end{aligned} \tag{150}$$

where here

$$\begin{aligned} [\partial_z a] &= -\frac{2}{l}\,, \\ [\partial_z n] &= -\frac{h'(z_0)}{\sqrt{h(z_0)}}\,. \end{aligned} \tag{151}$$

The Shortest Cut Equation

We consider the metric (140) with $k = 0$

$$ds^2 = -n^2(z)dt^2 + a^2(z)f^2(r)dr^2 + b^2(z)dy^2 + d^2(z)dz^2\,, \qquad (152)$$

where the graviton path is defined equating (152) to zero. Therefore,

$$\int_{r_0}^{r} f(r')dr' = \int_{t_0}^{t} \frac{\sqrt{n^2(z) - b^2(z)\dot{y}^2 - d^2(z)\dot{z}^2}}{a(z)}dt \equiv \int_{t_0}^{t} \mathcal{L}\left[y(t), \dot{y}(t), z(t), \dot{z}(t); t\right] dt \qquad (153)$$

which naturally defines a lagrangian density. The Euler-Lagrange equations of $\mathcal{L}$ define the graviton path. We first choose to work at a constant y to check on the very possibility of (152) allowing shortcuts. In this case the resulting equation is

simple but far from trivial,

$$\ddot{z} + \left(\frac{a'}{a} - 2\frac{n'}{n} + \frac{d'}{d}\right)\dot{z}^2 + \left(\frac{nn'}{d^2} - \frac{a'}{a}\frac{n^2}{d^2}\right) = 0\,. \tag{154}$$

For $z \leq z_0$, $a = z/l$, $n = \sqrt{h(z)}$, and $d = 1/\sqrt{h(z)}$. For $z \geq z_0$ we have to use the Z_2 symmetry showed up in (149).

Notice that this case is equivalent to consider the problem in five dimensions with the metric shown in [12].

The most general case includes a y dependence on the graviton path; however, as we will show in what follows, this dependence turns to be superflous and does not affect z-equation since (154) is independently satisfied. This conclusion is not surprising if we notice that the metric (152) is y-independent.

The two Euler-Lagrange equations considering a y dependence are then given by

$$(n^2-d^2\dot{z}^2)\ddot{y}+\dot{z}\left\{\left(-\frac{a'}{a}+2\frac{b'}{b}\right)(n^2-d^2\dot{z}^2)-nn'+\right.$$
$$\left.+dd'\dot{z}^2+d^2\ddot{z}\right\}\dot{y}+b^2\left(\frac{a'}{a}-\frac{b'}{b}\right)\dot{z}\dot{y}^3=0 \qquad (155)$$

and

$$(n^2-b^2\dot{y}^2)\ddot{z}+\left\{\left(\frac{a'}{a}+\frac{d'}{d}\right)(n^2-b^2\dot{y}^2)-2nn'+\right.$$
$$\left.+2bb'\dot{y}^2\right\}\dot{z}^2+(b^2\dot{y}\ddot{y})\dot{z}+$$
$$+\left\{-\frac{a'}{ad^2}(n^2-b^2\dot{y}^2)+\frac{nn'-bb'\dot{y}^2}{d^2}\right\}(n^2-b^2\dot{y}^2)=0\,. \qquad (156)$$

It is clear that the case $\dot{y}=0$ is a solution of this set of equations when at the same time z obeys (154).

This set of equations can be handled leading to

$$\begin{aligned}\frac{z\dot{z}\dot{y}}{h(z)}F_z+\left(h(z)-\frac{\dot{z}^2}{h(z)}\right)F_y &= 0\,,\\ \left(1-\frac{z^2\dot{y}^2}{h(z)}\right)F_z+\frac{z\dot{z}\dot{y}}{h(z)}F_y &= 0\,,\end{aligned}\tag{157}$$

where

$$\begin{aligned}F_y &= \ddot{y}+\dot{z}\left(\frac{2}{z}-\frac{h'(z)}{h(z)}\right)\dot{y}\,,\\ F_z &= \frac{\ddot{z}}{z}+\frac{\dot{z}^2}{z^2}\left(1-\frac{3}{2}z\frac{h'(z)}{h(z)}\right)+\frac{h(z)}{z}\left(\frac{h'(z)}{2}-\frac{h(z)}{z}\right)\,.\end{aligned}\tag{158}$$

Since the determinant of the set (157) is non-zero, the solutions of (155) and (156) must satisfy $F_y = 0$ and $F_z = 0$ independently. Furthermore, let us notice that $F_y = 0$ and $F_z = 0$ are the null geodesic equations for y and z respectively obtained from

$$\ddot{x}^\alpha + \Gamma^\alpha_{\mu\nu}\dot{x}^\mu\dot{x}^\nu = \lambda\dot{x}^\alpha \,. \tag{159}$$

Thus, a null curve is extreme if and only if it is a null geodesic.

Then, as (158) is the same as (154), our problem is reduced to the previous case with constant y described by (154).

For $k \neq 0$ cases we can also consider (154) as the shortcut equation if we assume the existence of a y-symmetry in our problem. In this way, our model represents a generalization of [12].

AdS-Schwarzschild Bulk

From the Darmois-Israel conditions (150) together with (151) we have

$$\frac{h}{z_0^2} = \frac{\kappa_{(6)}^4\rho^2}{64}, \tag{160}$$

$$\frac{h'}{2z_0} = -\frac{\kappa_{(6)}^4\rho^2}{64}(4\omega+3), \tag{161}$$

and we can obtain the black hole mass M as a function of the brane energy density ρ, while ρ is fixed by a *fine-tunning*,

$$\frac{M}{z_0^5} = \frac{2}{5}\frac{k}{z_0^2} - (\omega+1)\frac{\kappa_{(6)}^4\rho^2}{40}, \tag{162}$$

$$\frac{\kappa_{(6)}^4 \rho^2}{64} = -\frac{3k}{z_0^2(8\omega+3)} - \frac{5}{(8\omega+3)l^2}\,, \tag{163}$$

where $\omega = p/\rho$.

[htb!]

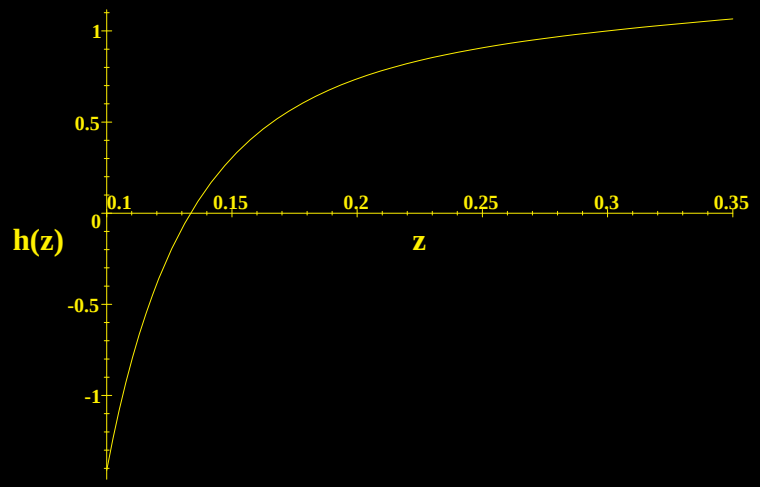

$h(z)$ in six-dimensional AdS-Schwarzschild bulk with the brane located at $z = 1/3$. Notice that the singularity is shielded by a horizon.

[htb!]

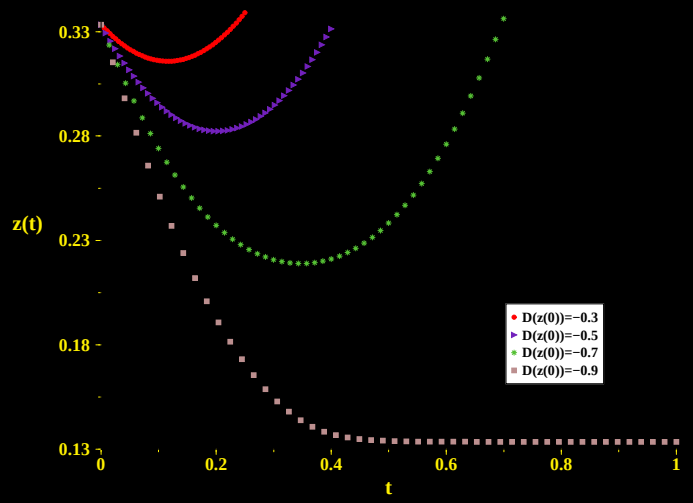

Shortcuts for several initial velocities in six-dimensional AdS-Schwarzschild bulk. Notice that there is a threshold initial velocity for which the graviton can not return to the brane and falls into the event horizon.

[htb!]

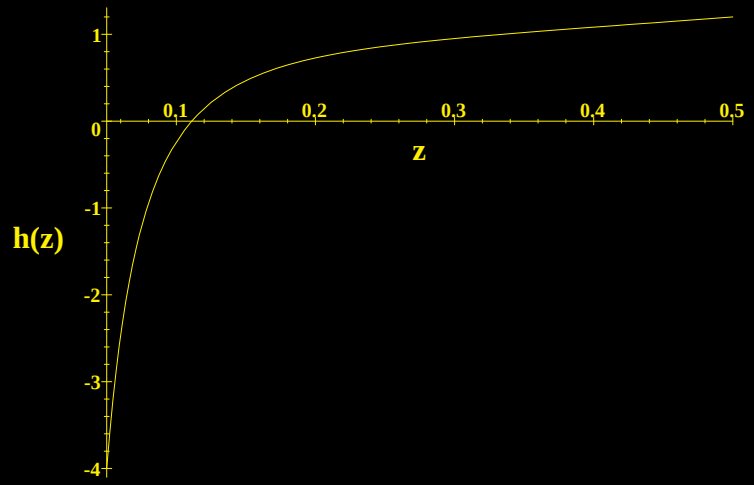

$h(z)$ in five-dimensional AdS-Schwarzschild bulk with the brane located at $z = 1/2$. Notice that the singularity is shielded by a horizon.

[htb!]

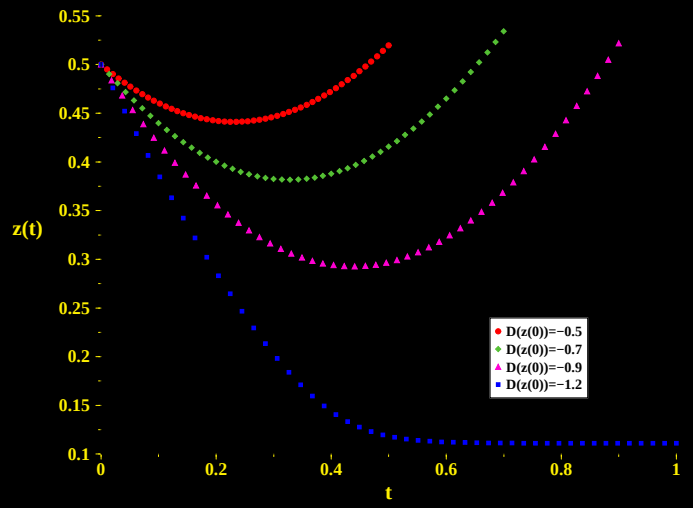

Shortcuts for several initial velocities in five-dimensional AdS-Schwarzschild bulk. As in the six dimensional case, there is a threshold initial velocity for which the graviton can not return to the brane and falls into the event horizon.

As we saw in the previous section, the shortcuts in six dimensions are determined from (154). We should also remember that the brane is static at $z = z_0$.

If a shortcut exists, there must be a time $t = v$ in the graviton path when $\dot{z}(v) = 0$ and $\ddot{z}(v) \geq 0$. Thus, (154) evaluated at this point will give

$$\ddot{z}(v) + h(z_v)\left(\frac{h'(z_v)}{2} - \frac{h(z_v)}{z_v}\right) = 0\,. \tag{164}$$

It is obvious that this minimum must be between the brane and the event horizon z_h, if a horizon exists. Otherwise, there is no turning point in the path since the graviton can not return after it goes through the event horizon. Hence, $h(z_v) > 0$. Thus, from (164) we require

$$F(z_v) = \frac{h'(z_v)}{2} - \frac{h(z_v)}{z_v} \leq 0 \quad \text{for} \quad z_h < z_v < z_0 \,. \tag{165}$$

Using (146) this implies

$$F(z_v) = \frac{5}{2}\frac{M}{z_v^4} - \frac{k}{z_v} \leq 0 \,. \tag{166}$$

This equation has a zero in $z = z_f \neq 0$ for $k \neq 0$

$$z_f^3 = \frac{5}{2k} M \,.$$

Thus, for the $k = 0$ or $k = -1$ cases there is no positive root. Since the mass, M, is positive, $F(z) > 0$ everywhere preventing the coexistence of shortcuts and horizons.

On the other hand, for $k=1$ there is one real and positive root, which must satisfy $z_f < z_0$ in order to have shortcuts. This is

$$\frac{5M}{2z_0^3} - 1 < 0\,.$$

Taking into account (162) and the fact that ε^2 must be positive in (163) [1]

$$-4(\omega+1)\varepsilon^2 z_0^2 < 0\,, \tag{167}$$

then

$$\omega + 1 > 0\,. \tag{168}$$

[1] From now on, we will denote $\varepsilon^2 = \kappa_{(6)}^4 \rho^2/64$ in six dimensions.

Now, let us study the conditions under which the event horizon must appear. In general, the horizons occur at the zeros of $h(z)$, or equivalently at the zeros of

$$z^5 + z^3 l^2 - l^2 M \,.$$

In the meantime, the non-vanishing zeros of $h'(z)$ occur when

$$2z^5 + 3l^2 M = 0 \,.$$

Since the derivative has no positive zeros with $M > 0$, there is just one event horizon. Then as $h(z)$ goes to $-\infty$ at the origin, the conditions

$$M > 0 \tag{169}$$

and

$$h(z_0) > 0 \tag{170}$$

are necessary and, in fact, enough to have a horizon and assure that the brane lies after it.

The condition (170) is automatically satisfied due to equation (160).

To fulfill (169) let us substitute (163) into (162) to have

$$(\omega+\frac{3}{4})+(\omega+1)\frac{z_0^2}{l^2}<0\,.$$

If $\omega+1\leq 0$, this condition is always satisfied, but this configuration does not produce shortcuts as we would like. However, the condition is also satisfied with $\omega+1>0$ if we require

$$-1<\omega<-\frac{3}{4}\,, \tag{171}$$

and

$$\frac{z_0^2}{l^2}<-\frac{\omega+3/4}{\omega+1}\,. \tag{172}$$

If we follow both (171) and (172) together with the fine-tunning for the energy (163), we will have several shortcuts in AdS-Schwarzschild bulks with shielded singularity. In figures 20 and 21 we illustrate an example with $\omega = -4/5$, $z_0 = 1/3$, and $l = 1$. Notice in figure 20 that the horizon appears before the brane.

Since this case is equivalent to consider the problem in five dimensions with $h(z)$, M and ρ given in [12], analogous results are obtained. In this case, the fine-tunning in the energy is given by [2]

$$\varepsilon^2_{(5)} = -\frac{1}{3\omega+1}\left(\frac{1}{z_0^2}+\frac{2}{l^2}\right), \tag{173}$$

and ω is confined to

$$-1 < \omega < -\frac{2}{3}, \tag{174}$$

while the brane position is given by

$$\frac{z_0^2}{l^2} < -\frac{\omega+2/3}{\omega+1}. \tag{175}$$

[2] In this case $\varepsilon^2_{(5)} = \kappa^4_{(5)}\rho^2/36$.

An example is shown in figures 22 and 23 for $\omega = -3/4$, $z_0 = 1/2$, and $l = 1$.

AdS-Reissner-Nordström Bulk

From the Darmois-Israel conditions (150) we will have for the black hole mass and charge,

$$\begin{aligned} \frac{M}{z_0^5} &= \frac{2k}{z_0^2} + \frac{8}{3l^2} + \frac{\kappa_{(6)}^4}{24}\rho^2\omega\,, \\ \frac{Q^2}{z_0^8} &= \frac{k}{z_0^2} + \frac{5}{3l^2} + \frac{8\omega+3}{3}\frac{\kappa_{(6)}^4\rho^2}{64}\,. \end{aligned} \tag{176}$$

At this stage it is convenient to carefully study the possibility of existence of shortcuts for every value of k.

$k = 0$ and $k = -1$ Cases As it was found in the AdS-Schwarzschild case, (165) determines the existence of shortcuts. Using (147) we see that (165) has a zero in $z = z_f \neq 0$ when

$$\frac{5}{2} M z_f^3 - 4Q^2 - k z_f^6 = 0 \,. \tag{177}$$

If $k = 0$, we have a real root in

$$z_f^3 = \frac{8Q}{5M} \,. \tag{178}$$

If $k = 1$, we have two roots in

$$z_f^3 = \frac{5}{4} M \pm \frac{1}{4} \sqrt{25M^2 - 64Q^2} \,. \tag{179}$$

Finally, if $k = -1$, we have

$$z_f^3 = -\frac{5}{4} M \pm \frac{1}{4} \sqrt{25M^2 + 64Q^2} \,. \tag{180}$$

Notice that $F(z)$ has at most one real and positive zero if $k = 0, -1$ and at most two positive zeros if $k = 1$.

Analyzing $h(z)$ and its derivative we see that $h(z)$ tends to $+\infty$ both at the singularity and at infinity, while $h'(z)$ tends to $-\infty$ at the singularity and to $+\infty$ at infinity.

The horizons occur at the zeros of $h(z)$, or equivalently, at the zeros of

$$z^8 + l^2 k z^6 - l^2 M z^3 + l^2 Q^2 = 0\,. \tag{181}$$

On the other hand, the non-vanishing zeros of $h'(z)$ occur when

$$2z^8 + 3l^2 M z^3 - 6l^2 Q^2 = 0\,. \tag{182}$$

This polynom grows at infinity being negative at the origin. Its derivative has non-vanishing roots when

$$16z^5 + 9l^2 M = 0\,. \tag{183}$$

For $M > 0$ this equation is never satisfied. Thus, as the derivative of (182) does not vanish and is positive outside the origin, the polynom (182) grows monotonically and has just one root. The zeros of this polynom are all non-vanishing zeros of $h'(z)$. Therefore, we conclude that for positive mass there is just one zero for $h'(z)$, and hence, at most two horizons for $h(z)$.

When there is one horizon, $h'(z)$ is negative before it and positive after, crossing $h(z)$ at the very horizon. If there are two horizons, $h'(z)$ vanishes at a point between Cauchy and event horizons, being negative before this point and positive after, while $h(z)$ is positive at all points except between both horizons. Taking into account both the sign and zeros of these functions, $h'(z)$ crosses $h(z)$ between the Cauchy horizon and the point at which $h'(z)$ vanishes.

Since $h'(z)/2$ has the same sign as $h'(z)$ and vanishes at the same point, and in the same way $h(z)/z$ has the same sign of $h(z)$ and vanishes at the same points, we conclude that, existing horizons, $F(z)$ necessarily vanishes at some point $z = z_c$ such that $0 < z_c \leq z_h$. However, as we pointed out before, for $k = 0$ or $k = -1$ there is only one positive root of $F(z)$. As $F(z) < 0$ for $z < z_c$, then $F(z) > 0$ for $z > z_c$. Thus, because $z_c \leq z_h$, $F(z) > 0$ for $z > z_h$ contrary to what was required in (165). This implies that there are no shortcuts with $k = 0$ or $k = -1$ when horizons exist.

In five dimensions the proof is very similar and we arrive to the same conclusion.

$k = 1$ Case As we saw in the previous section, $F(z)$ has two real, positive and distinct roots for $k = 1$,

$$r_1^3 = \frac{5}{4}M - \frac{1}{4}\sqrt{25M^2 - 64Q^2}\,, \tag{184}$$

$$r_2^3 = \frac{5}{4}M + \frac{1}{4}\sqrt{25M^2 - 64Q^2}\,. \tag{185}$$

This is the only situation where the shortcuts can coexist with a shielded singularity. In fact, this situation necessarily requires the second root of $F(z)$ being at some point before the brane position z_0. This also implies $F(z_0) < 0$.

In addition, we must have both Q^2 and M positive.

Given the fact that we have horizons, if the brane is not between them or at a horizon position, then $h(z_0) > 0$. Furthermore, in order to guarantee that the brane is located after the event horizon, we also need $h'(z_0) > 0$.

From the discussion in the previous section we will have one or two horizons if and only if $h(r_1) \leq 0$.

In summary, shortcuts in bulks with shielded singularities can occur only if $k = 1$ and also if the following conditions are supplied,

1. $h(z_0) > 0$ and $h'(z_0) > 0$ to have both horizons before the brane.

2. $F(z_0) < 0$ and $r_2 < z_0$ to have shortcuts with shielded singularity.

3. $Q^2 > 0$ and $M > 0$, which assures the positivity of the black hole mass and charge.

4. $h(r_1) \leq 0$ in order to have horizons.

We will analyze each condition and impose certain restrictions on ω, ρ^2, and z_0.

Existence of Both Horizons Before the Brane These conditions are the simplest to analyze since they restrict ω directly from the Darmois-Israel conditions (150) together with (151)

$$\frac{h(z_0)}{z_0^2} = \varepsilon^2\,, \tag{186}$$

$$\frac{h'(z_0)}{2z_0} = -(4\omega+3)\varepsilon^2\,. \tag{187}$$

The condition (186) is automatically satisfied since $\varepsilon^2 > 0$.

From the condition (187)

$$-(4\omega+3)\varepsilon^2 > 0\,, \tag{188}$$

we have our first restriction

$$\omega < -3/4\,. \tag{189}$$

Existence of Shortcuts with Shielded Singularity From the definition of $F(z)$, (165), and using (186) and (187) we see that

$$0 > F(z_0) = -4(\omega+1)\varepsilon^2 z_0\,. \tag{190}$$

Thus we find another condition on ω

$$\omega + 1 > 0\,. \tag{191}$$

Besides, from $r_2 < z_0$

$$\frac{5M}{4} - z_0^3 < -\frac{1}{4}\sqrt{25M^2 - 64Q^2}\,. \tag{192}$$

This equation will be satisfied if [3]

$$\frac{5M}{4} - z_0^3 < 0\,, \tag{193}$$

or using (176)

$$\frac{3}{2}z_0^3 + \frac{10}{3}z_0^5 + \frac{10}{3}z_0^5\omega\varepsilon^2 < 0\,, \tag{194}$$

and as $\omega < -3/4$

$$z_0^2\varepsilon^2 > \frac{1}{\omega}\left(-\frac{9}{20} - \frac{z_0^2}{l^2}\right)\,. \tag{195}$$

[3] We assume that $25M^2 - 64Q^2 > 0$. We will return to this condition when we discuss the existence of horizons, where we will impose a stronger restriction, $M^2 - 4Q^2 > 0$.

Positivity of the Black Hole Mass and Charge Because we require the positivity of the black hole mass, from (176) we have

$$\frac{M}{z_0^3} > 0 \quad \Rightarrow \quad \frac{z_0^2}{l^2} + \omega\varepsilon^2 z_0^2 > -\frac{3}{4}, \tag{196}$$

thus,

$$z_0^2\varepsilon^2 < \frac{1}{\omega}\left(-\frac{3}{4} - \frac{z_0^2}{l^2}\right). \tag{197}$$

Since $3/4 > 9/20$ this condition is certainly compatible with (195).

On the other hand, the positivity of the squared black hole charge requires

$$\frac{Q^2}{z_0^6} > 0 \quad \Rightarrow \quad 1 + \frac{5z_0^2}{3l^2} + \left(\frac{8}{3}\omega + 1\right) z_0^2\varepsilon^2 > 0\,, \tag{198}$$

so that

$$z_0^2\varepsilon^2 < \frac{1}{8\omega + 3}\left(-3 - \frac{5z_0^2}{l^2}\right). \tag{199}$$

In spite of not being trivial, this equation is also compatible with (195). This requires

$$\frac{1}{\omega}\left(-\frac{9}{20}-\frac{z_0^2}{l^2}\right)<\frac{1}{8\omega+3}\left(-3-\frac{5z_0^2}{l^2}\right), \tag{200}$$

or

$$-\frac{1}{5}\left(\omega+\frac{9}{4}\right)-\frac{z_0^2}{l^2}(\omega+1)<0\,, \tag{201}$$

what is always true for $-1<\omega<-3/4$.

Existence of Horizons This is the last and the more complicated of our conditions. We must have $h(r_1) \leq 0$. Let x be r_1^3,

$$\frac{x^{8/3}}{l^2} + x^2 - Mx + Q^2 \leq 0\,. \tag{202}$$

We do not need to do a complete study of this equation. For our purposes it will be enough to require

$$x^2 - Mx + Q^2 < 0\,. \tag{203}$$

Using (184) this implies

$$M^2 - 4Q^2 > 0\,. \tag{204}$$

This condition is necessary but not enough to have horizons. However, this restriction added to the others developed in this section will be enough to construct shortcuts with horizons as we will see. Notice that this condition is stronger than that one assumed before, $M > 8/5\,Q$.

Using (176) in (204),

$$(1-\varepsilon^2 l^2)+\frac{16}{9}\frac{z_0^2}{l^2}\left(1+\omega\varepsilon^2 l^2\right)^2>0\,. \tag{205}$$

We know from (195) that $1-\varepsilon^2 l^2$ must be negative. Therefore, we must very carefully analyze (205). We can interpret (205) as a quadratic equation in the energy

$$\left(1+\frac{16}{9}\frac{z_0^2}{l^2}\right)+\left(\frac{32}{9}\omega z_0^2-l^2\right)\varepsilon^2+\left(\frac{16}{9}l^2 z_0^2\omega^2\right)\varepsilon^4>0\,, \tag{206}$$

what implies

$$z_0^2\varepsilon^2>\frac{1}{32}\left(-32\omega z_0^2+9l^2+3\sqrt{-64\omega z_0^2 l^2+9l^4-64l^2 z_0^2\omega^2}\right)/(\omega^2 l^2)\,, \tag{207}$$

or

$$z_0^2\varepsilon^2<\frac{1}{32}\left(-32\omega z_0^2+9l^2-3\sqrt{-64\omega z_0^2 l^2+9l^4-64l^2 z_0^2\omega^2}\right)/(\omega^2 l^2)\,. \tag{208}$$

Notice that because $-1 < \omega < -3/4$,

$$-64\omega z_0^2 l^2 - 64 l^2 z_0^2 \omega^2 = -64\omega(\omega+1) z_0^2 l^2 > 0$$

and all the previous roots are real and positive.

Summarizing, from the considerations in the previous sections, we must have for ω

$$-1 < \omega < -3/4\,. \tag{209}$$

For the energy,

$$\frac{1}{\omega}\left(-\frac{9}{20}-\frac{z_0^2}{l^2}\right) < z_0^2\varepsilon^2 < \frac{1}{\omega}\left(-\frac{3}{4}-\frac{z_0^2}{l^2}\right)\,, \qquad \text{or} \tag{210}$$

$$\frac{1}{\omega}\left(-\frac{9}{20}-\frac{z_0^2}{l^2}\right) < z_0^2\varepsilon^2 < \frac{1}{8\omega+3}\left(-3-\frac{5z_0^2}{l^2}\right)\,, \tag{211}$$

depending on which condition is more restrictive.

In addition,

$$z_0^2\varepsilon^2 > \frac{1}{32}\left(-32\omega z_0^2 + 9l^2 + 3\sqrt{-64\omega z_0^2 l^2 + 9l^4 - 64l^2 z_0^2\omega^2}\right)/(\omega^2 l^2)\,, \quad (212)$$

or

$$z_0^2\varepsilon^2 < \frac{1}{32}\left(-32\omega z_0^2 + 9l^2 - 3\sqrt{-64\omega z_0^2 l^2 + 9l^4 - 64l^2 z_0^2\omega^2}\right)/(\omega^2 l^2)\,. \quad (213)$$

Now we are going to analyze the situations in which all these conditions are compatible.

Let us begin our analysis with equation (213). To be compatible with (210) and (211), we just need

$$\frac{1}{\omega}\left(-\frac{9}{20}-\frac{z_0^2}{l^2}\right)<\frac{1}{32}\left(-32\omega z_0^2+9l^2-3\sqrt{-64\omega z_0^2 l^2+9l^4-64l^2 z_0^2\omega^2}\right)/(\omega^2 l^2)\,, \tag{214}$$

that is,

$$-\frac{9}{20}\omega-\frac{9}{32}+\frac{3}{32}\sqrt{-64\omega\frac{z_0^2}{l^2}+9-64\frac{z_0^2}{l^2}\omega^2}<0\,. \tag{215}$$

Since $3/4 <\mid \omega \mid< 1$,

$$-\frac{9}{20}\omega-\frac{9}{32}$$

will always be positive and thus, (215) will never be satisfied. Then, we conclude that (213) is not compatible either with (210) or (211). This implies that $z_0^2\varepsilon^2$ must satisfy (212) together with (210) or (211).

Let us initially compare (210) with (212). We must have

$$\frac{1}{\omega}\left(-\frac{3}{4}-\frac{z_0^2}{l^2}\right)>\frac{1}{32}\left(-32\omega z_0^2+9l^2+3\sqrt{-64\omega z_0^2 l^2+9l^4-64l^2z_0^2\omega^2}\right)/(\omega^2 l^2)\,, \tag{216}$$

that is,

$$-\frac{3}{4}\omega-\frac{9}{32}-\frac{3}{32}\sqrt{-64\omega\frac{z_0^2}{l^2}+9-64\frac{z_0^2}{l^2}\omega^2}>0\,. \tag{217}$$

In this case, since ω is negative and $3/4<\mid\omega\mid<1$,

$$-\frac{3}{4}\omega-\frac{9}{32}>0$$

and (217) can be satisfied if

$$\left(-\frac{3}{4}\omega-\frac{9}{32}\right)^2>\frac{9}{1024}\left(-64\omega\frac{z_0^2}{l^2}+9-64\frac{z_0^2}{l^2}\omega^2\right)\,, \tag{218}$$

or

$$\frac{9}{16}\omega(\omega+1)\frac{z_0^2}{l^2}+\frac{9}{64}(3+4\omega)\omega>0\,. \tag{219}$$

Since $\omega+1>0$ and $3+4\omega<0$, for positive z_0 the inequality will be only fulfilled if

$$\frac{z_0}{l}<\frac{1}{2}\sqrt{-\frac{3+4\omega}{1+\omega}}\,. \tag{220}$$

So that (212) and (210) can be compatible.

Now we are going to analyze the compatibility between (212) and (211). We must have

$$\frac{1}{8\omega+3}\left(-3-\frac{5z_0^2}{l^2}\right)+\frac{z_0^2}{\omega l^2}-\frac{9}{32\omega^2}>\frac{3}{32\omega^2}\sqrt{-64\omega z_0^2 l^2+9l^4-64l^2z_0^2\omega^2}\,. \quad (221)$$

or using that $8\omega+3<0$, simplifying, and squaring both sides we can write (221) as

$$\frac{1}{16}\omega^2(3+4\omega)^2+\omega^2(\omega+1)^2\left(\frac{z_0^2}{l^2}\right)^2+\frac{\omega^2}{2}(3+4\omega)(\omega+1)\frac{z_0^2}{l^2}>0\,. \quad (222)$$

This polynom has just one root for z_0^2/l^2

$$\frac{z_0^2}{l^2}=-\frac{1}{4}\left(\frac{3+4\omega}{1+\omega}\right)\,.$$

Since the coeficient of z_0^4/l^4 is positive, the inequality is satisfied with the same condition (220), so we verify that both (211) and (210) are compatible with (212) under the same restrictions.

Furthermore, let us compare the upper limits of (210) and (211). Suppose

$$\frac{1}{\omega}\left(-\frac{3}{4}-\frac{z_0^2}{l^2}\right) > \frac{1}{8\omega+3}\left(-3-\frac{5z_0^2}{l^2}\right), \tag{223}$$

what can also be written as

$$-\frac{3}{4}(4\omega+3)-\frac{3z_0^2}{l^2}(\omega+1) > 0\,. \tag{224}$$

Thus, (223) is satisfied if and only if

$$\frac{z_0^2}{l^2} < -\frac{1}{4}\left(\frac{3+4\omega}{1+\omega}\right), \tag{225}$$

which is just the same inequality (220), that z_0 must satisfy. Hence, between (210) and (211), it is enough to take into account the latter. Nevertheless, from (222) notice that (211) would be also compatible with (212) if

$$\frac{z_0^2}{l^2} > -\frac{1}{4}\left(\frac{3+4\omega}{1+\omega}\right),$$

and (223) would be satisfied with a change of sign implying that we should consider (210) instead of (211); however, as stated before, the compatibility of (210) and (212) requires

$$\frac{z_0^2}{l^2} < -\frac{1}{4}\left(\frac{3+4\omega}{1+\omega}\right),$$

which contradicts our hypothesis. Therefore, the only possible configuration is (225).

At last, we compare the lower limits of (211) and (212). Suppose

$$\frac{1}{\omega}\left(-\frac{9}{20}-\frac{z_0^2}{l^2}\right)<\frac{1}{32\omega^2 l^2}\left(-32\omega z_0^2+9l^2+3\sqrt{-64\omega z_0^2 l^2+9l^4-64l^2 z_0^2\omega^2}\right), \tag{226}$$

or

$$-\frac{9}{20}\omega-\frac{9}{32}<\frac{3}{32}\sqrt{-64\omega\frac{z_0^2}{l^2}+9-64\frac{z_0^2}{l^2}\omega^2}\,.$$

Squaring and simplifying we obtain

$$\frac{z_0^2}{l^2}>-\frac{9}{20(\omega+1)}\left(\frac{4}{5}\omega+1\right)\,.$$

For $-1<\omega<-3/4$ this inequality is always satisfied since the right hand side is negative. Hence, we conclude that (226) is valid and between the lower limits for the energy in (211) and (212), we just need to choose the latter.

[htb!]

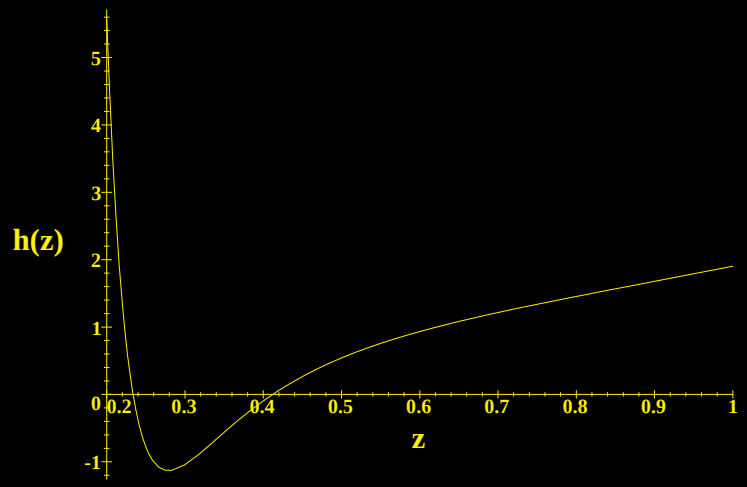

$h(z)$ in six-dimensional AdS-Reissner-Nordström bulk with the brane located at $z = 1$. Notice that the singularity is shielded by two horizons.

[htb!]

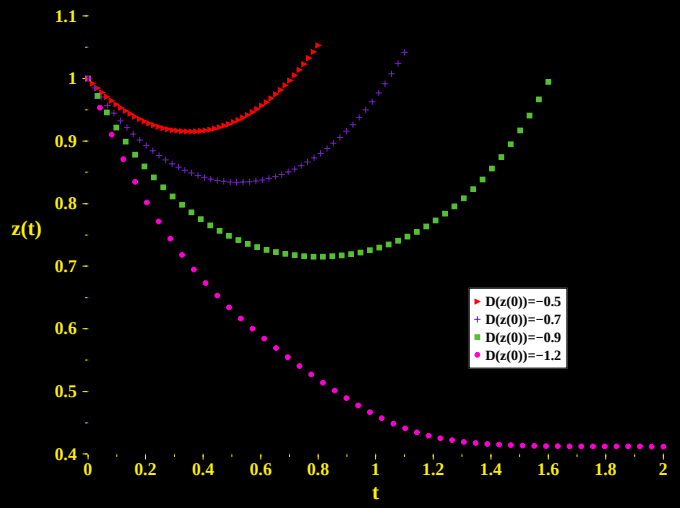

Shortcuts for several initial velocities in six-dimensional AdS-Reissner-Nordström bulk. Notice that there is threshold initial velocity for which the graviton can not return to the brane and falls into the event horizon.

[htb!]

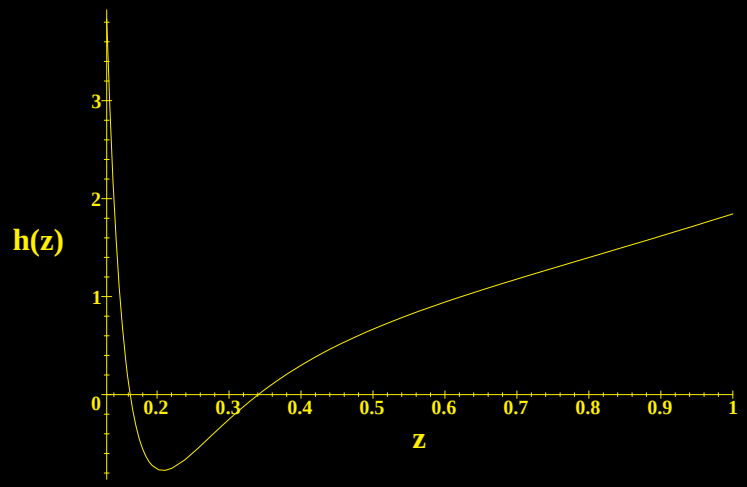

$h(z)$ in five-dimensional AdS-Reissner-Nordström bulk with the brane located at $z = 1$. We see that the singularity is protected by two horizons.

[htb!]

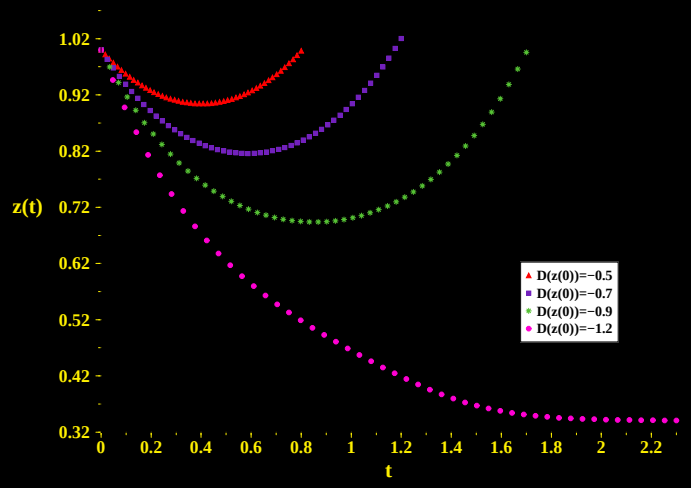

Shortcuts for several initial velocities in five-dimensional AdS-Reissner-Nordström bulk. We see that there is threshold initial velocity for which the graviton can not return to the brane and falls into the event horizon.

In short, by purely analytic considerations we conclude that shortcuts in bulks having no naked singularities and a static brane embedded in can only appear if $k = 1$ and if the following conditions are satisfied,

1. We must choose ω such that $-1 < \omega < -3/4$;

2. Given ω, the brane must be located at a position such that

$$\frac{z_0}{l} < \frac{1}{2}\sqrt{-\frac{3+4\omega}{1+\omega}}\,, \tag{227}$$

   which is the same condition as AdS-Schwarzschild case (172);

3. Given (227), the energy ε must satisfy

$$\frac{1}{32\omega^2}\left(-\frac{32\omega z_0^2}{l^2}+9+3\sqrt{-64\omega\frac{z_0^2}{l^2}+9-64\frac{z_0^2}{l^2}\omega^2}\right) < z_0^2\varepsilon^2 < \frac{1}{8\omega+3}\left(-3-\frac{5z_0^2}{l^2}\right). \tag{228}$$

In this way, it turns out to be simple to find shortcuts in bulks with shielded singularities.

As an example, let us choose $\omega = -9/10$. From (227) we must have

$$\frac{z_0}{l} < \frac{\sqrt{6}}{2},$$

then we choose $l = 1$ and $z_0 = 1$.

From (228) we have

$$\frac{35}{24} + \frac{5}{72}\sqrt{41} < \varepsilon^2 < \frac{40}{21},$$

so we choose $\varepsilon = \sqrt{238/125}$.

In figure (24) we plot $h(z)$ with these conditions. Notice that the singularity is protected by an event horizon and the brane is at $z = z_0 = 1$.

In figure (25) we plot the graviton paths obtained from (154) under the previous conditions for a variety of initial velocities showing that, in fact, shortcuts appear when we choose the parameters following the complete analysis shown in this section.

The analysis in five dimensions can be performed analogously to six-dimensional one with

$$h(z) = 1 + \frac{z^2}{l^2} - \frac{M}{z^2} + \frac{Q^2}{z^4}\,, \tag{229}$$

and

$$\frac{M}{z_0^4} = \frac{2}{z_0^2} + \frac{3}{l^2} + 3\omega\varepsilon_{(5)}^2\,, \tag{230}$$

$$\frac{Q^2}{z_0^6} = \frac{1}{z_0^2} + \frac{2}{l^2} + 3\omega\varepsilon_{(5)}^2 + \varepsilon_{(5)}^2\,, \tag{231}$$

arriving to the following restrictions:

1. We must choose ω such that $-1 < \omega < -2/3$;

2. Given ω, the brane must be located at a position such that

$$\frac{z_0}{l} < \sqrt{-\frac{\omega + 2/3}{1+\omega}}; \tag{232}$$

3. Given (232), the energy $\varepsilon^2_{(5)} = \kappa^4_{(5)}\rho^2/36$ must satisfy

$$\frac{1}{9\omega^2}\left(2 - 9\frac{z_0^2}{l^2}\omega + 2\sqrt{1 - 9\frac{z_0^2}{l^2}\omega(\omega+1)}\right) < z_0^2\varepsilon^2_{(5)} < \frac{1}{3\omega+1}\left(-1 - \frac{2z_0^2}{l^2}\right). \tag{233}$$

As an example, we choose $\omega = -7/8$. From (232) we must have

$$\frac{z_0}{l} < \frac{\sqrt{15}}{3},$$

so we choose $l = 1$ and $z_0 = 1$.

From (233) the energy must fulfill

$$\frac{632}{441} + \frac{16}{441}\sqrt{127} < \varepsilon_{(5)}^2 < \frac{24}{13},$$

then we choose $\varepsilon_{(5)} = \sqrt{461/250}$.

In figure (26) we can see $h(z)$ according to the previous conditions. As in the six dimensional case, the singularity is protected by an event horizon, and the brane is at $z = z_0 = 1$.

In figure (27) we show several graviton paths obtained under the previous conditions for several initial velocities showing that shortcuts appear when we choose the parameters following the analysis shown in this section analogously to the six dimensional case.

The FRW-Brane evolving in the Bulk

The main reason to study the evolution of the brane from the point of view of the bulk is to simplify the analysis of gravitational signs leaving and subsequently returning to the brane. In fact in the static AdS backgound, the equation for a null geodesic in the bulk, $a = a(t)$, is particularly simplified [11],

$$\frac{\ddot{a}(t)}{a} + \frac{\dot{a}^2(t)}{a^2}\Big(1 - \frac{3h'(a)a}{2h(a)}\Big) + \frac{h(a)}{a}\Big(\frac{h'(a)}{2} - \frac{h}{a}\Big) = 0 \quad . \tag{234}$$

On the other hand, the evolution of the brane in the bulk, $a = a_b(t)$, at early times, $a_b << L_c$, is dictated by

$$\frac{da_b}{dt} = \frac{h(a_b)}{\sqrt{1+\frac{h(a_b)}{\dot{a}_b(\tau)^2}}} = h(a_b)\Big(1+\frac{k+\frac{a_b^2}{l^2}}{\frac{\Omega_0^2}{4(1+l^2\Lambda_4)}\frac{L_c^{2q}}{l^2 a_b^{2q-2}}}\Big)^{-1/2} \quad ,$$

where we used the fact that the quadratic term in the energy prevails. Thus,

$$\frac{da_b}{dt} = h(a_b)\Big(1+\frac{4(1+l^2\Lambda_4)}{\Omega_0^2}\frac{a_b^{2q}}{L_c^{2q}}(1+kl^2/(a_b^2))\Big)^{-1/2} \quad ,$$

and, for $a_b << L_c$, since the observed cosmological constant is at most $\Lambda_4 \sim H_0^2$, $\Lambda_4 l^2 << 1$ we have

$$\frac{da_b}{dt} \approx h(a_b)\Big(1-\frac{2(1+l^2\Lambda_4)}{\Omega_0^2}\frac{a_b^{2q}}{L_c^{2q}}(1+kl^2/(a_b^2))\Big) \quad . \tag{235}$$

Substituting the result for the evolution of the brane, $\dot{a}(t) = h(a)$, in the geodesic equation (234), we verify that it is satisfied. Therefore, the trajectory of the brane differs from the trajectory of the null geodesic by a term of the order $\left(\frac{a_b}{L_c}\right)^{2q}$.

This means that for $a_b << L_c$, the trajectory of the brane in the bulk is governed by

$$\frac{da_b(t)}{dt} = k + \frac{a_b^2}{l^2} \quad . \tag{236}$$

Thus, if $k = 0$,

$$a_b(t) = \frac{a_b(0) l^2}{l^2 - a_b(0) t} \tag{237}$$

and, if $k = -1$,

$$a_b(t) = \frac{2l(l + a_b(0))}{e^{2t/l}(l - a_b(0)) + l + a_b(0)} - l \quad . \tag{238}$$

In this last situation, if the Universe begins under the Randall-Sundrum scale, $a(0) < l$, it will recolapse to the singularity in a finite time,

$$t = \frac{l}{2} \ln\Big(\frac{l + a_b(0)}{l - a_b(0)}\Big) \quad .$$

Indeed, there is an event horizon when $a = l$ if $k = -1$.

In the case of an eliptic Universe,

$$a_b(t) = l \tan\Big(\frac{t}{l} + \tan^{-1}\Big(\frac{a_b(0)}{l}\Big)\Big) \quad . \tag{239}$$

Starting at the singularity $t_0 = \tau_0 = a_b(t_0) = 0$, we have

$$a_b(t) = l \tan\Big(\frac{t}{l}\Big) \quad . \tag{240}$$

Note that the evolution of the brane in the bulk is linear near the initial singularity ($a(t) \sim t$ for $t << l$), diverging at the critical time $t_c = \frac{\pi}{2} l$. In fact, the behaviour of all solutions is similar near the critical time

$$\begin{aligned} t_c &= \frac{l^2}{a_b(0)} \quad ; \\ t_c &= \frac{l}{2} \ln\Big(\frac{l + a_b(0)}{a_b(0) - l}\Big) \quad ; \end{aligned}$$

$$t_c \quad = \quad \frac{\pi}{2} l - l \tan^{-1}\left(\frac{a_b(0)}{l}\right) \tag{241}$$

for $k = 0,\ -1,\ +1$ respectively.

As we approach the critical time $a_b(t)$ increases quickly. When $a_b(t) \sim L_c$ equation (236) is no longer valid, and the trajectory of the brane is no longer a geodesic. Thus, for a very short period, from the point of view of the bulk the brane undergoes a phase transition. In figure 28 this behaviour is shown in terms of the numerical solution of eq. (**??**) for a radiation dominated eliptic Universe.

Before the critical time, from the point of view of the bulk, there is no time left for the remaining graviton geodesics to reach the brane. This is in fact the kind of behaviour that we find in numerical studies of the complete equation for the evolution of the brane and null geodesics as in the example of figure 29.

On the other hand, for later times the evolution of the brane is softer, and shortcuts appear, as exhibited in fig. 30.

[htb!]

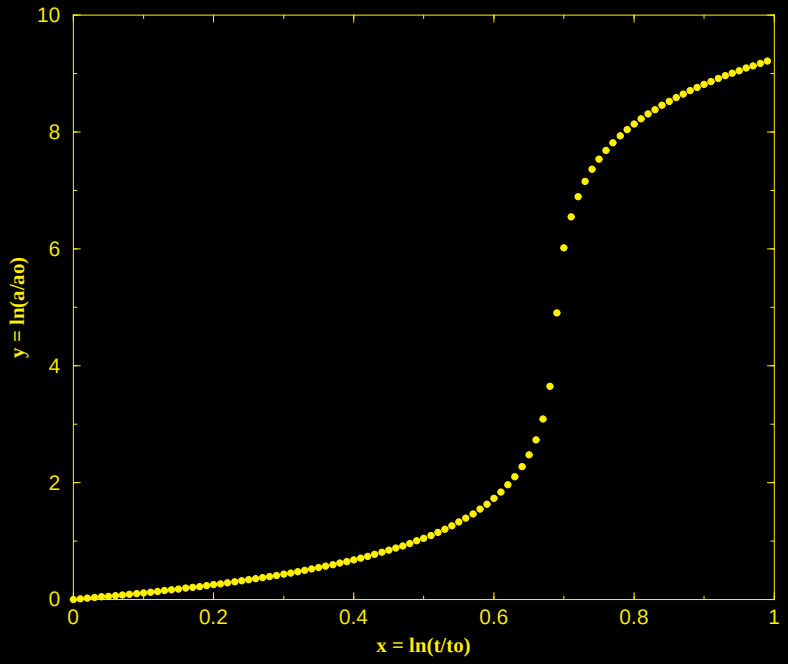

Evolution of the brane in the bulk at the intermediate epoch $a_b \sim 0.01 L_c$ until $a_b \sim 200 L_c$, radiation dominated era (RDE), $\Omega_0 = 2$.

[htb!]

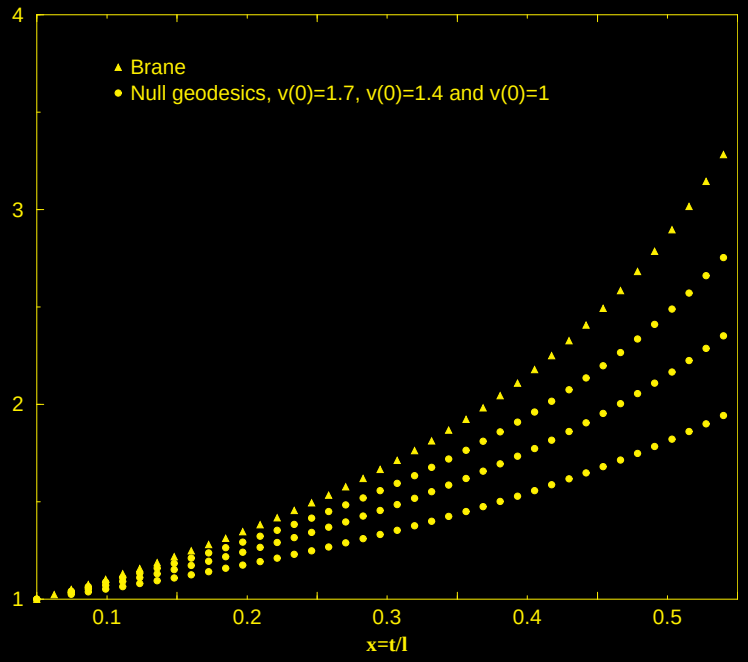

The trajectory of the brane in the bulk for $\Omega_0 = 2$. Other curves are geodesics that start in the brane with different initial velocities.

[htb!]

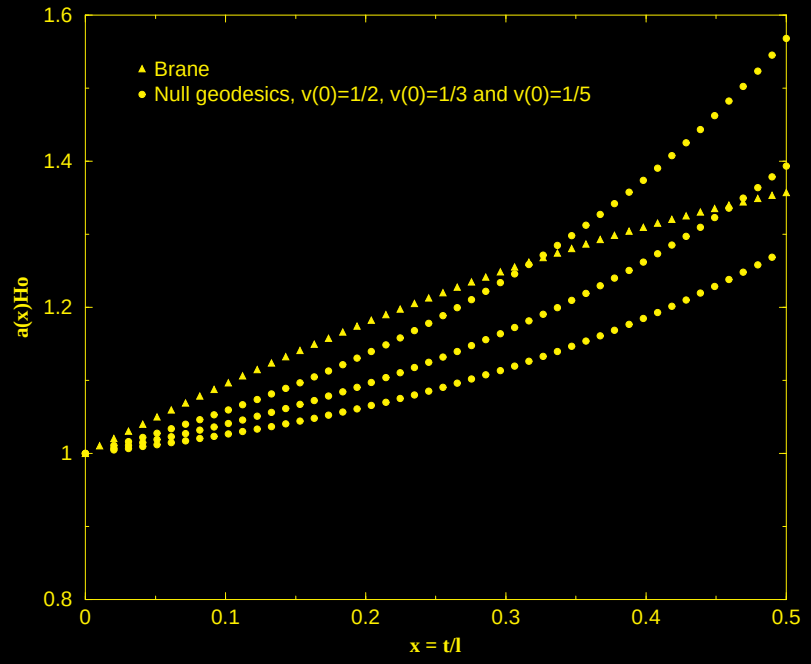

The trajectory of the brane in the bulk for $\Omega_0 = 2$, matter dominated era (MDE) with $k = 1$. Also null geodesics starting in the brane with various initial velocities.

The Effect of Shortcuts in Late Times Universes

The shortcuts just found for late times Universes could be used to probe the extra-dimensionality by the aparent violation of causality in the brane. Thus, suppose that in $\tau = t = 0$ an object could emit eletromagnetic and gravitational waves and that we could be able to detect both signs in times τ'_γ and τ'_g. We compute now the order of magnitude of the advance in time of the graviton. Since the signals cover the same distance in the brane,

$$\int_0^{\tau'_\gamma} \frac{d\tau_\gamma}{a_b(\tau_\gamma)} = \int_0^{t'_g} \frac{dt_g}{a(t_g)} \sqrt{h(a) - \frac{\dot{a}(t_g)^2}{h(a)}} \quad . \tag{242}$$

Here, a denotes the coordinate defining the geodesic in the bulk, and differs from the coordinate of the brane a_b. In terms of the dimensionless parameters y and x,

$a = Ly$ and $t = Tx$ the last integral reads

$$\int_0^{t'_g} \frac{dt_g}{a(t_g)} \sqrt{h(a) - \frac{\dot{a}(t)^2}{h(a)}} \;=\; \int_0^{t'_g} \frac{dt_g}{l} \sqrt{1 + \frac{l^2}{L^2 y^2} - \frac{l^2}{T^2} \frac{\dot{y}(x)^2}{y^2 + y^4 \frac{L^2}{l^2}}} \quad . \text{(243)}$$

Using the relation between the time in the brane and that of the bulk we convert the above expressions in terms of the interval of time of the observer in the brane,

$$\begin{aligned} \int_0^{\tau'_\gamma} \frac{d\tau_\gamma}{a_b(\tau_\gamma)} \;&=\; \int_0^{\tau'_g} \frac{d\tau_g}{l} \frac{dt_g}{d\tau_g} \sqrt{1 + \frac{l^2}{L^2 y^2} - \frac{l^2}{T^2} \frac{\dot{y}(x)^2}{y^2 + y^4 \frac{L^2}{l^2}}} \\ &=\; \int_0^{\tau'_g} \frac{d\tau_g}{l} \frac{1}{h(a_b)} \sqrt{h(a_b) + \dot{a}_b(\tau_g)^2} \sqrt{1 + \frac{l^2}{L^2 y^2} - \frac{l^2}{T^2} \frac{\dot{y}(x)^2}{y^2 + y^4 \frac{L^2}{l^2}}} \, . \end{aligned}$$

The Friedmann equation implies

$$\int_0^{\tau_g'} \frac{d\tau_g}{l}\frac{1}{h(a_b)}\sqrt{\frac{y_b^2L^2}{l^2}+\Lambda_4L^2y_b^2+\frac{\Omega_0}{y_b^{q-2}}\frac{L_c^q}{l^2L^{q-2}}}\sqrt{1+\frac{l^2}{L^2y^2}-\frac{l^2}{T^2}\frac{\dot{y}(x)^2}{y^2+y^4\frac{L^2}{l^2}}}$$

$$=\int_0^{\tau_g'} \frac{d\tau_g}{l}\frac{1}{h(a_b)}\frac{y_bL}{l}\sqrt{1+l^2\Lambda_4+\frac{\Omega_0}{y_b^q}\frac{L_c^q}{L^q}}\sqrt{1+\frac{l^2}{L^2y^2}-\frac{l^2}{T^2}\frac{\dot{y}(x)^2}{y^2+y^4\frac{L^2}{l^2}}}$$

$$=\int_0^{\tau_g'} \frac{d\tau_g}{a_b(\tau_g)}\frac{1}{1+\frac{l^2}{L^2y_b^2}}\sqrt{1+l^2\Lambda_4+\frac{\Omega_0}{y_b^q}\frac{L_c^q}{L^q}}\sqrt{1+\frac{l^2}{L^2y^2}-\frac{l^2}{T^2}\frac{\dot{y}(x)^2}{y^2+y^4\frac{L^2}{l^2}}}\quad .$$

Therefore, if $L >> L_c >> l$ we obtain, at second order in L_c/L and l/L,

$$\int_0^{\tau_g'} \frac{d\tau_g}{a_b(\tau_g)}\left(1-\frac{l^2}{L^2}\frac{1}{y_b^2}\right)\left(1+\frac{1}{2}l^2\Lambda_4+\frac{1}{2}\frac{\Omega_0}{y_b^q}\frac{L_c^q}{L^q}\right)\left(1+\frac{1}{2}\frac{l^2}{L^2y^2}-\frac{1}{2}\frac{l^2}{T^2}\frac{\dot{y}(x)^2}{y^2+y^4\frac{L^2}{l^2}}\right) \quad .$$

Finally,

$$\int_0^{\tau_\gamma'} \frac{d\tau_\gamma}{a_b(\tau_\gamma)} = \int_0^{\tau_g'} \frac{d\tau_g}{a_b(\tau_g)}\Big[1+\frac{1}{2}\frac{\Omega_0}{y_b^q}\frac{L_c^q}{L^q}+\frac{1}{2}l^2\Lambda_4-\frac{l^2}{L^2}\frac{1}{y_b^2} + \frac{1}{2}\frac{l^2}{L^2y^2}-\frac{1}{2}\frac{l^4}{T^2L^2}\frac{\dot{y}(x)^2}{y^4}\Big] \quad .$$

Thus, at first order, the time difference between the photon and the graviton is corrected in the integrand by terms of the order $\frac{L_c^q}{a_b^q}$. Today this factor is at most 10^{-58} and in the time of decoupling 10^{-46}, showing that the time advance of the graviton can be safely neglected and is of no physical significance, in spite of the fact that the trajectory of the brane is distinctively different from the null geodesic.

The Effect of Shortcuts in Early Times Universes

From the analysis developed so far we learned that the periods of evolution of the Universe differ by the scale that defines the physical significance of the shortcuts. In an era where $a_b << L_c$, the trajectory of the brane in the bulk differs from the extreme geodesics by $(a_b/L_c)^{2q}$ and the shortcuts do not appear, since the brane itself provides the graviton geodesic.

In the period when $a_b >> L_c$, the trajectory of the brane is far from a null geodesic and shortcuts appear, but they are not significant, since the $skin\ depth$ of the graviton in the bulk is defined by the parameter $l << L_c << a_b$. The difference between the time intervals of the photon and the graviton is of the order $(L_c/a_b)^q$.

However, from the continuity of the evolution of the brane in the bulk, we expect that there is also an intermediate situation $a_b \sim L_c$ when physically important shortcuts could appear, since the evolution of the brane is far enough from a geodesic. Indeed, in figure 31, rescaling the geodesics in the bulk we can observe the behaviour of the brane as compared to the geodesics that start in it at a later time. It is clear that these shortcuts are serious mediators of homogenization of the matter in the brane in the era before nucleosynthesis [13], [14].

From the evolution of the brane in the bulk in the intermediate epoch we thus conclude that there is a critical age t_c, after which the gravitational waves leaving the brane return before the arrival of the photons released at the same time as the gravitons. The behaviour of the geodesic in the bulk shows that any geodesic starting in the brane at a certain instant will be singular at a time later than the critical time, indicating that it will return to the brane. Thus, information leaks between regions which apparently are causally disconnected at times $t > t_c$.

[htb!]

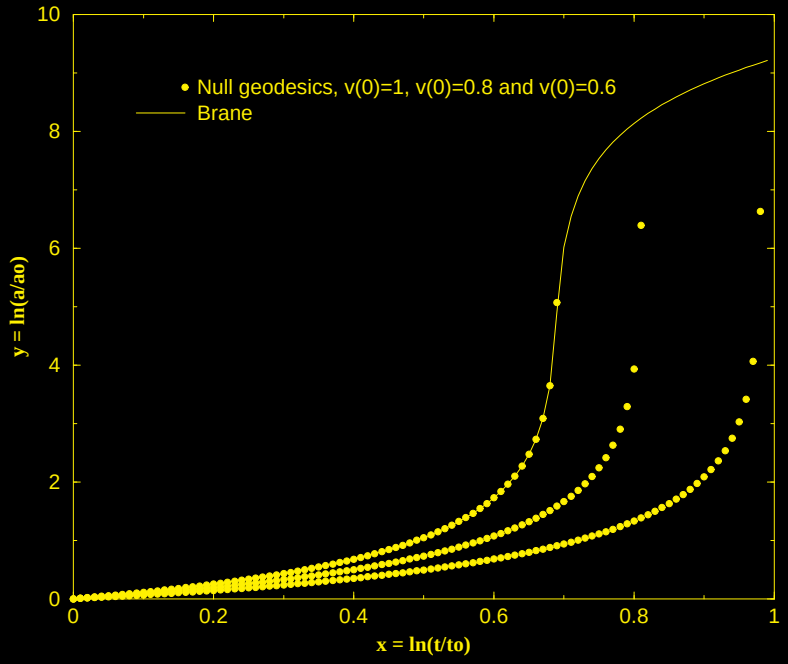

The trajectory of the brane in the bulk leaving $a = 0.01 L_c$ in the RDE. Geodesics in the bulk with different initial velocities are exhibited intercepting the brane after the critical time t_c.

In order to study the horizon problem, we now compare, at a certain time τ_n previous to nucleosynthesis, the graviton horizon R_g with the observable proper distance of the universe (from the radiation decoupling until today) [15]. Since the graviton evolves in a bulk geodesic,

$$
\begin{aligned}
R_g &\equiv \int \frac{dr}{\sqrt{1-kr^2}} = \int \frac{dt}{a}\sqrt{h(a)-\frac{\dot{a}^2}{h(a)}} = \int \frac{d\tau}{a}\frac{\sqrt{h(a_b)+\dot{a}_b^2}}{h(a_b)}\sqrt{h(a)-\frac{\dot{a}^2}{h(a)}} \\
&= \int_0^{\tau_n} \frac{d\tau}{a_b}\frac{1}{1+l^2/a_b^2}\sqrt{1+\Lambda_4 l^2+\frac{\Omega_0 L_c^q}{a_b^q}\Big(1+\frac{\Omega_0 L_c^q}{4a_b^q(1+\Lambda_4 l^2)}\Big)}\times \\
&\quad \times\sqrt{1+\frac{l^2}{L^2y^2}-\frac{l^2}{T^2}\frac{\dot{y}(x)^2}{y^2+y^4\frac{L^2}{l^2}}} \quad , \qquad (244)
\end{aligned}
$$

while in the brane, the size of the observable Universe is $R=\int \frac{d\tau}{a_b(\tau)}$.

We use the known results for the usual particle horizon

$$R = \frac{1}{\sqrt{\Omega_0} H_0 a_{b0}} \int_{z(\tau)}^{z(0)} z^{-q/2} dz = \frac{2}{(q-2)\sqrt{\Omega_0} H_0 a_{b0}} (z(\tau)^{1-q/2} - z(0)^{1-q/2}) \quad .$$

where $z(\tau) = a_{b0}/a_b(\tau)$. Today,

$$R \sim \frac{2}{\sqrt{\Omega_0} H_0 a_{b0}} \equiv R_0 \quad .$$

For the computation of the graviton horizon, we work in a primordial era before nucleosynthesis. Thus, in the Friedmann equation we can neglect the usual cosmological term as well as the curvature term. At an epoch between Planck era and nucleosynthesis, $l << a_b << H_0$, it is safe to neglect terms involving l^2/L^2 in (244), and we find

$$R_g \approx \int_0^{\tau_n} \frac{d\tau}{a_b} \sqrt{1 + \frac{\Omega_0 L_c^q}{a_b^q} + \frac{\Omega_0^2 L_c^{2q}}{4 a_b^{2q}}} \quad .$$

Using the Friedmann equation we get

$$R_g = \frac{1}{\Omega_0^{1/2} H_0 a_{b0}} \int_{z(\tau_n)}^{z(0)} \frac{dz}{z^2} \frac{\left(1 + \frac{\Omega_0 H_0^2 l^2}{2} z^4\right)}{\sqrt{1 + \frac{\Omega_0 H_0^2 l^2}{4} z^4}} \quad . \tag{245}$$

The integral diverges for arbitrarly high redshifts, proving that the horizon problem is potentially solvable. The behaviour of this integral can be determined. We have

$$R_g \approx \frac{l}{a_{b0}} z(0) \quad .$$

Comparing with the size of the Universe today,

$$\frac{R_g}{R_0} \sim \frac{\sqrt{\Omega_0}}{2} H_0 l z(0) \quad .$$

It looks like shortcuts are not enough to solve the horizon problem, since we would need to go back in time to $z(0) \sim (H_0 l)^{-1} \sim 10^{29}$, 10^{11} times higher than the redshift at the Planck time in the brane associated with the fundamental scale of gravity, κ_5.

For the time being, lets assume the validity of the theory in such high energies. In the next section we will argue that, in order to provide a solution to the usual cosmological problems, inflationary models must use of those high redshifts. We may note, however, that there are actually two related time scales. In the primordial Universe the brane is evolving as a part of the bulk, with velocities close to that of light, and time intervals in the brane correspond to much longer

intervals in the bulk. In fact, the relation between these scales is obtained from $t_0 = \tau_0 = a_b(\tau_0) = 0$ and from

$$t = \int_0^\tau d\tau \frac{\sqrt{h(a_b) + \dot{a}_b^2(\tau)}}{h(a_b)} \quad .$$

For $a_b << L_c$ we have $\tau << l$, and one finds, as a consequence

$$t \approx \int_0^{\tau} d\tau \frac{\dot{a}_b(\tau)}{h(a_b)} = \int_0^{a_b(\tau)} \frac{da_b}{k + a_b^2/l^2} \quad .$$

This implies, for the example of a closed universe with $\Omega_0 = 2$,

$$t = l \arctan\Big(\frac{a_b(\tau)}{l}\Big) \quad .$$

Therefore, when $a_b(\tau) \sim l$, that is, when the brane time is $\tau \sim 10^{-67} s$, the corresponding bulk time $t \sim \frac{\pi}{4} l \sim 10^{-11}$s is much larger than the Planck scale, $t >> M_{(5)}^{-1}$.

If we assume that quantization is mandatory according to the bulk Planck energy scale, geodesics that start in the bulk with $z(0) \sim (H_0 l)^{-1}$ should be sufficient to homogenize the Universe before nucleosynthesis, reaching $R_g \sim 1$. In order to verify this, we have numerically integrated the expression for the distance reached by geodesics $a(t)$ starting in the brane at $a_b = l$, corresponding to a time $t = \pi/4l$, for $k = 1$ with $\Omega_0 \sim 2$ ($a_{b0} \sim H_0^{-1}$):

$$R_g = \int_{l\pi/4}^{t_f} \frac{dt}{a} \sqrt{h(a) - \frac{\dot{a}^2}{h(a)}} \quad . \tag{246}$$

[htb!]

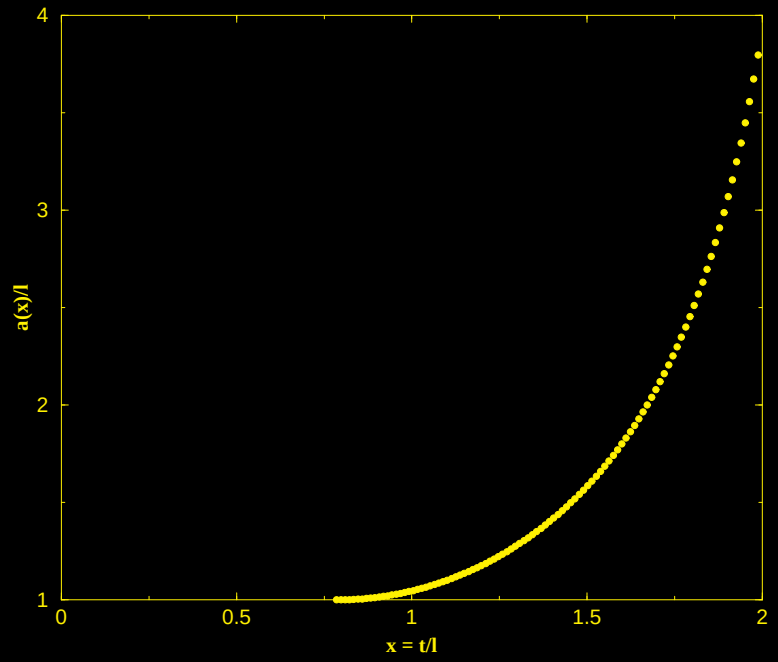

Null geodesic starting at $a = l$, $t = \pi/4l$ with initial velocity $v(\pi/4) = 0$.

The solution of the geodesic equation is given in figure 32. The brane evolves initially as a geodesic with speed $v_b \sim 2$ ($a_b \sim l$) and we exhibit a geodesic with zero initial speed in the bulk. The point of inflexion in its trajectory is $t_f = 2.356l > t_c = \frac{\pi}{2}l$. As we saw before, the brane evolves smoothly after the transition and the geodesics return to the brane if we wait until t_f, see (246). Although the trajectory diverges near this point, the integrand in (246) is finite and we can perform the integration, finding

$$R_g = 2.526 \quad .$$

Thus, the observable Universe is smaller than the reach of the relic gravitons that start in a previous era.

Causal Gravitational Structure

In the last section we learned about the behaviour of null-geodesics for closed Universes. We can, however, study analytically the whole causal structure of the gravitational signs for a $k = 0$ Universe.

The geodesic equation, (234), is quite simple for purely AdS $k = 0$ space-times

$$\frac{1}{a^2}\frac{da}{dt} = \frac{v(0)}{a(0)^2} \quad . \tag{247}$$

Thus, a geodesic that starts in the brane at $a = a(0)$ ant $t = 0$, with initial veolcity $v(0)$, returns to it when

$$t_r \approx \frac{a(0)}{v(0)} \quad .$$

The expression for the gravitational horizon can also be integrated

$$\begin{aligned} R_g &= \int_0^{t_r} \frac{dt}{a}\sqrt{h(a)-\frac{\dot{a}^2}{h(a)}} = \int_0^{t_r} \frac{dt}{l}\sqrt{1-\frac{l^4\dot{a}^2}{a^4}} \\ &= \frac{t_r}{l}\sqrt{1-\frac{v(0)^2 l^4}{a(0)^4}} \quad . \end{aligned} \tag{248}$$

Using the relation between the returning time and the initial velocity,

$$R_g = \frac{t_r}{l}\sqrt{1-\frac{l^4}{a(0)^2 t_r^2}} \quad . \tag{249}$$

In order to relate the returning time to the redshift, we must integrate the relation between time of the bulk and time of the brane (**??**). We already know that from

$a(0)$ to the critical period of transition a time of $t_c \sim \frac{l^2}{a(0)}$ has passed. After that, the evolution is dominated by the usual term in Friedmann equation and we can approximate

$$\begin{aligned} t_r &\approx \frac{l^2}{a(0)} + \int_{L_c}^{a_r} l \frac{da_b}{a_b^2 H} \approx \frac{l^2}{a(0)} + \int_{L_c}^{a_r} da_b \frac{l}{\sqrt{\Omega_0} H_0} a_b^{q/2-2} \\ &\approx \frac{l^2}{a(0)} + \frac{2l}{(q-2)\sqrt{\Omega_0} H_0 a_{b0}} \left(z_r^{-q/2+1} - 10^{-15} \right) \quad , \end{aligned} \tag{250}$$

where z_r must, of course, be greater than the redshift in the transition, $z_{Lc} \sim 10^{15}$.

Substituting back in the expression of the gravitational horizon,

$$
\begin{aligned}
R_g &= \left[\frac{l}{a(0)}+\frac{2}{(q-2)\sqrt{\Omega_0}H_0 a_{b0}}\left(z_r^{-q/2+1}-10^{-15}\right)\right] \\
&\times \sqrt{1-\left[1+\frac{2a(0)}{(q-2)\sqrt{\Omega_0}lH_0 a_{b0}}\left(z_r^{-q/2+1}-10^{-15}\right)\right]^{-2}} \quad . \quad (251)
\end{aligned}
$$

When considering the interesting situation of a high initial redshift $z(0) = a_{b0}/a(0) > (H_0 l)^{-1}$, this expression can be approximated by

$$R_g \approx \frac{l}{a(0)}\sqrt{\frac{4a(0)}{(q-2)\sqrt{\Omega_0} l H_0 a_{b0}}\left(z_r^{-q/2+1} - 10^{-15}\right)} \quad . \tag{252}$$

Comparing with the size of the horizon today, we find

$$\left(\frac{R_g}{R_0}\right)_{z_r} \approx \sqrt{\sqrt{\Omega_0}\frac{l H_0}{(q-2)}}\sqrt{z(0)\left(z_r^{-q/2+1} - 10^{-15}\right)} \quad . \tag{253}$$

We note, as we did in the last section, that if sufficiently large redshifts were available, the graviton horizon in a past epoch could be larger than the present size of the observable Universe.

We argue, however, that those high redshifts could be available even when the energy density in the brane is not quantized yet. Indeed, if inflation takes place in the brane high redshifts could be present in the beginning of the inflationary epoch.

Denoting the redshift when inflation ends by z_e, if the size of the present Universe, R_0, is expected to be in causal contact during inflation, we must reach at least a redshift in the beginning of inflation, $z(0)$, that solves

$$\frac{a_{b0}R_0}{z(0)} = H^{-1}(z_e) \quad .$$

The unusual results in brane-world cosmology are expected if inflation ends before the transition time, when the quadratic term in Friedmann equation dominates. In this case, we get

$$\frac{a_{b0}R_0}{z(0)} = \frac{1}{\Omega_0 H_0^2 l z_e^4}$$

and

$$z(0) = 2\sqrt{\Omega_0} H_0 l z_e^4 \quad . \tag{254}$$

If $H(z_e)l >> 1$, it is simple to note, from equation (**??**), that the evolution of the brane in the bulk is not altered during inflation. Thus, we can substitute the result(254) in the complete expression for the causal gravitational horizon (253),

$$\left(\frac{R_g}{R_0}\right)_{z_r} \approx \sqrt{\frac{2\Omega_0}{(q-2)}} H_0 l z_e^2 \sqrt{\left(z_r^{-q/2+1} - 10^{-15}\right)} \quad . \tag{255}$$

This equation tells us that, in the time of nucleosyntesis, when $z_r \sim 10^{10}$, $R_g/R_0 \sim 1$ for a model with inflation ending just before what would be the Planck era, with $z_e \sim 10^{17}$ (where $z_{Pl} \sim 10^{18}$). This proves that successfully inflationary models ending before the transition time necessarily make relevant changes in the causal structure of the universe.

We are able to sketch the gravitational horizon for this kind of configuration. In figure 33 we show the behaviour of the Hubble horizon in comoving coordinates $H^{-1}a_b^{-1}/R_0$ and the graviton horizon R_g/R_0 for an inflationary model ending just before the Planck era, $z_e = 10^{17}$ and producing the necessary number of e-folds to solve the horizon problem. The fraction of the Universe in causal contact by gravitational signs in the nucleosynthesis epoch is just the present horizon R_0. Today, the gravitational horizon would be $10^5 R_0$.

[htb!]

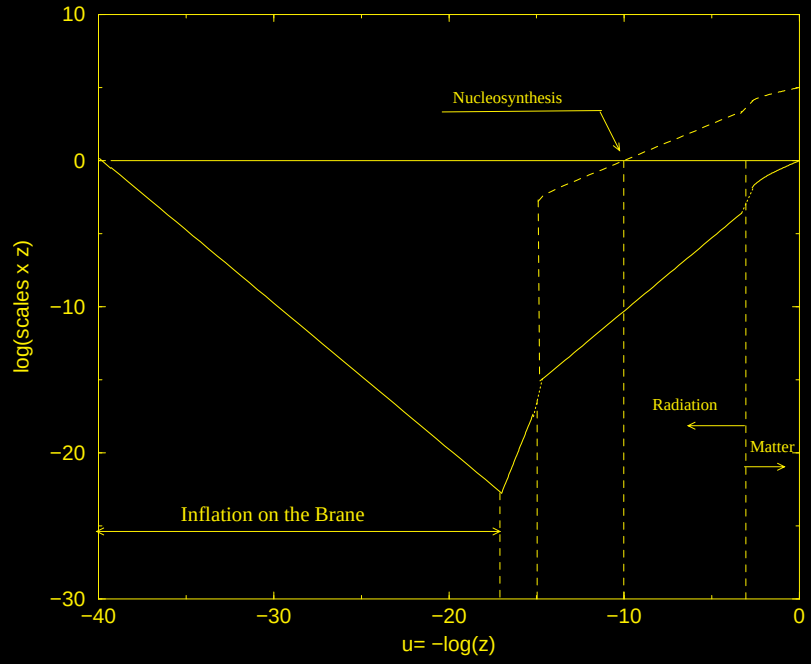

We plot in log-log scale the evolution of the fraction of graviton horizon and the present observable size, R_g/R_0 (dashed line) and the same for the Hubble horizon $a_b^{-1}H^{-1}/R_0$ (solid line), for an inflationary model in the brane that ends after Planck time ($u_{PL} = -\log(z_{PL}) = -18$), and before transition time ($u_{TR} = -15$), in $u_{end} = -\log(z_{end}) = -17$. The present scale would be under the de-Sitter horizon if redshifts like $u(0) = -39$ were available. This imply in strong modifications of the causal structure for gravitational signs after the transition time.

Conclusions

Studying the shortcut problem in braneworld cosmology from the point of view of the bulk we have explicitly shown that shortcuts are indeed common in late time Universes, though they are extremelly small and the time advance of the graviton can be safely neglected. However, we have also learned that gravitational signs may leave and subsequently return to the brane even in early times Universes. We have showed that those shortcuts exist and that the new scale of the model, l, implies in a minimum time scale for the reception of those signs by an observer in the brane. Before that critical time, the brane itself evolves like a null-geodesic in the bulk.

If high initial redshits were available the shortcuts just found could solve the horizon problem without inflation. More important however, may be the effect of those shortcuts with an inflationary epoch in the brane.

Brane-world models incorporate two changes in the cosmology, namely, the modified Friedmann equation and the possibility of leaking of gravity in the extra dimension. Using the first of those modifications, it was shown that, remarkably, the consistency equation is mantained in the brane-world formalism when the inflation is guided by a scalar field minimally coupled in the brane [59]. This consists in bad news for those who expect that brane cosmological configurations could probe the extra dimensionality of our Universe.

However, we have showed that if there was an inflationary epoch in the brane evolution, the causal structure of the universe could be strongly modified. This could be a sign of an unusual evolution of the perturbations from the time they cross the de Sitter horizon, H^{-1}, during inflation, through the time they became causally connected again. In this case, there could be distinct predictions for the microwave background radiation structure even with the same consistency equation during inflation. Thus, further investigation on the dynamics of perturbations in inflationary brane-world models may prove useful to probe the dimensionality of space-time.

Acknowledgements: This work has been supported by Fundação de Amparo à Pesquisa do Estado de São Paulo **(FAPESP)** and Conselho Nacional de Desenvolvimento Científico e Tecnológico **(CNPq)**, Brazil.

References

[1] M. Gasperini, G. Veneziano, The pre big-bang scenario in String Cosmology, **CERN-TH** (2002) 104; [hep-th/0207130].

[2] J. Polchinski, *Superstring Theory* vols. 1 and 2, Cambridge University Press 1998.

[3] G. t'Hooft

[4] Sugra

[5] Green Schwarz

[6] Duality

[7]

[8] kaluzaklein

[9] Arkani Hamed

[10] Horava and E. Witten

[11] E. Abdalla, A. Casali, B. Cuadros-Melgar, *Nucl. Phys.* **B644** (2002) 201; [hep-th/0205203].

[12] C. Csáki, J.Erlich, C. Grojean, *Nucl. Phys.* **B604** (2001) 312; [hep-th/0012143].

[13] H. Ishihara, *Phys. Rev. Lett.* **86** (2001) 381.

[14] R. Caldwell and D. Langlois, *Phys. Lett.* **B511** (2001) 129; [gr-qc/0103070].

[15] D. J. Chung and K. Freese, *Phys. Rev.* **D62** (2000) 063513; [hep-ph/9910235]. *Phys. Rev.* **D61** (2000) 023511; [hep-ph/9906542].

[16] C. Csáki, M.Graesser, L. Randall and J. Terning, *Phys. Rev.* **D62**, (2000) 045015, [hep-th/9911406]; P. Binetruy, C. Deffayet, D. Langlois *Nucl.Phys.* **B615**, (2001) 219, [hep-th/0101234].

[17] E. Abdalla, B. Cuadros-Melgar, S. Feng, B. Wang, *Phys. Rev.* **D65** (2002) 083512; [hep-th/0109024].

[18] G. Starkman, D. Stojkovic and M. Trodden, *Phys. Rev. Lett.* **87** (2001) 231303; *Phys. Rev.* **D63** (2001) 103511.

[19] D. J. Chung and K. Freese; [astro-ph/0202066].

[20] E. Abdalla and A. G. Casali; [hep-th/0208008].

[21] G. Dvali and S. H. Tye *Phys. Lett.* **B450** (1999) 72, hrp-th/9812483.

[22] F. Quevedo

[23] S. Kashru, R. Kallosh, A. Linde, J. Maldacena, L. McAllister and S. Trivedi, hep-th/0308055

[24] K. D. Kokkotas, B. G. Schmidt, gr-qc/9909058 and references therein.

[25] C. W. Misner, K. S. Thorne and J. A. Wheeler, Gravitation (Freeman, San Franciso, 1973).

[26] E. Poisson and W. Israel, Phys. Rev. D 41, 1796 (1990).

[27] R. H. Price, Phys. Rev. D 5, 2419 (1972); 5, 2439 (1972).

[28] C. Gundlach, R. H. Price and J. Pullin, Phys. Rev. D 49, 883 (1994).

[29] R. Gomez, J. Winicoar and B. G. Schmidt, Phys. Rev. D 49,2828 (1994).

[30] E. Leaver, J. Math. Phys. 27, 1238 (1986); Phys. Rev. D 34,384 (1986).

[31] N. Andersson, Phys. Rev. D 55, 468 (1997).

[32] J. Bicak, Gen. Relativ. Gravit. 3, 331 (1972).

[33] C. Gundlach, R. H. Price and J. Pullin, Phys. Rev. D 49, 890 (1994).

[34] L. M. Burko and A. Ori, Phys. Rev. D 56, 7820 (1997).

[35] S. Hod and T. Piran, Phys. Rev. D 58, 024017 (1998).

[36] S. Hod and T. Piran, Phys. Rev. D 58, 044018 (1998).

[37] P. R. Brady, C. M. Chambers, W. G. Laarakkers and E. Poisson, Phys. Rev. D 60, 064003 (1999).

[38] P. R. Brady, C. M. Chambers, W. Krivan and P. Laguna, Phys. Rev. D 55, 7538 (1997).

[39] E. S. C. Ching, P. T. Leung, W. M. Suen and K. Young, Phys. Rev. D 52, 2118 (1995); Phys. Rev. Lett. 74, 2414 (1995).

[40] J. M. Maldacena, Adv. Theor. Math. Phys. 2, 231 (1998).

[41] E. Witten, Adv. Theor. Math. Phys. 2, 253 (1998).

[42] S. S. Gubser, I. R. Klebanov and A. M. Polyakov, Phys. Lett. B428, 105 (1998).

[43] G. T. Horowitz and V. E. Hubeny, hep-th/9909056; G. T. Horowitz, Class. Quant. Grav. 17, 1107 (2000).

[44] Gravitational wave experiments.

[45] Accelerated Expansion.

[46] de Sitter

[47] B. Wang, C. Molina and E. Abdalla, *Phys. Rev.* **D63**, 084001 (2001), hep-th/0005143.

[48] B. Wang, C. Lin and E. Abdalla, *Phys. Lett.*

[49] Jiong-Ming Zhu, Bin Wang and Elcio Abdalla, *Phys. Rev.* **D63** (2001)124004 hep-th/0101133; Bin Wang, Elcio Abdalla and R.B. Mann, *Phys. Rev.* **D65** (2002) 084006 hep-th/0107243.

[50] Leaver

[51] Gamow

[52] Elcio Abdalla, Bin Wang, A. Lima-Santos and W.G. Qiu, *Phys. Lett.* **B538** (2002) 435-441 hep-th/0204030; E. Abdalla, K.H.C. Castello-Branco, A. Lima-Santos, *Mod. Phys. Lett.* **A** gr-qc/0301130.

[53] B. F. Schutz and C. M. Will, *Astrophys. J.* **291**, L33 (1985).

[54] S. Iyer and C. M. Will, *Phys. Rev.* **D35**, 3621 (1987).

[55] J. W. Moffat; [hep-th/0208122].

[56] E. W. Kolb and M. S. Turner, *The Early Universe*, Addinson-Wesley 1990.

[57] G. Giudice, E. Kolb, J. Lesgourgues and A. Riotto, **CERN-TH** (2002) 149; [hep-ph/0207145].

[58] Shin'ichi Nojiri, Sergei D. Odintsov, Akio Sugamoto, *Mod. Phys. Lett.* **A17** (2002) 1269; [hep-th/0204065]. Shin'ichi Nojiri, Sergei D. Odintsov, *JHEP* **0112** (2001) 033; [hep-th/0107134]. Bin Wang, Elcio Abdalla, Ru-Keng Su, *Mod. Phys. Lett.* **A17** (2002) 23; [hep-th/0106086].

[59] G. Huey and J. Lidsey, *Phys. Lett.* **B514**, 217 (2001), [astro-ph/0104006]; A. Liddle and A. Taylor, *Phys. Rev.* **D65**, 041301 (2002), [astro-ph/0109412].

[60] A. R. Liddle and D. H. Lyth *Phys. Rep.* V. F. Mukhanov, H. A. Feldman and R. H. Brandenberger *Phys. Rep.* **215** (1992) 203.

[61] A. H. Guth *Phys. Rev.* **23** (1981) 347; A. A. Starobinsky *Phys. Lett.* **B 91** (1980) 99.

[62] J. R. Oppenheimer and H. Snyder *Phys. Rev.* **56** (1939) 455; S. Weinberg *Gravitation and Cosmology*.

[63] Gibbons and S. Hawking, *Phys. Rev.* **D15** (1977) 2738.

[64] C. Lanczos, *Phys. Zeits.* **23** (1922) 539; *Ann. der Phys.* **74** (1924) 518.

[65] W. Israel, *Nuovo Cimento* **44B** (1966) 1. Erratum: **48B** (1967) 2.

[66] G. Darmois, *Mem. Sciences Math.* **XXV** (1927) ch. V.

[67] H.A. Chamblin and H.S. Reall, *Nucl. Phys.* **B562** (1999) 133.

[68] G. Gibbons and S. Hawking, *Phys. Rev.* **D15** (1977) 2752.

[69] P. Binétruy, C. Deffayet and D. Langlois, *Nucl. Phys.* **B565** (2000) 269.

[70] P. Binétruy, C. Deffayet, U. Ellwanger and D. Langlois, *Phys. Lett.* **B477** (2000) 285.

[71] H. A. Chamblin and H. S. Reall, *Nucl.Phys.* **B562** (1999) 133; [hep-th/9903225].

[72] P. Kanti, R. Madden and K. A. Olive, *Phys. Rev.* **D64** (2001) 044021; [hep-th/0104177].

[73] D. Ida, *JHEP* **0009** (2000) 014; [gr-qc/9912002].

[74] L. Randall and R. Sundrum, *Phys. Rev. Lett.* **83**, (1999) 3370, [hep-th/9905221]; *Phys. Rev. Lett.* **83**, (1999) 4690, [hep-th/9906064].

[75] P. Kraus, *JHEP* **9912** (1999) 011; [hep-th/9910149].

[76] P. Bowcock, C. Charmousis and R. Gregory, *Class. Quant. Grav.*, **17** (2000) 4745 ; [hep-th/0007177].

[77] P. Binétruy, C. Deffayet and D. Langlois, *Nucl. Phys.* **B565** (2000) 269; [hep-th/9905012].

[78] C. Csáki, M. Graesser, C. Kolda and J. Terning, *Phys. Lett.* **B462** (1999) 34; [hep-ph/9906513].

[79] J. Cline, C. Grosjean and G. Servant, *Phys. Rev. Lett.* **83** (1999) 4245; [hep-ph/9906523].

[80] P. Binétruy, C. Deffayet, U. Ellwanger and D. Langlois, *Phys. Lett.* **B477** (2000) 285; [hep-th/9910219].

[81] P. Binétruy, C. Deffayet and D. Langlois, *Nucl. Phys.* **B565** (2000) 269; [hep-th/9905012].

[82] P. de Bernardis *et al.*, *Nature* **404** (2000) 955; *Astrophys. J.* **536** (2000) L63; [astro-ph/9911445]. R. Stompor *et al.*, *Astrophys. J.* **561** (2001) L7; [astro-ph/0105062].

[83] T. Regge and J.A. Wheeler, Phys. Rev. **108**, 1063 (1957).

[84] S. Chandrasekhar, *The Mathematical Theory of Black Holes*, (Oxford University Press, Oxforf, 1983).

[85] K. D. Kokkotas and B. G. Schmidt, Living Rev. Relativity **2** (1999).

[86] A. Riess et al. Astrophy. J., **116**, 1009 (1998).

[87] V. Cardoso and J. P. S. Lemos, Phys. Rev. D **64**, 084017 (2001);

[88] B. Wang, C. Lin and E. Abdalla, Phys. Lett. B, **481**, 79 (2000); B. Wang, C. Molina and E. Abdalla, Phys. Rev. D **63**, 084001 (2001); V. Cardoso, R. Konoplya, J. P. S. Lemos, gr-qc/0305038.

[89] B. Wang, C. Molina and E. Abdalla, Phys. Rev. D **63**, 084001 (2001);

[90] V. Cardoso and J. P. S. Lemos, Class.Quant.Grav. **18**, 5257 (2001); V. Cardoso and J. P. S. Lemos, Phys. Rev. D **63**, 124015 (2001); J. Zhu, B. Wang and

E. Abdalla, Phys. Rev. D **63**, 124004 (2001); B. Wang, E. Abdalla and R. B. Mann, Phys. Rev. D **65**, 084006. (2002).

[91] H. Nariai, Sci. Rep. Tohoku Univ. **34**, 160 (1950); H. Nariai, Sci. Rep. Tohoku Univ. **35**, 62 (1951).

[92] E. Leaver, Phys. Rev. D **34**, 384 (1986).

[93] E. S. C. Ching, P. T. Leung, W. M. Suen and K. Young, Phys. Rev. D **52**, 2118 (1995).

[94] G. Gamow, Zeits. F. Phys. **51** 204 (1928).

[95] Elcio Abdalla, Bin Wang, A. Lima-Santos and W.G. Qiu, Phys. Lett. B **538**, 435 (2002); E. Abdalla, K.H.C. Castello-Branco, A. Lima-Santos, Mod. Phys. Lett. A **18**, 1435 (2003).

[96] B. F. Schutz and C. M. Will, Astrophys. J. **291**, L33 (1985).

[97] S. Iyer and C. M. Will, Phys. Rev. D **35**, 3621 (1987).

[98] S. Iyer, Phys. Rev. D **35**, 3632 (1987); K. D. Kokkotas and B. F. Schutz, Phys. Rev. D **37**, 3378 (1988).

[99] R. Ruffini, J. Tiomno, C. Vishveshwara, Lettere al Nuovo Cimento **3**, 211 (1972).

[100] R. Price, Phys. Rev. D **5**, 2419 (1972).

[101] V. Cardoso and J. P. S. Lemos, Phys. Rev. D **67**, 084020 (2003).

[102] C. Molina, gr-qc/0304053, to be published on Phys. Rev. D.

[103] A. Zhidenko, gr-qc/0307012.

[104] R. A. Konoplya, gr-qc/0303052.

[105] P. Brady, C. Chambers, W. Krivan and P. Laguna, Phys. Rev. D **55**, 7538 (1997).

[106] P. Brady, C. Chambers, W. Laarakkers and E. Poisson, Phys. Rev. D **60**, 064003 (1999).

[107] E. Abdalla, B. Wang, A. Lima-Santos and W. G. Qiu, Phys. Lett. B **538**, 435 (2002).

[108] E. Abdalla, K. Castello Branco and A. Lima Santos, Mod. Phys. Lett. A, **18**, 1435, (2003).

[109] *Higher Transcedental Functions, V.* ***II*** *(Bateman Manuscript Project)*, ed. by A. Erdélyi (McGraw-Hill, New York, 1953); I. S. Gradshteyn and I. M. Ryzhik, *Tables of Integrals, Series and Products* (Academic Press, 2000).

[110] G. 't Hooft, gr-qc/9310026; L. Susskind, *J. Math. Phys.* **36** (1995) 6377.

[111] J. Maldacena, *Adv. Theor. Math. Phys.* **2** (1998) 231; S. Gubser, I. Klebanov and A. Polyakov, *Phys. Lett.* **B 428** (1998) 105; E. Witten, *Adv. Theor. Math. Phys.* **2** (1998) 253.

[112] E. Witten, *Adv. Theor. Math. Phys.* **2** (1998) 505.

[113] S. W. Hawking and D. Page, *Comm. Math. Phys.* **87** (1983) 577.

[114] W. Fischler and L. Susskind, hep-th/9806039; N. Kaloper and A. Linde, *Phys. Rev.* **D 60** (1999) 103509; R. Easther and D. A. Lowe, *Phys. Rev. Lett.* **82** (1999) 4967; G. Veneziano, *Phys. Lett.* **B454** (1999) 22; R. Brustein, *Phys. Rev. Lett.* **84** (2000) 2072; R. Brustein, G. Veneziano, *Phys. Rev. Lett.* **84** (2000) 5695; R. Bousso, *JHEP* **7** (1999) 4, ibid **6** (1999) 28, *Class. Quan. Grav.* **17** (2000) 997; B. Wang, E. Abdalla, *Phys. Lett.* **B 466** (1999) 122, **B 471** (2000) 346.

[115] R. Tavakol, G. Ellis, *Phys. Lett.* **B 469** (1999) 37; B. Wang, E. Abdalla and T. Osada, *Phys. Rev. Lett.* **85** (2000) 5507.

[116] E. Verlinde, hep-th/0008140

[117] B. Wang, E. Abdalla and R. K. Su, hep-th/0101073, Phys. Lett. B 503 (2001) 394.

[118] S. Nojiri and S. D. Odintsov, Int. J. Mod. Phys A16 (2001) 3237; D. Kutasov, F. Larsen, JHEP 0101 (2001) 001, hep-th/0009244; F. Lin, Phys. Lett. B 507 (2001) 270; R. Brustein, S. Foffa and G. Veneziano, Nucl. Phys. B 601 (2001) 380; D. Klemm, A. C. Petkou and G. Siopsis, hep-th/0101076; R. G. Cai, Phys. Rev. D 63 (2001) 124018 hep-th/0102113; D. Birmingham and S. Mokhtari, Phys. Lett. B 508 (2001) 365 hep-th/0103108.

[119] I. Savonije and E. Verlinde, Phys. Lett. B 507 (2001) 305.

[120] L. Randall and R. Sundrum, Phys. Rev. Lett. 83, 3370 (1999); ibid 83, 4690 (1999).

[121] A. K. Biswas and S. Mukherji, JHEP 0103 (2001) 046; S. Nojiri and S. D. Odintsov, hep-th/0103078; Y. S. Myung, hep-th/0102184

[122] D. Youm Phys. Lett. B 515 (2001) 170; S. Nojiri, O. Obregon, S. Odintsov, H. Quevedo and M. Ryan Mod. Phys. Lett. A16 (2001) 1181; D. Klemm, A. Petkou, G. Siopsis and D. Zanon hep-th/0104141.

[123] T. Banks and W. Fischler astro-ph/0307459.

[124] Bin Wang, Elcio Abdalla and Ru-Keng Su *Mod. Phys. Lett.* **A17** (2002) 23.

[125] S. Dodelson and L. Hui, astro-ph/0305113.

[126] A. R. Liddle and S. M. Leach astro-ph/0305263.

[127] W. Israel, *Nuovo Cim.* **44B** (1966) 1; erratum: **48B** (1967), 463.

[128] E. Abdalla and B. Cuadros-Melgar

[129] A. Chamblin, R. Emparan, C. V. Johnson and R. C. Myers, Phys. Rev. D 60, 064018 (1999)

[130] J. Garriga and M. Sasaki, Phys. Rev. D 62, 043523 (2000)

[131] P. Kraus, JHEP 12, 011 (1999)

[132] R. Maartens, D. Wands, B. A. Bassett and I. P. C. Heard, *Phys. Rev.* **D62** (2001) 041301.